NERC-LV-539-6

NRDS NUCLEAR ROCKET EFFLUENT PROGRAM
1959-1970

by
D. E. Bernhardt, R. B. Evans, R. F. Grossman,
F. N. Buck, and M. W. Carter
National Environmental Research Center

U. S. ENVIRONMENTAL PROTECTION AGENCY
Las Vegas, Nevada

June 1974

This report was written under a Memorandum
of Understanding No. AT(26-1)-539
for the
U. S. ATOMIC ENERGY COMMISSION

This report was prepared as an account of work sponsored by the United States Government. Neither the United States nor the United States Atomic Energy Commission, nor any of their employees, nor any of their contractors, subcontractors, or their employees, makes any warranty, express or implied, or assumes any legal liability or responsibility for the accuracy, completeness or usefulness of any information, apparatus, product or process disclosed, or represents that its use would not infringe privately-owned rights.

Available from the National Technical Information Service,
U. S. Department of Commerce,
Springfield, VA. 22151

Price: Paper copy $5.45 Microfiche $1.45

NERC-LV-539-6

NRDS NUCLEAR ROCKET EFFLUENT PROGRAM
1959-1970

by
D. E. Bernhardt, R. B. Evans, R. F. Grossman,
F. N. Buck, and M. W. Carter
National Environmental Research Center

U. S. ENVIRONMENTAL PROTECTION AGENCY
Las Vegas, Nevada

June 1974

This report was written under a Memorandum
of Understanding No. AT(26-1)-539
for the
U. S. ATOMIC ENERGY COMMISSION

ABSTRACT

This report reviews the health implications of radioactive effluent released during nuclear rocket engine tests at the Nuclear Rocket Development Station (NRDS), Jackass Flats, Nevada, prior to 1970.

During this period, nuclear rocket engine concepts incorporated an open-cycle hydrogen-cooled reactor with core operating temperatures of approximately 4,000°F, which cause small quantities of fission products to migrate from the fuel and to be released in the rocket engine exhaust as gases or micrometer-sized particulates; radioactivity released in this manner is called the "aerosol effluent." Core operating conditions caused minor fuel element erosion and corrosion, releasing particles with high radioactivity content (roughly 10^{11} fissions per particle) and diameters of tens of micrometers; these particles are referred to as the "particulate effluent."

NRDS adjoins the Nevada Test Site and the Nellis Air Force Range and is located about 80 miles northwest of Las Vegas, Nevada, in an area of low population density and limited agricultural usage. Lathrop Wells (population less than 100), the nearest town, is about 15 miles from the testing locations.

Estimates of doses, both potential and actual, resulting from exposure of the off-site population to aerosol effluent from past tests have been 15% or less of the appropriate Federal Radiation Council (FRC) guides and Atomic Energy Commission (AEC) standards.

Possible modes of interaction of the particulate effluent with humans which have been investigated include deposition of particles on skin, in or near the eye, in the respiratory system, and in the GI tract. The most limiting mode of interaction, considering biological consequences and probability of occurrence, appears to be deposition on skin. There are no AEC or FRC guides or standards applicable to this type exposure, but the testing organization with the assistance of consultants has established an operational guide. The guide stipulates that the probability of a deleterious interaction (defined

as a certain dose to the skin) should be less than 10^{-4}. Several tests have resulted in potential probabilities of interaction near or above this guide in off-site unpopulated areas. However, there are no known instances of interaction of the particulate effluent with individuals in the off-site population.

PREFACE

This report is a compendium of information about the Project Rover ground testing at the Nuclear Rocket Development Station, Jackass Flats, Nevada, prior to 1970. The testing program was directed by the Space Nuclear Systems Office (SNSO), formerly the Space Nuclear Propulsion Office, a joint administration of the Atomic Energy Commission (AEC) and the National Aeronautics and Space Administration.

Quantities and characteristics of effluent for future tests cannot be directly inferred from the material presented here because of continued efforts to improve reactor fuel element operating integrity and to reduce the quantity of radioactive effluent. The effluent from the nuclear furnace test conducted in June 1972, the first test since 1969, was passed through a liquid scrubber which significantly reduced the quantity of radioactive effluent released to the environment. In addition, the nuclear furnace was fueled with a new type fuel with fission product release characteristics varying from those discussed in this report.[1]

This report refers to a number of Federal Agencies, several of which have been reorganized in the last several years. The report was written at the request of SNSO, under the auspices of a Memorandum of Understanding between the Environmental Protection Agency (EPA) and the AEC. Per this Memorandum the National Environmental Research Center-Las Vegas (NERC-LV) is responsible for conducting an off-site radiological safety program for Nevada Test Site and NRDS activities. This Memorandum was originated between the AEC and the Public Health Service, Department of Health, Education, and Welfare, but, with the formation of the EPA, was subsequently transferred to the NERC-LV. Similarly, the Air Resources Laboratory, Las Vegas, Nevada, (ARL-LV), which provides meteorological services for the testing program, is under the administration of the National Oceanic and Atmospheric Agency, but was formerly under the Environmental Sciences and Services Administration.

TABLE OF CONTENTS

Subject	Page
ABSTRACT	i
PREFACE	iii
LIST OF FIGURES	vi
LIST OF TABLES	vii
I. INTRODUCTION	1
II. REACTOR DESCRIPTION AND EFFLUENT DEFINITION	4
A. Reactor	4
B. Reactor Effluent	7
1. Effluent Release -- Normal Operation	8
(a) Aerosol Effluent	8
(b) Particulate Effluent	11
2. Effluent Release -- Accident Condition	14
C. Source Term Measurements	16
1. Aerosol Effluent	16
2. Particulate Effluent	19
III. EFFLUENT TRANSPORT AND DISTRIBUTION	23
A. Effluent Transport	23
1. Test Location and Site Geography	23
2. Factors Affecting Transport and Deposition	25
3. Plume Rise	26
4. Aerosol Effluent Transport	28
5. Particulate Effluent Transport	34
B. Effluent Distribution	38
IV. DOSE MODELS	40
A. Aerosol or Gas-Cloud Model	42
1. External Gamma Exposure	43
2. Other Approaches to External Gamma Exposure Predictions	45
3. Evaluation	46

Subject	Page
4. Thyroid Dose via Inhalation Pathway	47
5. Thyroid Dose via Ingestion -- Milk-Food Chain	52
B. Particle Dose Prediction Models	53
1. Particle Skin Dose Model	57
V. RADIATION PROTECTION GUIDES	61
A. Guides for Total Body and Internal Organ Doses	62
1. Normal Operation	62
2. Accident Conditions	63
B. Guides for Exposure to Discrete Particles	64
VI. ENVIRONMENTAL LEVELS AND DOSES	68
A. Aerosol Effluent	69
1. Off-Site	69
2. On-Site	75
B. Deposition of Particulate Effluent	79
VII. SUMMARY AND CONCLUSIONS	88
REFERENCES	92
APPENDICES	102
DISTRIBUTION	

LIST OF FIGURES

Figure Number	Title	Page
1.	Conceptual Reactor Schematic.	5
2.	Fraction of Isotope Chain Assumed Released During Full Power Run.	12
3.	Population Centers Near NRDS.	24
4.	XE Prime, EP-IXA, Normal Run Centerline Dose Estimates.	33
5.	XE Prime, EP-IXA, Particle Prediction.	37
6.	Locations Where Fresh Fission Products Were Detected (Phoebus-1B, EP-IV).	39
7.	Dose Models.	41
8.	Off-Site Whole-Body Gamma Exposures and Infant Thyroid Doses Resulting from Reactor Engine Tests from CY 1959 to 1969.	72
9.	Pre-Event Dose Predictions and Dose Estimates from Surveillance Results.	76
10.	Relative Quantity of ^{131}I On Natural Vegetation.	78
11.	Cloud Centerlines for Selected Reactor Tests.	80
12.	Estimated Hypothetical Whole-Body External Gamma Exposures from Activity Deposited by Selected Tests Indicated on Figure 11.	81
13.	Cloud Centerlines for Reactor Engine Tests for which Particle Deposition was Documented in Detail.	83
14.	Three Dimensional Representation of Particle Deposition for Pewee I, EP-III.	85
15.	Probability of Receiving Critical Dose at Kreb's Depth for Four Tests.	86
16.	Normalized Maximum Particle Concentration.	89

LIST OF TABLES

Table Number	Title	Page
1.	Summary of NERVA Reactor Development.	3
2.	Estimated Migration Releases.	20
3.	Estimated Corrosion Releases.	22
4.	Effluent Parameters.	27
5.	Parameters for Radioiodine.	48
6.	Biological Parameters for Radioiodine Isotopes.	50
7.	Occupational Dose Standards.	62
8.	Comparison of Maximum Hypothetical Whole-Body Gamma Exposures and Infant Thyroid Doses with Radiation Protection Standards.	73
9.	Summary of NRDS Nuclear Rocket Testing Results.	74
10.	Typical Effluent Prediction Parameters.	77

I. INTRODUCTION

From the conception in 1958 of Project Rover, the program to develop a nuclear powered rocket engine, through June 1970, nineteen nuclear reactors or engines were tested at the Nuclear Rocket Development Station (NRDS). About 80 miles northwest of Las Vegas, Nevada, NRDS is part of a large complex of government-controlled testing reservations known as the Test Range Complex and including the Nevada Test Site, the Nellis Air Force Range, and the Tonopah Test Range. The distance between testing facilities at NRDS and the outer boundaries of the access-controlled Test Range Complex varies between ten and 80 miles. The closest populated area beyond the Test Range Complex is Lathrop Wells, about 15 miles to the south.

This report summarizes information concerning the public health implications of the radioactive effluent released from past Project Rover Reactor tests. The report includes descriptions of the mechanisms of production and release of the radioactive effluent, the mechanisms of environmental transport of the effluent and its potential interaction with man, and the implications of this interaction with man. Emphasis has been placed on the public health versus occupational health aspects of the program.

Engines tested recently have utilized a single-pass open-cycle hydrogen-cooled reactor. During rocket engine tests, airborne radioactive gases and particles have been transported to and detected in areas beyond the Test Range Complex. As part of this testing program, considerable effort has been devoted to determining the physical, chemical, and radiological characteristics of the radioactivity releases, evaluating the potential biological effects of the releases, and maintaining a radiological safety program to insure the safety of on-site workers and off-site residents.

Table 1 contains the highlights of the development of the nuclear rocket engine.[2,3,4] The development of the nuclear rocket began in early 1955 under joint sponsorship of the Air Force and the Atomic Energy Commission.[2]

The development of nuclear rocket engine technology was the responsibility of the Los Alamos Scientific Laboratory (LASL), Los Alamos, New Mexico. The Air Force was responsible for the non-nuclear portion of the project. The National Aeronautics and Space Administration (NASA) was formed by executive order in 1958. In 1960 a joint AEC-NASA agency, the Space Nuclear Propulsion Office (now known as the Space Nuclear Systems Office), was created to administer development of an operational nuclear rocket.

The first reactors of the program were called KIWI's after the flightless Kiwi bird of New Zealand. Initially the KIWI reactor was intended as a low-power ground test engine of roughly 1,000 Mw; it was proposed that a larger version, the Phoebus class of reactors with a power of 5,000 Mw, would be developed for flight engines. The Phoebus program was cancelled after several tests, and the present concept is based on development of a rocket engine of lower power and thrust than the Phoebus or Kiwi designs.

The success of the first nuclear reactor test, KIWI-A, on July 1, 1959, encouraged SNSO to initiate industrial participation in the program. In July 1961, Aerojet General Corporation was chosen to develop a Nuclear Engine for Rocket Vehicle Application (NERVA) with Westinghouse Astronuclear Laboratory (WANL) as the subcontractor to provide the nuclear reactors. The NRX or NERVA experiments were aimed at developing the basic KIWI reactor into a nuclear rocket engine. The NERVA program includes reactor development and development of equipment for and testing of a breadboard system.

The NERVA program progressed to the "Experimental Engine" (XE) phase with the test of the XE Prime in the winter and spring of 1968-69. The engine was tested in the down-firing configuration (as opposed to the up-firing attitude of previous tests), with auxiliary components in a semi-flight configuration and in a partial vacuum to simulate the environment to be encountered in space. The Pewee Reactor tested in 1968 and the Nuclear Furnace Reactors are scaled-down models for testing changes in technology in a nuclear environment.

Table 1. Summary of NERVA Reactor Development.

Year	Reactor Test Series	Configuration
1957		Program started.
July 1959	KIWI-A	First power reactor test. Gaseous H_2 coolant, 5 min. test, 70 Mw power used micrometer-sized UO_2 particles in a carbon matrix--plate geometry.(2)
Sept. 1962	KIWI-B1B	First liquid H_2 cooled reactor, 800 Mw. Internal core structure failed.(2)
Aug. 1964	KIWI-B4E	First all bead (UC_2) fueled reactor which contained a redesigned core support structure. 900 Mw, run of 5 x 10^5Mw-sec. (Ref.2)
Sept. 1964	NRX-A2	First NERVA reactor test, 1100 Mw, 3.5 x 10^5 Mw-sec. Demonstrated flow control characteristics.
Jan. 1965	KIWI-TRANSIENT NUCLEAR TEST	Reactor nuclear safety test experiment.
June 1965	PHOEBUS-1A	First Phoebus reactor test. 1100 Mw, 7 x 10^5 Mw-sec. Ran out of run tank hydrogen and had loss of coolant incident. (Ref.3) Some of the fuel elements had exterior cladding.(Ref.4)
Feb.-Mar. 1966	NRX-A4/EST	First experiment with breadboard design* and first bootstrap startup to power. Maximum power 1140 Mw, peak integral power during a test 1.1 x 10^6 Mw-sec. Demonstrated that a nuclear rocket system could start and operate on its own power and operate over a wide range of conditions. The total series nominal full power operating time was 30 min.(Ref.2)
Jan. 1967	NRX-A6	Operated at full power (1100-1200 Mw) for 60 min., 4.5 x 10^6 Mw-sec.(Ref.2)
June 1968	PHOEBUS-2A	Nominal full power 4200 Mw. Several short runs, 15 min. run.
Nov.-Dec. 1968	PEWEE-I	Scaled down KIWI type reactor for fuel development, 500 Mw, 20 min. run time. Exterior surface of all elements coated.
Feb.-Sept. 1969	XE PRIME	First test of a NERVA reactor in a flight type configuration. Reactor in down-firing position with components clustered in a semi-flight configuration.

*A breadboard engine contains the principal components of a flight-test system with the components arranged for test convenience rather than flight.

II. REACTOR DESCRIPTION AND EFFLUENT DEFINITION

A. Reactor

The Kiwi/NERVA reactor design uses highly enriched uranium in a graphite-base core cooled by hydrogen (the propellant of the rocket engine) which is expelled to the atmosphere. The reactor operates at high power densities (Megawatts per litre) with core and coolant exit temperatures of about 4,000°F, well above the melting point of most metals. The core structure is largely composed of graphite and metal carbides.[2] By its design, the reactor is under-moderated and consequently operates on an intermediate energy neutron spectrum.

Figure 1 is a general schematic of a conceptual design for the NERVA engine. The hydrogen coolant flowrate is roughly 90 lb/sec at 1,500 Mw. For ground testing the hydrogen is ignited as it exits the nozzle to minimize explosion hazards.

The reactor can be controlled either by the control drums in the periphery of the core or by changes in the coolant flowrate. Power is measured by neutronics measurements and by temperature, pressure, and flowrate measurements at power.

Three different cryogenic systems are used in the ground test program. Hydrogen is used as the coolant and propellant. The specific impulse of a propellant is inversely proportional to the square root of the molecular weight of the exhaust gases, making non-oxidized hydrogen the most preferable propellant. (In actual rocket operation in space the hydrogen would not be oxidized.) Nitrogen is used in various phases of reactor cooldown and for providing an inert atmosphere for some of the test areas. Helium is used to purge the coolant system of nitrogen prior to the use of hydrogen.

The pressure vessel is the only containment for the reactor. The only housing is a three-sided shed set up around the reactor during non-testing periods.

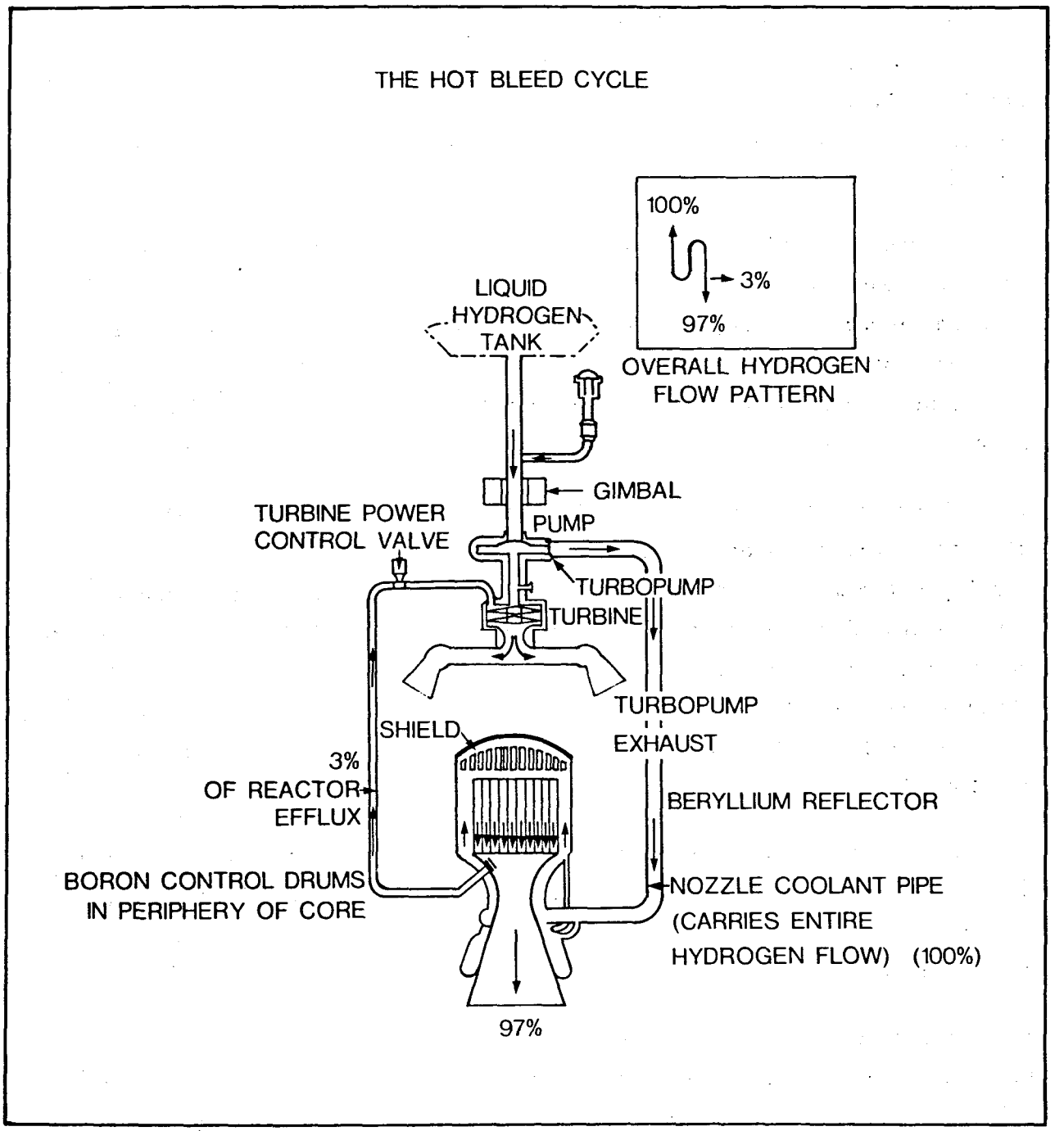

Figure 1 Conceptual Reactor Schematic[1]

The core of recent reactors, about 4 feet long and 4 feet in diameter, has been composed of clusters of fuel elements, hexagonal rods composed of UC_2 beads (containing oralloy uranium--93% enriched in ^{235}U) in a graphite matrix. The core structure design limits the core coolant flow to the coolant channels in the fuel rods; coolant does not flow between the rods or rod clusters.

High reactor operating temperatures cause fission products to migrate from the fuel beads through the graphite matrix into the coolant. To reduce fission product release, coating or cladding materials (not cladding in the sense of metallic claddings for other types of reactor fuels) are used on the beads and the elements to protect the elements and to reduce the migration of fission products from the fuel.

There have been continual changes in the design of the reactor core support structure, the means of incorporating the uranium into the fuel, and the coating materials for the fuel beads and elements. Additional changes are contemplated for the future. The changes are made to improve core integrity and thus increase the design operating power and potential run time. These changes have resulted in significant decreases in the fraction of the fission inventory released by present day reactors as compared to the early Kiwi reactors.[4,5]

The reactor engines are tested at test stands or test cells, which contain coolant storage and distribution systems and auxiliary equipment needed for testing the reactors. The reactors are, so to speak, plugged into the test stands or cells.

The initial tests were conducted at Test Cell A. When the reactor power and run time were increased, Test Cell C, with its increased coolant storage capacity, was used. Reactors were tested at Cells A and C in an "upside down" configuration, with the exhaust expelled vertically upward rather than downward. Structural support for the test vehicle was easier to construct with the engine in this position.

The XE Prime test was the first of the Engine Test Stand Experiments (ETS-1). The ETS-1 tests positioned the reactor "normally," with the gases exhausting vertically downward and being ducted out at an angle above the horizontal. The component clustering for the ETS-1 tests approached flight configuration, and the engine was operated in a partial vacuum to simulate a space environment.

Reactor engine tests are termed Experimental Plans (EP's). The first EP is normally a criticality checkout of the general neutronics of the reactor and its control systems and instrumentation. Other tests prior to the full power tests include intermediate power tests. Subsequent tests include the full power tests, operating systems tests, restarts, etc. As discussed later, the amount of effluent released is a function of the operating temperature as well as core design and total operating time. Significant effluent release is largely limited to the full power tests, the primary subject of this paper. (Radioactive effluent has been released not only during the actual tests but also during reactor cooldown after full power tests.) Coolant must be passed through the core to remove the fission product decay heat. The required cooldown period depends on the experimental plan operating power and time integral. A general rule-of-thumb for the basic reactor is one day of cooling per 10^6 Mw-sec power integral.

After the Phoebus-1B test in February 1967, LASL developed a filtration system to be placed over the reactor nozzle during reactor cooldown. Called the "FROG" (Filter Reactor Outlet Gas), this filter is part of a rail-mounted shed which can be placed around the reactor during non-testing periods. This system has not been used on the test stands.

B. Reactor Effluent

The full power operating parameters for reactors (temperature, flowrate, etc.) result in the release of a small fraction of the fission products. This fraction has varied from test to test from about 10% to less than 1% of most of the fission products (50% for ^{115}Cd).[6,7] The releases have occurred through two modes: migration of fission products from the fuel elements into

the coolant stream, and actual release of fuel fragments through erosion and corrosion of the fuel.[8,9,10] Since some of the fuel fragments have disintegrated into aerosol-sized particles, field measurements have not been able to fully distinguish between the two modes.

Fission products released by migration tend to condense or agglomerate on to atmospheric dust particles or small particulate matter released from the reactor, and on surface dust entrained by the reactor plume forming a composite gaseous and small particulate (micrometer size or less) effluent.[11,12] This composite will be called an aerosol since it acts as suspended material and essentially follows the air stream.

The core fragments are generally in the size range of tens of micrometers. (Ref. 13,14,15,16,17,18) Because of their size and density they act as particles and fallout along the effluent track. Some of the material released as UC_2 may be oxidized to UO_2, and the associated fission products may be released from the particle either by migration or as a result of oxidation, and become part of the aerosol effluent.

Two categories of effluent release are discussed, the normal case and the accident case. "Normal operation" refers to an experiment following the nominal experimental plan. For the postulated accident situations abnormally large quantities of radioactive effluent are assumed to be released. For safety evaluation purposes, two types of accidents, the loss of coolant accident and the control-drum roll-out accident, are discussed.

Reactor tests and effluent release predictions and evaluations have been performed by two organizations, LASL and WANL. Their prediction techniques are generally similar; significant differences are indicated in the following discussions:

1. <u>Effluent Release--Normal Operation</u>

   a. Aerosol Effluent

   The quantity of material released by migration depends on the fuel temperature, operating time and power (inventory), the specific fuel design, and the radioactive element.

Prediction of migration releases is based on two empirically supported assumptions: (1) the rate of loss of any fission product, dN/dt, is proportional to the amount of that fission product (N) in the portion of the element or core being considered; and (2) the migration coefficient (K) for the fission product of interest is a function of temperature (T). Based on the previous assumptions[9,10, 19]

$$dN/dt = -KN \qquad \text{II-1}$$

and

$$K = K_o \exp(-F/RT) \qquad \text{II-2}$$

WHERE:

- N - amount of fission product in the fuel.
- t - time
- K - rate constant or migration coefficient; K_o, migration coefficient at reference temperature
- F - activation energy based on laboratory data
- R - gas-constant
- T - absolute temperature of the fuel being considered
- K, K_o, and F are empirical constants that are established from data from past reactor tests and laboratory experiments.

WANL has noted that the release of some of the radionuclides can be described better by two release constants. They relate this to a "slow migration" for the coating material and a "fast migration parameter" for the graphite matrix.[10] This interpretation results in equation II-3.

$$dN/dt = -(K_1N_1 + K_2N_2) \text{ where } N = N_1 + N_2 \qquad \text{II-3}$$

The parameters for these equations vary according to the design and are empirically determined.

In estimating the releases of various fission products, the yield and decay sequence of the complete chain must be considered. For example, the ^{131}I chain may be represented as:(20,21)

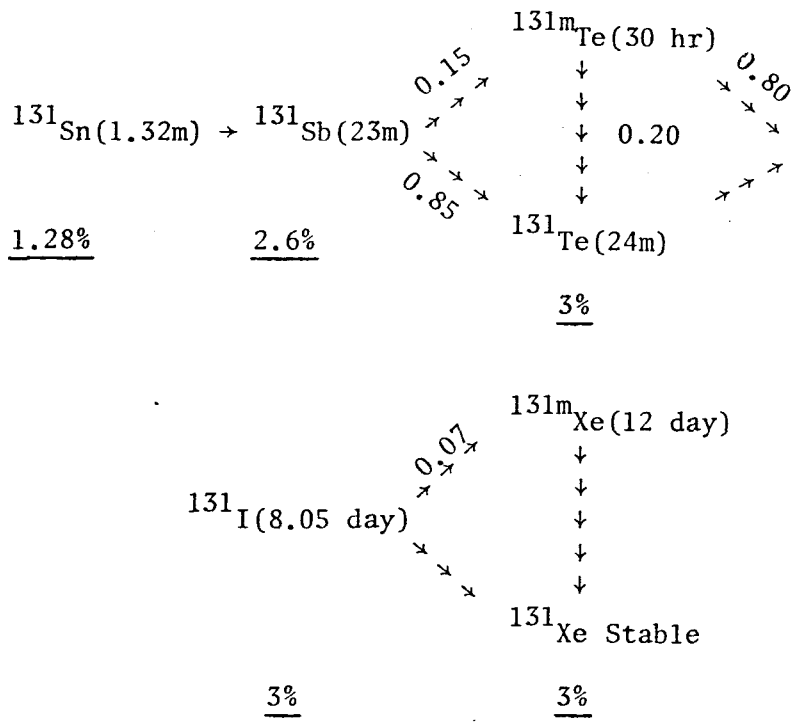

The underlined numbers indicate the fission product yield (cumulative up to the indicated point in the chain). Two things should be observed: (1) the isotope ^{131}I has a small direct yield; i.e., its total yield is derived largely from precursors; and, (2) the quantity of ^{131}I increases after the fission reaction stops because of decay of its precursors.

The migration coefficients of Sn and Sb for beaded fuels are greater than that of iodine.[4,6,7] Thus the important mechanism for release of ^{131}I from the reactor is not the migration of ^{131}I from beaded fuel, but rather the migration of Sn and Sb. This brings about two additional considerations:

1. If a reactor with beaded fuel is re-started several days after a previous test, the primary source of ^{131}I release is the Sn and Sb iodine precursors from the second test. The actual iodine release fraction is less than its precursors.

2. The release fraction has not been the same for all of the iodine isotopes because of differences in their production chains.

Figure 2 indicates release fractions predicted for various isotope chains for the Phoebus-2A reactor test.[7] The curve was determined from measurements on the Phoebus-1A. The curve was utilized for subsequent tests by estimating the release for several mass chains (based on changes in design) and then transposing the curve to fit those points.[4,7] In general the mass chains with the highest fractional releases are those of relatively low fission yield.

b. Particulate Effluent

Release of core material through corrosion and/or erosion is more difficult to describe and measure than the migration of fission products from the core. The hydrogen coolant reacts with graphite at operating temperatures to produce methane and other hydrocarbons.[22] The release mechanism has been described as chemical corrosion which in its later stages is accompanied by physical erosion of the fuel.[3,13] The release mechanism has been related to both minor breakage of fuel elements and reaction of hydrogen with the fuel as a result of defects or failure of the fuel element cladding, in some cases absence of cladding on sections of the fuel. (Ref. 4,9,22,23). The fuel element losses have been related to thermal and/or mechanical stresses.[23] The quantity of material released by corrosion has been found to increase approximately exponentially with fuel core operating time [4,10] and has been related to the number of operating cycles.[10]

The primary purpose of the cladding material is to protect the graphite core matrix material. Graphite loss has been the predominant factor in the loss of core reactivity from corrosion. It has been estimated that roughly 10 grams of graphite per element could be lost before a significant amount of uranium is lost.[10,22]

Modes of corrosion can be separated into three categories:

1. Bore corrosion--from the coolant channel. This can be further subdivided into mid-band (horizontal plane centered on the vertical axis) or hot-end (exit end of core) corrosion.

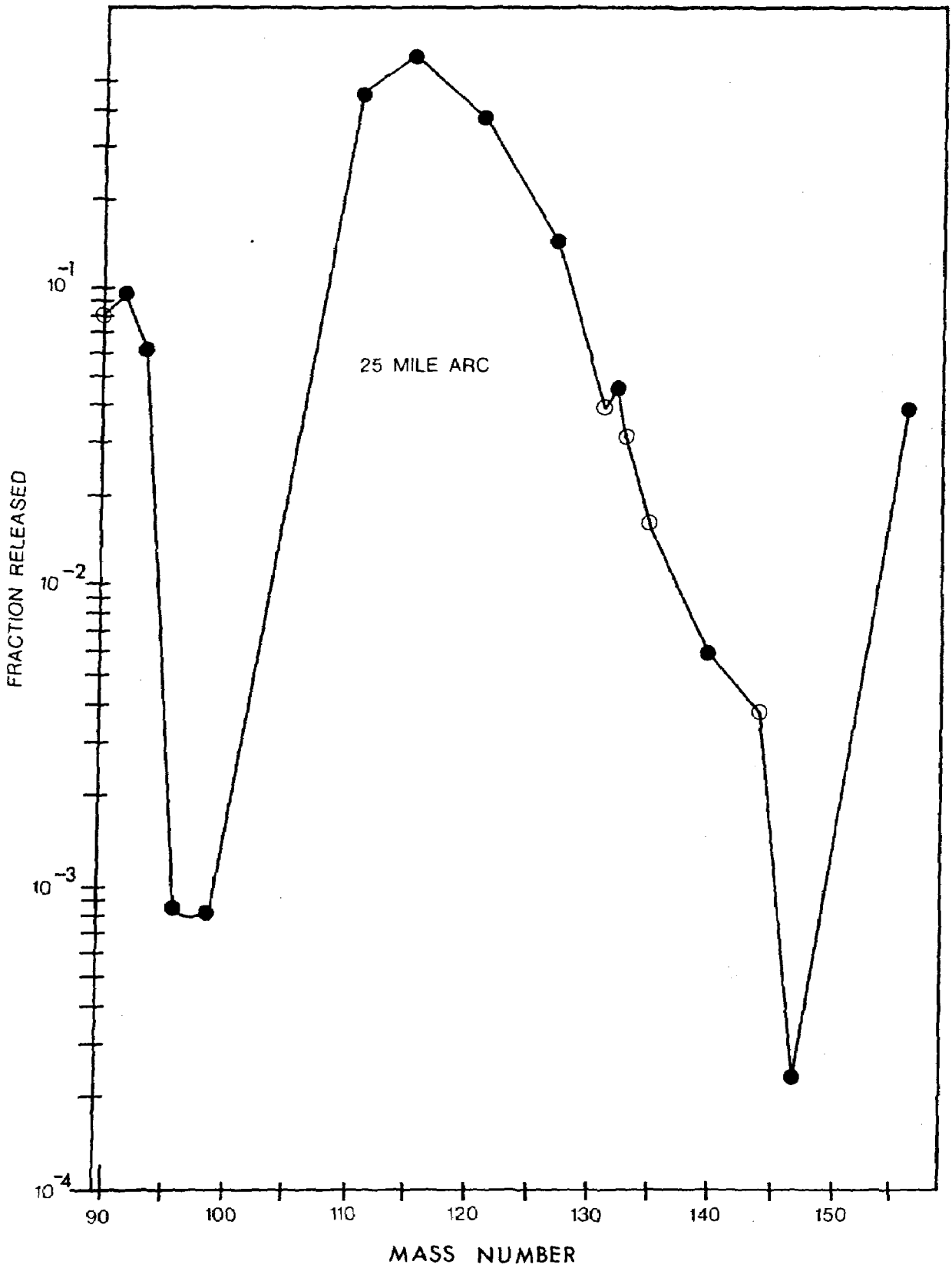

Figure 2 Fraction of Isotope Chain Assumed Released During Full Power Run (Phoebus 2A)[7]

2. External corrosion of elements (external surface, not coolant channel). The reactor design minimizes, but does not completely prevent, the flow of hydrogen around the exterior of the fuel elements.

3. Corrosion and erosion of broken fuel elements.

The relative significance and extent of these mechanisms has varied from reactor to reactor according to the design and type of fuel.

Corrosion can also create a feedback effect. Reactivity loss and possibly gain as a result of corrosion is compensated for by adjusting the control drums. Adding reactivity by withdrawing the control drums from their optimum position results in greater power peaking in the periphery of the core, thus accentuating not only corrosion, but also diffusion losses. The normal variation of fission density (fission/gram of U) with physical position in the core has been as high as a factor of 15.[10]

Bore corrosion takes place as a result of flaking and/or cracking and possibly imperfections of the bore coating. Hydrogen attacks the graphite fuel matrix through these breaks in the fuel surface protection causing either pinholes or holes in the bore surface.[4,22] If the breach in coating is small, a cavity may be produced within the matrix leaving only a pinhole at the surface. However, the cavity wall may also collapse, resulting in a hole.

Lyon[22] indicates that uranium release from the Pewee-I reactor was primarily from broken and massively corroded fuel. The type of corrosion was not identified, but it was probably extensive bore corrosion. Lyon concluded that about 170 grams of U from broken or massively corroded fuel elements was released, but that about 100 grams from exterior and pinhole corrosion was probably retained in the reactor.[22]

Quantitative projections for releases have been based on releases from past reactors, releases from laboratory tests if there has

been a significant change in fuel design, and scaling factors for variations in reactor operating parameters and fuel changes.

The following outlines the WANL prediction technique.[10]

1. Postulate reactivity loss for the proposed reactor tests (considering temperature, time, fuel channel coating, proposed number of operating cycles).

2. Estimate the uranium loss associated with the reactivity loss. This estimate is evidently based on inspection and analysis of the NRX-A5 reactor. It assumes analogous modes of fuel loss and similar axial fuel loss distribution.

3. Estimate the fission product loss associated with the uranium loss. There is a significant variation in fission product production per gram of uranium in the core because of the axial and radial variation of power density. Also, fuel may be lost prior to the end of the reactor test. For the NRX-A5 reactor, it was estimated that 1.2% of the fission product inventory was released per percent of uranium lost from the core.

From this information, the uranium release for the NRX-A6 was estimated to be 650 grams. This was three times the amount that Pan American Airways (PAA) accounted for by an integration of ground deposition.[10]

LASL estimates have been based on a similar approach where past results were extrapolated to future tests. The pertinent factors included operating temperatures, number of temperature cycles, and changes in fuel design.[22]

2. Effluent Release--Accident Condition

The parameters for evaluating accident releases for nuclear rocket engine reactors have varied with time. The changes have been largely due to availability of information and changes in reactor design.

The maximum design accident, related to uncontrolled drum roll-out, is assumed to occur without coolant flow.

The following criteria have been used to evaluate the control-drum roll-out accident:

a. LASL - For Kiwi and Pewee reactors:

   2×10^{19} fissions have been postulated to occur as a result of a drum rotation rate of 45° per second. (Ref. 3,4,13,24) The associated energy release is near the threshold of dynamic destruction, but little if any dynamic destruction has been expected.[25] The release assumptions of TID-14844[26] have been used: 1% solids, 50% halogens, and 100% of the volatile fission products, the cumulative total of which is equivalent to 15% fission product release. (Ref. 3,13,27) An excursion of 2×10^{20} fissions was estimated to be possible for the Phoebus-2A.

b. WANL - For NERVA or NRX type reactors:

   7,000 Mw-sec, which is equivalent to about 2×10^{20} fissions, has been postulated to occur as a result of a drum rotation rate of 55° per second. WANL has applied a general release assumption of 50% for all of the fission products. The release assumption is based on results from Kiwi-TNT, laboratory experiments, and predicted reactor core temperatures.[10]

The difference in the energy release assumptions appears to be due to the different rates of control drum rotation. The estimates have been based on the reactor criticality neutronic calculation computer codes of LASL and WANL, respectively. The difference in release assumptions is minor.

The loss-of-coolant accident is limiting for a reactor with a significant fission product inventory remaining from a power test. For conservatism the loss of coolant was assumed to occur at the end of the power run, the time when the reactor would have a substantial fission product inventory. An analogous accident would be a control drum roll-out (to provide the energy to melt the core) subsequent to a power test.

The following assumptions have been used to predict the consequences of such an accident:

LASL - The previously referenced TID-14844[26] assumptions. (Ref.3,13,24)

WANL - 50% of the fission products.[8,10]

Experience to date has indicated that fuel bead material should not be encountered in effluent under accident conditions. Material of this nature was not noted for the Kiwi-TNT test or the Phoebus-1A test (partial destruction of core due to loss of coolant and overheating).[3,13]

C. Source Term Measurements

1. Aerosol Effluent

Three methods have been used to document reactor releases:

Aircraft sampling

Elephant Gun sampler

Post mortem analysis of the reactor.

The results from these documentation techniques have been compared to the pre-event predictions and used to improve the estimates for future reactor tests. The first two techniques are based on:

a. Evidence that approximately 50% of the ^{115}Cd produced has been released. The fraction released was due to migration. This fraction has been fairly constant for the normal operating limits. Thus, the quantity of ^{115}Cd in a sample has been compared to the estimated total produced and from this

ratio the fraction of the total effluent sampled has been estimated. The release of ^{115}Cd is largely due to the rapid migration of its silver precursor.[4]

b. ^{99}Mo has not been released by diffusion. Thus, the quantity of fission product ^{99}Mo present in effluent has been taken to be an indication of the amount of corrosion.

The techniques of post mortem analysis have not been adaptable to quantitating the small fractions of release of most of the fission products. Also the time increment between the reactor test and analysis has been such that quantities of most of the fission products have been significantly decreased by radioactive decay. The primary objective of post mortem analysis has been to obtain reactor design information, but it has also been possible to quantitate the ^{115}Cd release by analysis of the core for ^{115m}Cd. Thus, the ^{115}Cd release fraction has been refined and used to scale the quantities of other radioisotopes to the total quantity released.

Both LASL and NERC-LV have used aircraft sampling to estimate effluent releases. The LASL technique, used on NRX/EST and subsequent tests prior to XE Prime, involved aerial sampling of the plume at numerous heights and transects within about six miles of the reactor. Particulate samples taken during the plume transects were analyzed for specific radionuclides and the quantities related to total effluent based on the ^{115}Cd results. Analysis of the samples was performed by LASL and/or WANL. The results of this technique have served as the official source term for most of the reactor tests prior to XE Prime. The LASL aircraft sampling program has been largely discontinued since 1967.

The NERC-LV aircraft sampling technique is based on sampling on a pre-fixed coordinate system to obtain an estimate of the cloud size and concentration profile within the cloud. The sampling equipment aboard the aircraft includes a mass particulate sampler and

charcoal bed (to obtain continuous samples), sequential sampler (for obtaining profile), cryogenic sampler or a "Grab Sampler" to obtain samples of gases in the cloud, electrostatic precipitator, Anderson impactor (particle size), and instruments for measuring external radiation exposure to obtain real-time position relative to the cloud. The LASL sampling has taken place at about one to five miles from the test location prior to significant depletion of the cloud due to fallout. The NERC-LV sampling is done at tens of miles from the test stand by which time depletion may have occurred. Reports have been written concerning the results for each event. Additional information concerning the sampling procedure and examples of results are given in references 11, 12, and 28.

The initial source term estimates based on radiochemistry and inspection of the core material suffered from lack of sensitivity and from inability to resolve the effluent release into components for specific experiments within a test series. Aircraft sampling improved the quantitation of effluent releases. However, variations of the effluent composition with time and difficulties in accurately locating the cloud (caused by wind shear with height and variations in wind speed and direction with time) have made accurate measurement difficult. Also, the LASL program was based on particulate sampling and thus obtained no samples of the noble gases and probably only a fraction of the sub-micron size particles.

In 1967, LASL developed a new sampling apparatus known as the Elephant Gun. The device is composed of a probe which can be extended into the effluent, directly over the nozzle, to obtain samples which can be stored in sampling tanks. Samples equivalent to several moles of hydrogen effluent may be taken at selected times throughout a reactor test. The sampling mechanism is sealed when it is removed from the effluent, thus

retaining any of the gases. The fission products are removed from the sampling tanks by acid leaching and the solution is then analyzed for appropriate radionuclides. Problems concerning sampling with the Elephant Gun relate to the concentration gradient across the plume and insuring proper and unbiased sampler operation at the effluent temperature and pressure.

Table 2 gives the pre-event predictions and post-test estimates of the ^{131}I and gross gamma releases for selected reactor tests. The data indicate a definite decrease in the fractional release from recent tests versus tests such as NRX/EST.

WANL and LASL have provided estimated source terms for such fission products as ^{89}Sr, ^{91}Y, ^{91}Sr, 95 and ^{97}Zr, ^{111}Ag, ^{115}Cd, ^{132}Te, $^{131-135}I$, ^{235}U, ^{99}Mo, and ^{144}Ce.[6,8,9] The NERC-LV reports present values for most of the isotopes indicated above (normally excluding ^{115}Cd and ^{235}U) in addition to results for the noble gases.[11,12,28]

2. Particulate Effluent

The presence of particulate matter in the effluent in the size range of tens of micrometers was observed prior to the early NRX tests.[5,29] However, there was only limited evaluation of the released material until the NRX/EST test in March of 1966.[5] Not until the Phoebus-1B reactor in February 1967 was emphasis placed on before-the-fact prediction and after-the-fact quantitation of particulate effluent releases.[14,15]

There are several ways of quantitatively estimating the amount of material lost as large particles:

a. Relate reactivity losses, as measured by relative control drum position, to the uranium loss.

b. Relate the quantity of uranium or number of particles collected by aerial sampling to the total release.

TABLE 2. ESTIMATED MIGRATION RELEASES[5]

Reactor Test	Date	Full Power Mw	Power Integral (10^6 Mw-sec)	Max. Chamber Temp. (°R)	Percent Release*			
					Pre-Event Predictions		Post-Event Estimates	
					^{131}I	Gamma	^{131}I	Gamma
NRX/EST-A4, EP-IVA	03/25/66	1200	1.1	4150	3.9	2.3	5.0	3.0
Phoebus-1B, EP-IV	02/23/67	1340	2.6	4000	4.0	N/A	1.0	0.5
NRX-A6, EP-III	12/15/67	1140	4.5	4150	2.7	2.1	0.6	0.8
Phoebus-2A, EP-IV	06/26/68	4010	4.5	4000	4.2	4.0	0.1	0.2
Phoebus-2A, EP-V	07/18/68	3430	2.5	4000	5.7	4.0	0.1	0.1
Pewee-I, EP-III	12/11/68	503	1.53	N/A	10.0	7.0	0.8	0.5

*This includes only releases due to migration (corrosion fraction subtracted from total).(5)

N/A = Not Available

c. Data from Elephant Gun: Although the Elephant Gun was originally intended only for aerosol sampling, it has been noted that the number of beads or large particles impacting on the probe can be estimated from autoradiographing the probe.[23,30] This estimate can be summed with time and integrated for the total nozzle cross-section to indicate the total release. The total release can also be estimated from the amount of uranium in the Elephant Gun samples.

d. Survey the fallout pattern to obtain the number of particles per unit area. Based on the particle size distribution and area distribution, the results can be integrated to obtain the total mass deposited.

e. Corrosion losses have also been estimated from post mortem data, but difficulties exist in distinguishing the quantity of material lost in the effluent from the quantity disturbed in reactor disassembly. This procedure does not allow losses to be related to specific tests.

In essence, a combination of the previously indicated techniques has been used. Not all of the techniques have been used for each of the tests; i.e., neither the Elephant Gun nor aerial sampling by LASL, (NERC-LV sampled) were used for the XE Prime reactor test series. The Elephant Gun has only been used at the test cells, not at the test stand. Table 3 indicates the release estimates for previous reactor tests. Both pre-test and post-test estimates are given.

TABLE 3. ESTIMATED CORROSION RELEASES[5]

Reactor Test	Date	Full Power Mw	Power Integral (10^6 Mw-sec)	Grams of Uranium	
				Pre-Event Estimate	Post-Event Estimate
Phoebus-1B, EP-IV	02/23/67	1340	2.6	500	200
NRX-A6, EP-III	12/15/67	1140	4.5	Not made	210[a]
Phoebus-2A, EP-IV	06/26/68	4010	4.53	125	60
Phoebus-2A, EP-V	07/18/68	3430	2.5	N/A	55[b]
Pewee-1, EP-III	12/11/68	503	1.53	150[c]	140[d]

[a] The reactivity loss corresponded to 650 grams of uranium. The PAA integration of the ground deposition indicated the value of 210 grams. WANL concluded that this indicated that only 0.3 of the uranium loss was related to particulate effluent.(10)

[b] Van Vleck[16] indicates 450 grams for Phoebus-1B, and 70 grams for Phoebus-2A, EP-IV.

[c] SNPO Operations Plan for Pewee-I.

[d] 170 grams,[22] 139 grams,[30] and 100 grams.[16]

III. EFFLUENT TRANSPORT AND DISTRIBUTION

A. Effluent Transport

1. Test Location and Site Geography

The NRDS test cells and stand are located southwest of the Nevada Test Site, approximately 80 miles northwest of Las Vegas, Nevada. Test Range Complex boundaries are approximately 10 miles to the south and west of the test cells and over 80 miles to the north. Lathrop Wells, Nevada, about 15 miles SSW of the test cell, population less than 100, is the nearest community. Beatty, Nevada, population about 500, lies about 30 miles to the west. The terrain surrounding the test cells is largely mountainous except for a long, flat valley extending for about 40 miles to the southwest.

The Nevada Test Site and the Nuclear Rocket Development Station encompass an approximately rectangular area 50 miles north to south and 30 miles east to west within a region of generally north-to-south trending ridges and valleys. The Nellis Air Force Range provides an additional buffer zone. The terrain is extremely irregular, with elevations ranging from a high of 7700 feet on Rainier Mesa in the north to lows of 3100 feet in Frenchman Flat in the southeast and 2700 feet in the extreme southwest corner on the edge of the Amargosa Desert. The test locations are at about 3800 feet MSL. There is a general but frequently interrupted downward slope from north to south.

The areas adjoining NRDS are sparsely populated and the desert environment limits agriculture. Locations and populations of communities near NTS and NRDS are shown on Figure 3. The Figures in Appendix A give a more detailed description of populated areas and the distribution of milk cows in the off-site area.

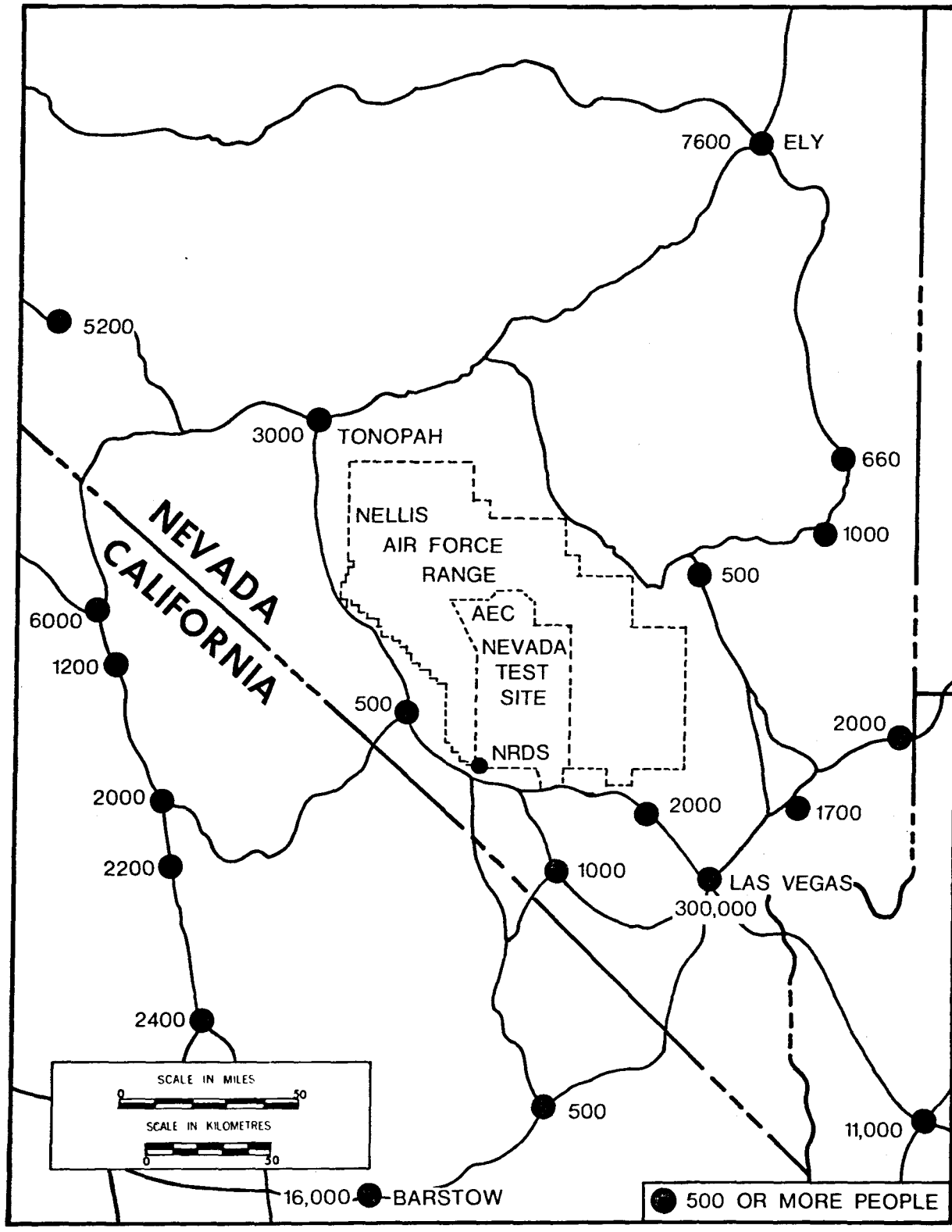

Figure 3 Population Centers Near NRDS

2. Factors Affecting Transport and Deposition

Quiring[31] has summarized the climatological data for the NTS and the NRDS. Van Vleck[32] presented a summary of diffusion parameters related to the NRDS testing program. Observations of meteorological variables have been recorded in certain locations at the NTS and NRDS since 1956, when the U. S. Weather Bureau began its observation program. Upper-air soundings have been made at the Yucca weather station since October 1956. Since that time more than 100 sites have been instrumented for various periods to measure wind, temperature, relative humidity, precipitation, or combinations of these parameters. Observations of winds aloft have been generally made at intervals of five or six hours, except during test support, when the interval has been shortened to one hour and occasionally to 15 minutes. Around-the-clock surface observations were started at the Yucca station in December 1961 and have continued with a few minor interruptions since that time. In addition to the continuous record at the Yucca station, observations of the winds aloft are made at various points around the NTS and NRDS for specific operations.

What is generally referred to as "good weather" is usually experienced at the NTS. Cloudy days are rare in summer and winter, and precipitation is even more rare. During late winter and spring, severe winds sometimes create dust storms. Operations can usually be scheduled months in advance with delays for weather conditions resulting only from undesirable wind directions. Fultyn[33] reported atmospheric temperature profiles taken very near to test times for ten reactor tests. All profiles were nearly equal to the dry adiabatic lapse rate through much of the atmospheric layer containing the plumes.

The Air Resources Laboratory, Las Vegas (ARL-LV), National Oceanic and Atmospheric Administration, Department of Commerce, is responsible for meteorological support (measurements and data evaluation) and effluent radiation dose predictions.

3. Plume Rise

The coolant gas in most tests has been expelled vertically upward (XE Prime is an exception) at speeds of about Mach 3 and discharge temperatures of about 4,000°F. The total thermal energy of the plume has been about four times as great as the nuclear energy of the reactor, because of the chemical energy generated in burning the hydrogen. The total thermal energy release rate for the Phoebus-1B, EP-IV plume while operating at a power of 1,500 megawatts was about 1.5×10^9 calories/second, of which about 3.6×10^8 calories/second were contributed by the nuclear energy of the reactor. Vertical momentum of the jet is believed to contribute negligibly to the height of rise of the plume; the controlling factor is thought to be the thermal energy of the plume.[34,35] For purposes of comparison, Briggs[34] indicates that thermal energy release rates for stack gases from the largest commercial power plants are on the order of 10^7 calories/second.

The effective plume rise has been important from several standpoints. The higher the plume rise, the lower the maximum ground level concentration will be and the further out from the point of release it will occur. Thus, underestimation of plume rise leads to conservative dose predictions. If the atmospheric wind velocity varies both in speed and direction with altitude, the plume rise determines the winds that provide the effective transport medium. Under atmospheric conditions with a large amount of shear, an incorrect estimate of the plume rise can result in gross errors in the predicted trajectory and transport speed. Estimates of average wind speeds and plume heights from several tests are given in Table 4.[36] The average altitude for the peak concentration with hydrogen coolant flow rates of about one hundred pounds per second has been about 10,000 feet MSL or above.

A variety of techniques for estimating plume rise have been proposed and used. Briggs[34] critically reviewed many of these models and

TABLE 4. EFFLUENT PARAMETERS

Reactor Test	Average Hydrogen Flow at Full Power(5) (lbs/sec)	Power Integral(5) (10^6 Mw-sec)	Wind Velocity(36)[a] (m/sec)	Effective Plume Height(36) (meters)
Kiwi-B4D, EP-IV	69	0.1	10.8	1000
Kiwi-B4E, EP-V	68	0.5	8.2	850
Kiwi-B4E, EP-VI	70	0.2	4.1	2050
NRX-A2, EP-IV	75	0.3	6.7	1200
NRX-A3, EP-IV	74	0.3	4.1	900
NRX-A3, EP-V	72	0.8	3.6	1350
Phoebus-1A, EP-IV	69	0.7	4.1	1500
NRX-A4, EP-IV	78	1.0	5.1	1500
NRX-A4, EP-IVA	80	1.1	4.6	2250
NRX-A5, EP-III	72	1.2	2.6	1350
NRX-A5, EP-IV	71	1.0	2.1	1800
Phoebus-1B, EP-IV	94	2.6	3.6	1650
NRX-A6, EP-III	72	4.5	12.4	725
Phoebus-2A, EP-IV	261	4.5	4.1	3475
Phoebus-2A, EP-V	244	2.5	5.1	2550
Pewee-1, EP-III	42	1.5	4.1	1200
Kiwi -TNT	0	0.009		

[a] Mean layer wind speed within the transport layer.

concluded that transitional plume rise could best be described by the "2/3 law":

$$h(x) = 1.6\ F^{1/3}U^{-1}x^{2/3} \qquad \text{III-1}$$

Where

$h(x)$ = plume rise or height of the cloud above the terrain as a function of downwind distance (feet).

F = flux of buoyancy force from stack, divided by the mean atmospheric density - $4.3 \times 10^{-3} Q_H$
Q_H = cal/sec and $F = ft^4/sec^3$

U = mean wind speed (ft/sec)

x = distance downwind from the point of release (in feet)

1.6 = empirical constant chosen by fit of data.

The plume rise is not a single value (equation III-1) but rather is a function of the distance downwind.* Measurements of plume rise should be associated with the distance from the test point at which the measurements were made.

In the past, plume rise predictions for NRDS tests have been based on a combination of plume rise equations (Briggs' and others), information from past reactor tests, and atmospheric lapse rate measurements. The occasional existence of a subsidence inversion at 8,000 to 10,000 feet MSL and the uncertainties of predicting penetration of the layer by the plume present additional difficulties in making accurate predictions.

4. Aerosol Effluent Transport

During the course of nuclear rocket testing, radioactive gases and small particulates that behave aerodynamically essentially like gases

*Equation III-1 becomes indeterminate for zero wind speed, and is thus inappropriate for such conditions.

have been released into the atmosphere. Initial concentrations of these materials are diluted by atmospheric turbulence as they are transported downwind. For each reactor test, the potential for downwind doses must be assessed based on the expected exposure to concentrations of ionizing radiation. Predictions of effluent release, transport, and human interaction have been presented to a review panel prior to each reactor test.

Radiation exposure levels downwind can be estimated by knowing the nature of the contaminating source and the parameters of the atmosphere that determine the dilution of the contaminant cloud as it moves away from the reactor. The initial properties of the source that need to be determined are: (1) the source strength and cloud composition, usually expressed in curies of activity; (2) the duration of the release; (3) the initial geometry of the source[i.e., whether it is a vertical line source, an elevated volume source, or an elevated point source] and (4) the available energy, both kinetic and thermal, for producing plume rise. The source strength and the duration of the run have been estimated by the laboratory conducting the test. The initial geometry of the source is difficult to determine because the cloud is invisible, but an elevated point source has been assumed because of the nature of the rising plume.

Dilution of atmospheric contaminants is a function of atmospheric turbulence related in part to seasonal and diurnal effects (e.g., solar heating), the influence of large scale weather regimes, and the ground surface roughness. All of these have superimposed effects that result in a wide spectrum of turbulent eddies which are quite random in their formation, individual behavior, and description. It is the random nature of turbulent eddies that makes statistical techniques essential in any practical dilution equation.

The dilution equations that have been used at the NRDS are special forms of the Gaussian distribution formulation adapted by Sutton and Pasquill and Gifford.[35,37,38,39] Since the first reactor test at NRDS, the Sutton diffusion equation has been used as the basic dilution model by ARL to predict air concentrations of gaseous and fine particulate matter released during full power tests.

Sutton's diffusion equation integrated with respect to time for a continuous elevated point source with anisotropic eddy diffusion downstream can be written as follows:

$$X_{(x)} = \frac{2Q_R}{\pi U C_y C_z x^{2-n}} \exp - \frac{h^2}{C_z^{\,2} x^{2-n}} \qquad \text{III-2}$$

Where (any compatable set of units)

$X(x)$ = Air concentration (Ci-sec/m^3) as a function of distance downwind

Q_R = Source strength (Ci)

U = Mean wind speed (m/sec)

C_y = Lateral diffusion coefficient ($\text{meters}^{n/2}$)

C_z = Vertical diffusion coefficient ($\text{meters}^{n/2}$)

x = Downwind distance (meters)

h = Effective stack height (meters) at a selected downwind distance; e.g., 1 mile.

n = Stability parameter (dimensionless)

This equation yields ground level values of the air concentration with the x-axis along the centerline. If isotropic eddy diffusion is assumed then $C_y = C_z = C$, and the equation becomes:

$$X(x) = \frac{2Q_R}{\pi U C^2 x^{2-n}} \exp - \frac{h^2}{C^2 x^{2-n}} \qquad \text{III-3}$$

The source strength, Q_R, has been estimated by the laboratory conducting the test. The mean wind speed, U, has been determined from the predicted wind structure of the atmosphere. C^2 and n have been assumed to be 0.10 (m^n) and 0.25 (dimensionless), respectively, for normal daytime cases. For normal reactor runs, the effective stack height, h, has usually been estimated to be between 1,000 and 1,500 meters above the ground depending on the atmospheric temperature profile (see Table 4).

Equation III-3 is based on several assumptions:

1. The cloud diffuses over a flat homogeneous surface which acts as a perfect reflector to the effluent.

2. The cloud is formed of gases or particles which do not fall out.

3. The meteorological situation is steady state, i.e., there are no variations in the various parameters in the diffusion equation in space or time.

4. The diffusion is isotropic.

5. The release can be described as an elevated point source.

None of these assumptions is strictly valid for reactor tests at the NRDS. The steady state assumption has been perhaps the most serious disparity as far as NRDS operations are concerned. It has been observed that the wind speed and direction both change, often quite drastically, in both space and time. Effluent clouds from reactor tests quickly mix through several thousand feet of atmosphere and, through this depth, there is often a considerable amount of wind shear. Wind shear is not quantitatively taken into account in the diffusion equation although it may be compensated for in the choice of eddy diffusion parameters. The effect of shear is to spread the cloud laterally and thus reduce the centerline concentrations.

Evaluations of past results have indicated that the effluent release cannot be described as a point source at the effective stack height. Fultyn[33] proposed describing the process as being equivalent to release of 1% of the effluent at ground level with the other 99% released at the effective stack height. ARL used this technique for a number of years, but more recently has adopted the practice of reshaping the near-in diffusion curve (out to 5-10 miles) to approximate past results.[35,39] Both of these techniques are methods of taking into account the fact that part of the plume "peels off" as it ascends; i.e., the entire effluent does not rise to the same altitude.

Figure 4 presents examples of pre-event dose predictions for the normal run accident dose estimates and for one of the XE Prime tests. Meteorological and trajectory information were also presented to the safety panel prior to tests. Dose prediction models are discussed in Section III.

Although the Sutton equation has been the basis for the dilution prediction model used by ARL, a generalized Gaussian equation with Pasquill/Gifford values for the diffusion parameters has proven valuable under unusual stability conditions. Gifford[35,37] gives values for the diffusion parameters as a function of the distance downwind for various atmospheric stability conditions.

Numerous attempts have been made to develop diffusion models to improve effluent prediction capabilities for NRDS operations. Several of these models were reviewed by Wilson in 1968.[38] Wilson concluded that, from the standpoint of availability of meteorological parameters and ease of calculation, the previously described Sutton model was preferable. Models reviewed by Wilson included:

1. Stigall and Calley[35,40] presented an empirical model based on effluent data for tests between May 1964

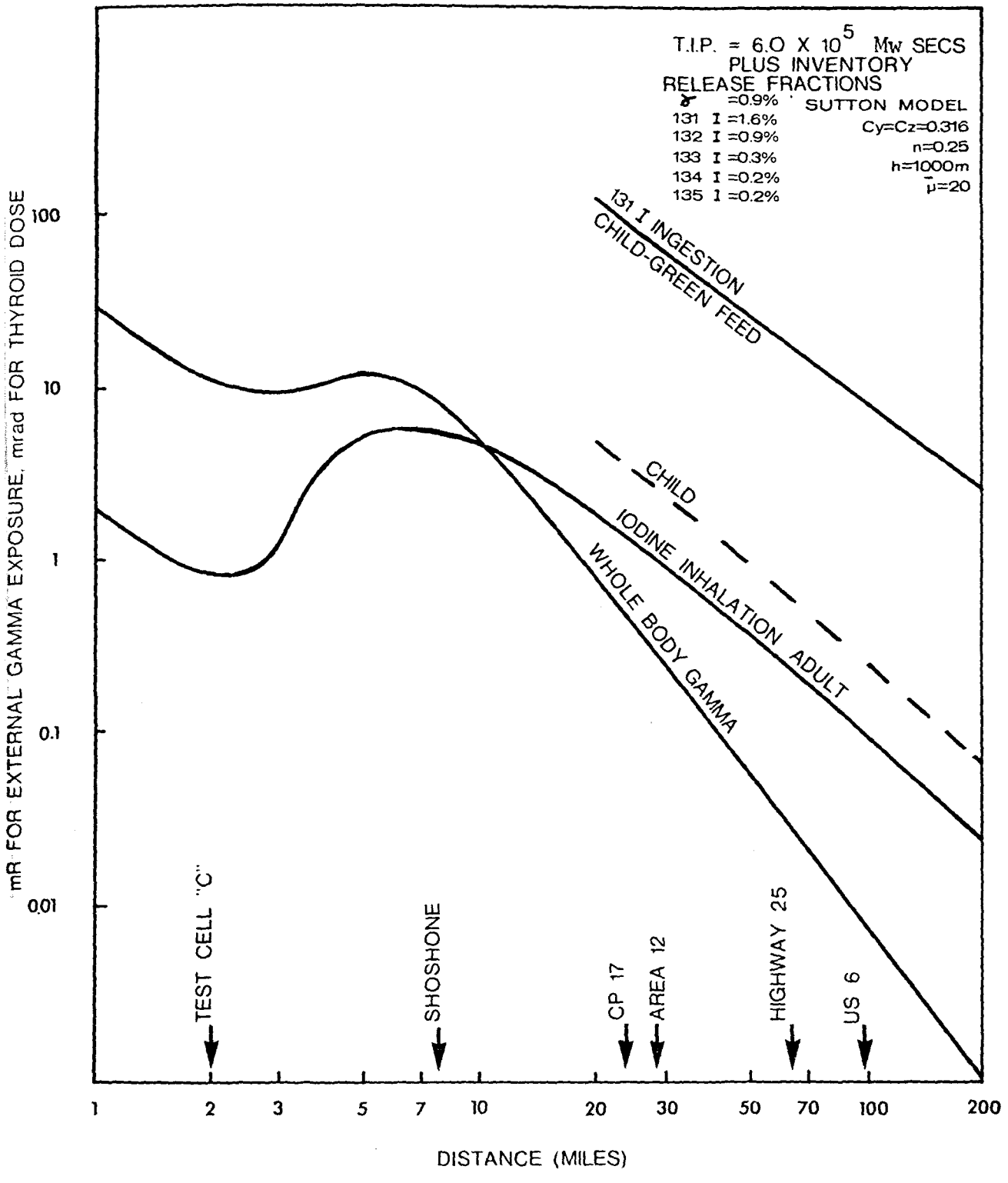

BRIEF 0900 PDT
VALID 1100PDT 8/28/69
(ARL-LV)

Figure 4 XE Prime, EP-IXA, Normal Run Centerline Dose Estimates (from ARL-LV)

and 1967. They determined empirical parameters analogous to the Gaussian model.

2. Fultyn[7,13,33] developed an empirical model for predicting downwind concentrations and doses from tests at NRDS. Results from past tests were normalized to yield an "average" diffusion curve of relative concentration as a function of distance which could be scaled to future tests. The dilution factor at a particular distance was assumed to be a log normally distributed statistical variable. The model not only predicts the geometric mean concentration at a particular point, but also yields an estimate of probable deviations from the mean. Predictions using this model were presented in several of LASL Safety Analysis Reports[7,13] although as of 1970, LASL adopted the Sutton approach for the sake of standardizing prediction techniques within the NRDS program.

5. Particulate Effluent Transport

Experience to date indicates that large particles have been encountered only as a result of operating a beaded fuel reactor in a normal-run, full-power mode for several minutes. Particles were not encountered as a result of the Kiwi-TNT Test (a planned reactivity insertion experiment of a modified reactor that resulted in violent disruptive disassembly of the reactor) or as a result of the Phoebus-1A incident (loss-of-coolant due to depletion of primary coolant supply--destructive overheating of the core with subsequent ejection of 5% of the fuel material from the nozzle). It has been considered appropriate, therefore, to estimate the probability of particles interacting with man only for the full-power normal-run tests and not for the accident case.

Henderson[16] reviewed several proposed particle prediction schemes contained in the literature. These include diffusion models such as

those used to predict exposures expected from gaseous or aerosol-type effluent; e.g., Sutton, Pasquill, Gifford[37] as well as the scaling model of Cluff and Palmer.[41] Several of these models have received limited use for NRDS evaluations, but none has been used as extensively as the Cluff-Palmer scaling equation.

The Cluff-Palmer equation uses data from one experiment to predict environmental concentrations expected from another event, taking into account differences in wind parameters and source terms. For prediction of ground deposition of particles, the appropriate form of the equation is

$$N'(x') = N(x) \left[\frac{\alpha}{\alpha'} \frac{Q'}{Q} \left(\frac{h}{h'}\right)^2 \left(\frac{u}{u'}\right)^2 \right] \qquad \text{III-4(a)}$$

and

$$x' = x \frac{u'}{u} \frac{h'}{h} \qquad \text{III-4(b)}$$

where

$N(x)$ = number of particles per unit ground surface area as a function of the distance x, downwind;

x = the distance downwind;

α = the total wind direction shear in the fallout hodograph;

Q = the amount of the reactor core released as particulate, generally stated in terms of mass of uranium;

h = the height of the plume top above the ground; and

$\bar{u}$ = the mean wind speed of the atmospheric layer containing the plume.

In each case, the primed symbol refers to a variable for the event for which deposition is to be predicted, and the unprimed symbols refer to data from past experiments. Techniques for the use of the Cluff-Palmer equation are more fully described by Hughes,[42] although Hughes' discussion is related to estimates of external gamma exposure expected

from nuclear explosive cratering applications. Fultyn[13] observed that the predictions of the Cluff-Palmer model depend strongly on the particular reference event used for scaling. The meteorological data required to use this model for prediction are routinely recorded by ARL. Some input parameters required by other models are not well-documented, such as atmospheric turbulence parameters, initial physical dimensions of the plume, and the distribution of particles along the vertical extent of the cloud or plume..

The particle concentration N(x) used in the Cluff-Palmer model to predict N'(x') may be taken from a set of results from a single test, from the mean of all tests, or some other composite of past experience.

Figure 5 presents the pre-event prediction for one of the XE Prime tests as an example of results from this technique.

Altomare and Coleman[43] developed another model for prediction of particle deposition on the basis of Van de Hoven's tilted plume formulation.[44] This formulation is based on the assumption that particles diffuse crosswind and vertically according to Sutton's equation and simultaneously settle with a constant fall velocity. For the case of an elevated plume such as the reactor effluent, the effect is to tilt the plume downward. This can be expressed by replacing the constant height of the plume centerline in the Sutton equation with a variable expression. Altomare and Coleman[43] adapted the modified Van der Hoven formulation for a computer model, DIFOUT, to predict particle deposition for reactor plumes. This technique approximates the distributed volume of the plume as a series of stacked cylinders, each containing several size ranges of particles with different fall velocities. The program accounts for the different volumes and size ranges to predict diffusion and deposition downwind. This model received some use in evaluating the Phoebus-1B EP-IV data and providing preliminary predictions for the NRX-A6 tests. Because of difficulties in adapting it to computers used by NRDS and a lack of the necessary meteorological parameters, the model has not received extensive use.

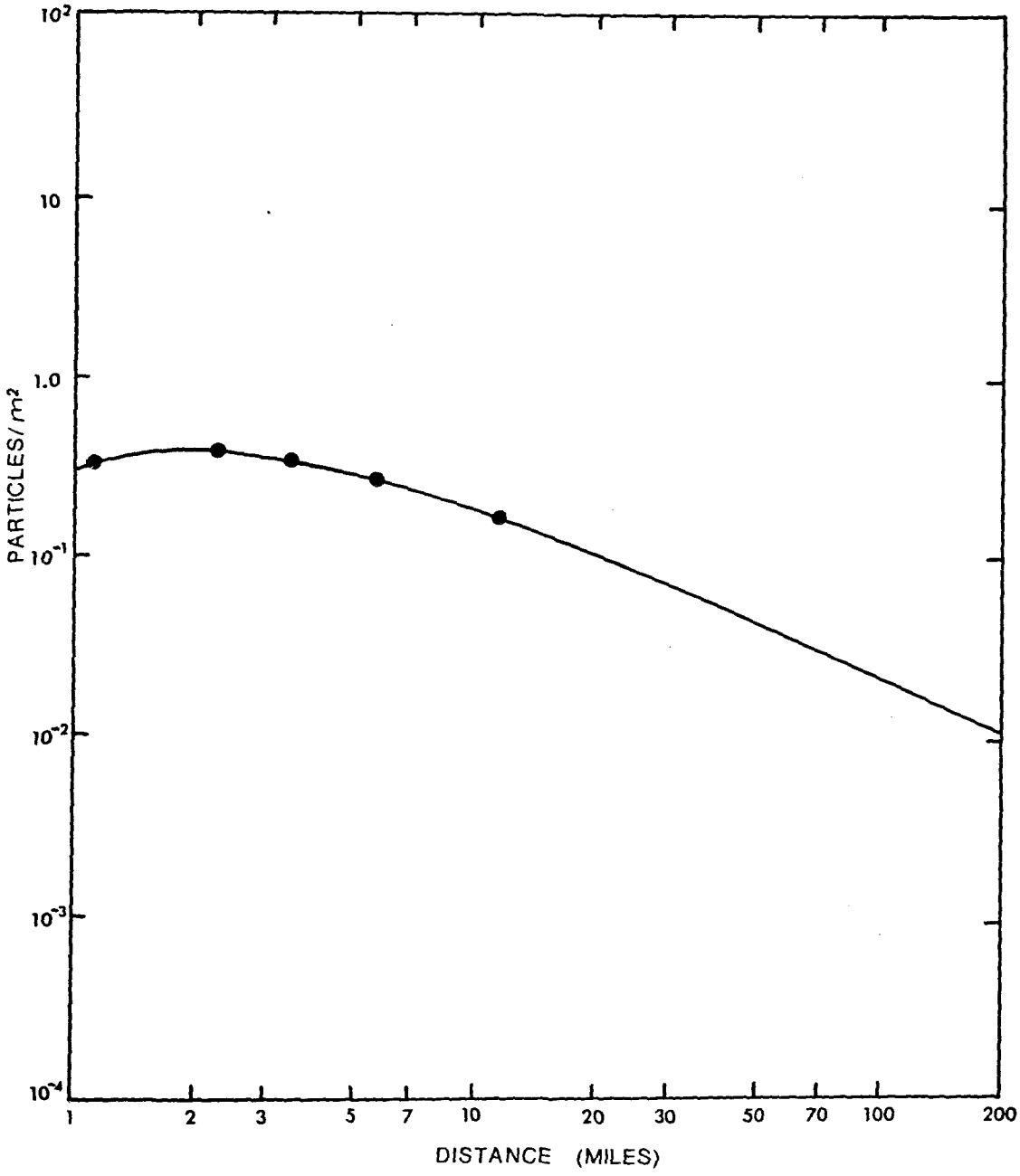

BRIEF 0900 PDT
VALID 1100 PDT 8/28/69
(ARL-LV)

Figure 5 XE Prime, EP-IXA, Particle Prediction (from ARL-LV)

B. Effluent Distribution

This section briefly indicates the geographic distribution of the effluent. The effluent program and environmental concentrations are described in Section IV.

NRDS effluent releases have taken place over a period of minutes to hours. The actual power tests, fifteen minutes to one hour in duration, are responsible for the most important effluent releases, but reactor cooldown has also produced effluent releases. The Filter Reactor Outlet Gas (FROG) was installed on up-firing reactors subsequent to the Phoebus-1B to eliminate cooldown releases, though it was not used for the down-firing XE Prime test.

Effluent from a given test can be distributed in several directions, as illustrated in Figure 6. Several factors contribute to such widespread distributions. Changes in wind direction, in addition to differences due to wind shear with height, can occur during the period of effluent release. The plume rise associated with reactor cooldown is usually less than that of effluent from power tests, and the wind velocities at these altitudes may be different. Also, as discussed earlier, a portion of the power test plume "peels off" as the plume ascends, and wind shear can act on this portion.[33,39] The samples containing effluent, Figure 6, north of the test site were primarily a result of effluent from the power test; whereas those to the south were primarily a result of effluent from reactor cooldown which was transported by the low-level valley flow (drainage) winds during the evening following the test.[45]

The prevailing winds at NRDS cause most of the effluent trajectories to be either to the northeast or southwest. At distances of a hundred to several hundred miles, these trajectories tend to veer easterly or westerly, respectively.

Particulate effluent (relative values of particles per square meter) has been detected out to about 80 miles,[14] ground level aerosol effluent to

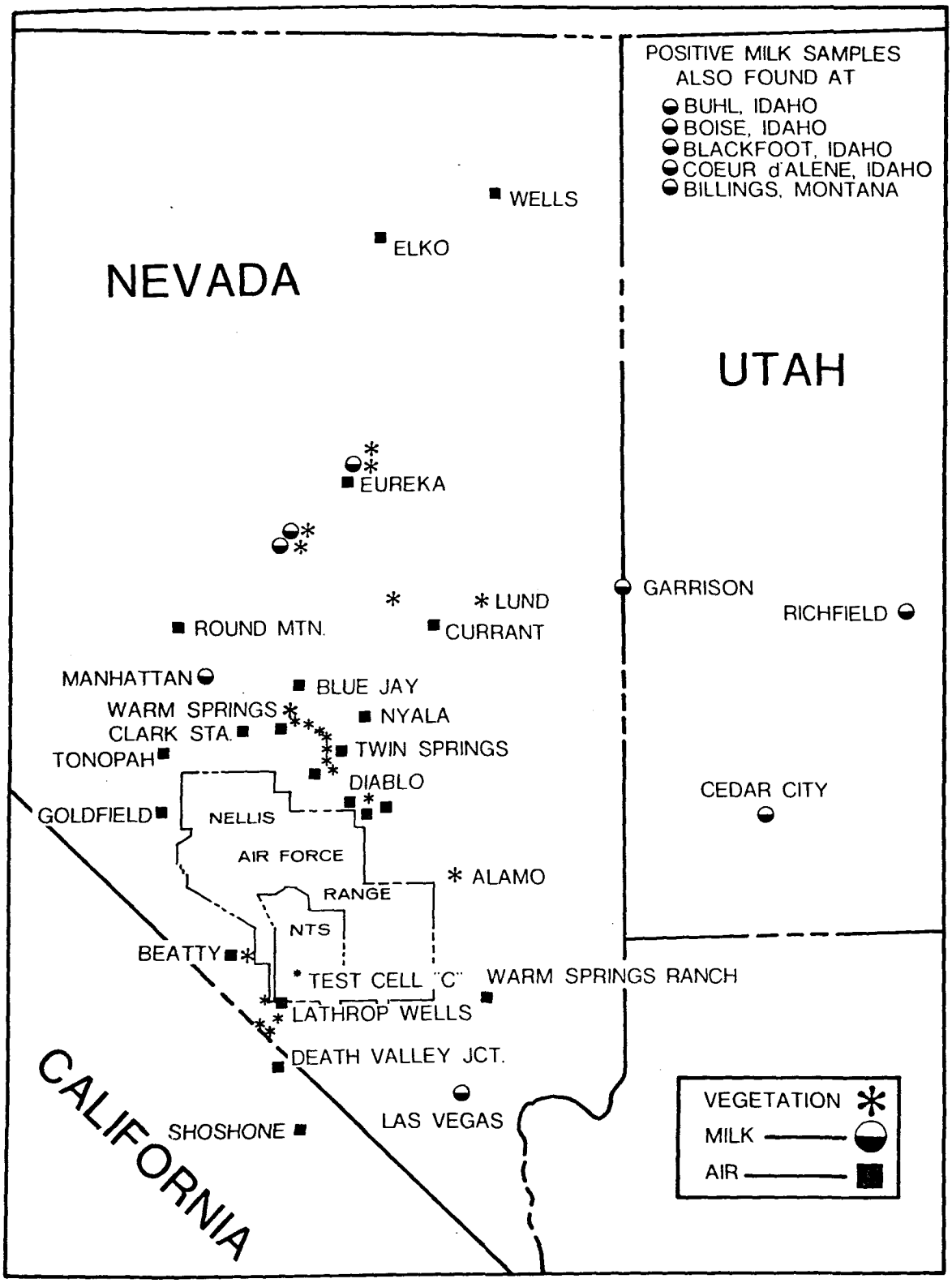

Figure 6 Locations Where Fresh Fission Products were Detected (Phoebus-1B, EPIV)

hundreds of miles (doses of mrads or less normally.)[45,46,47] The effluent cloud has been tracked to several thousand miles by aircraft utilizing sensitive sampling and monitoring instruments. The effluent transport altitude has ranged from the ground to better than 3 km above the ground.

IV. DOSE MODELS

Several models have been used to predict doses prior to reactor tests and to calculate postulated doses from surveillance results after tests. The models have included transport models for estimation of environmental concentrations, and factors and techniques for converting these concentrations to potential doses to man.

Figure 7 shows the major steps involved in each of the models. Since the arid environment of the NRDS includes very few bodies of water, the models are limited to atmospheric transport phenomena. Models for estimation or prediction of internal doses to man have been primarily concerned with radioiodine isotopes[7,8,13,47,48] and to some extent with the inhalation of large discrete particles. Evidence from past tests,[15,39,45,47,48,49,50,51,52] fission production ratios,[53] release rates,[5,7,54] factors of environmental transport,[35, 39,55] and biological uptake and dose factors[56,57,58,59] have led to the conclusion that the radioiodines have been the most important components of aerosol effluents from reactor tests. For fission product releases of the nature of past NRDS tests potential bone doses from strontium-89 and -90, as well as doses to other organs from other radionuclides, are lower than potential thyroid and/or external gamma doses. Techniques used to control the potential thyroid and external gamma dose also tend to control other potential doses.

The Aerosol or Gas-Cloud Model consists of steps, i, ii, iv, v, vi, vii, viii, ix, and x in Figure 7. The particulate model includes steps i, ii, iii, ix, and x. These two models will be treated separately; the gas-cloud model in Section A and the particulate model in Section B.

Steps i and ii in Figure 7, the estimation of source terms and transport, were discussed in Sections II and III. These steps yield environmental

Figure 7

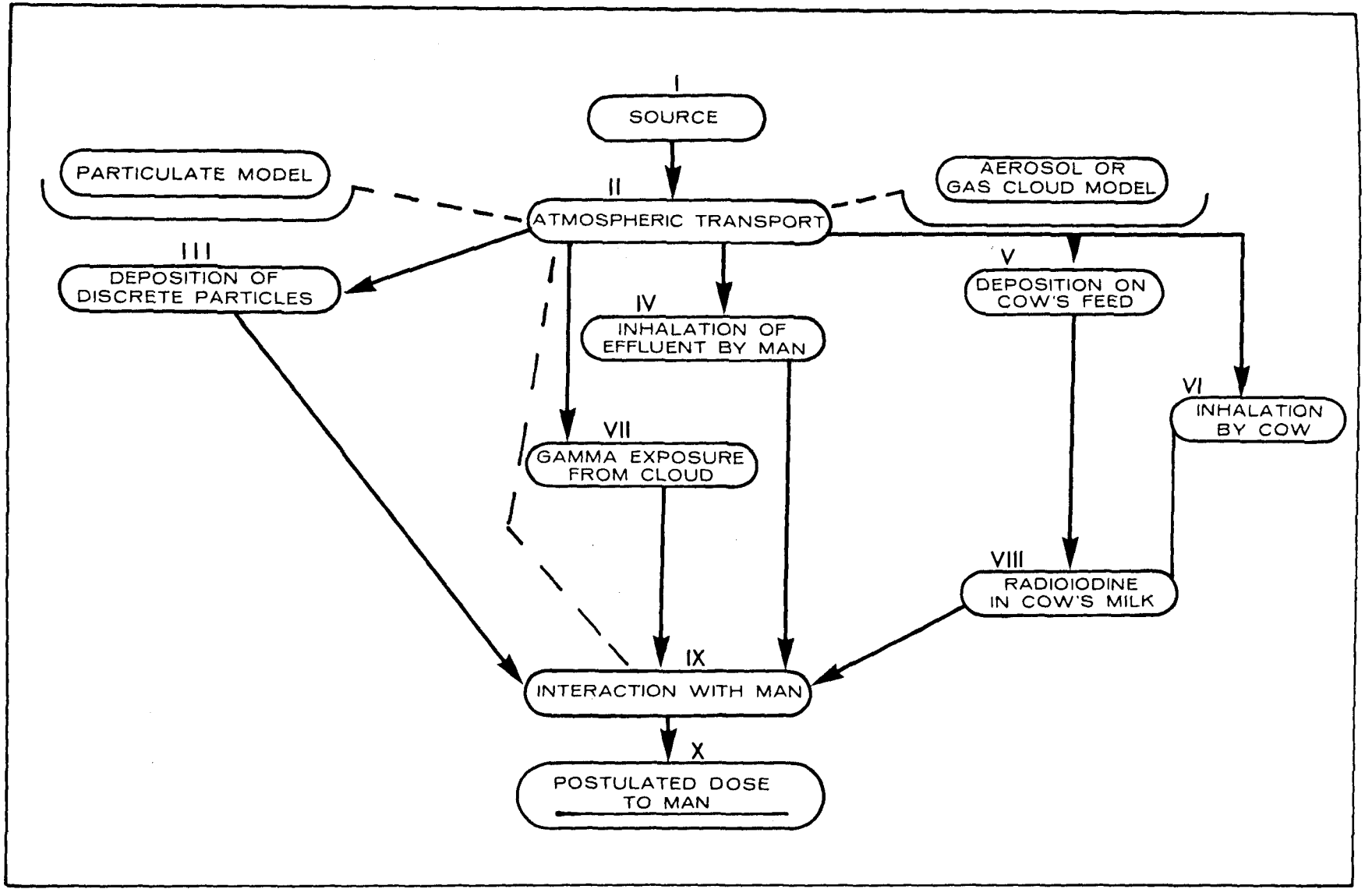

Dose Models

concentrations in Ci-sec/m^3 for the aerosol and particles/m^2 for the particulate effluent. The only difference between the normal run and accident predictions is in the source term.

A. Aerosol or Gas-Cloud Model

The basic model that has been used by ARL[35,39,52] considers three pathways of exposure:

- External gamma exposure from the radioactivity in the cloud during cloud passage (steps i, ii, vii, ix, and x in Figure 7),
- Thyroid dose via inhalation of radioiodine isotopes (steps i, ii, iv, ix, and x); and
- Thyroid dose via ingestion of radioiodine in cow's milk (i, ii, v, vi, viii, ix, and x).

Although this model does not consider external gamma exposure from fallout or ingestion of radioiodine via the vegetation pathway, these sources of exposure have been considered by agencies within the testing program.[7,60] Off-site surveillance results have indicated limited detectable external gamma exposure off-site (measurement made 3 feet above the ground) from deposition of the reactor effluent. (Ref. 40,46-49,61,62,63) Calculations by LASL[7] have indicated that the infinite exposure from residual fallout may have been similar to that from cloud passage.

Thompson[64] noted that the ^{131}I intake from non-milk food items may be significant compared to that from milk. For adults this is true, but for infants (the critical receptor for ^{131}I via ingestion), the intake path by milk is controlling (about 90% or more of total). Therefore, only the milk-food chain has been considered.

1. External Gamma Exposure

Steps i, ii, vii, ix, and x are included in the external gamma exposure model. The parameters for these steps are determined as follows:

i. The source term has been estimated to be the product of the gross fission product activity in the reactor and the gross fission product release fraction. Either the reactor inventory at the appropriate time after fission or the initial inventory decayed by the Way-Wigner relationship has been used. The fission product yield for instantaneous fission may also be used (100 Ci/Mw-sec at H+1 hour). This simplification produces a conservative estimate. Decay time has been assumed to be equal to transport time, (x/U), so the Way-Wigner decay factor may be presented as:

$$\left(\frac{x/U}{1\ \text{hr}}\right)^{-1.2}$$

ii. The diffusion coefficient, X/Q, may be calculated according to one of the variations of Sutton's equation, as outlined in Section II.

The product of steps i and ii yields

(release fraction) (Power integral, Mw-sec) (100 Ci/Mw-sec) $\left(\frac{x/U(\text{hr})}{1\ \text{hr}}\right)^{-1.2} \left(\frac{X}{Q}\ \frac{\text{sec}}{\text{m}^3}\right)$

vii. An infinite semispherical cloud model has been used to predict external gamma dose.(ref.35,51). The model includes the following assumptions:

a. The effluent cloud has been assumed to have dimensions large enough and concentrations uniform enough to approximate the dose to an individual on the surface from a cloud of uniform concentration and infinite dimensions. (dimensions large compared to the range of gamma photons). Several references outline techniques which might be used to consider finite clouds and/or the dose from a cloud passing aloft.(ref.37,65,66).

b. Since the receptor is at ground level, the dose has been assumed to be half that from a spherical infinite cloud. (ref.37,59).

c. It has been assumed that the individual does not perturb the gamma flux, so that the dose to the individual is the same as that to a similar volume of air except for differences in electron densities between tissue and air. (ref.37,59).

Imai and Iijima[65] note that the maximum external gamma dose does not occur at the point of maximum ground level air concentration. The distance at which the maximum ground-level gamma dose occurs is related to the effective stack height or plume rise, as is the distance of maximum air concentration. However, the maximum gamma dose occurs at a point nearer the release point than the point of maximum air concentration because of the contribution from the cloud aloft. Thus, although the homogeneous semi-spherical cloud model is generally conservative, it tends to underestimate doses at distances less than that of the maximum air concentration.[65]

The ARL model has compensated for this by shaping the dose curve, to match near-in results from previous tests.[35,38,39] Step vii yields the following conversion factor, when X is the integrated air concentration of gross fission products:

$$X(\text{Ci-sec/m}^3) \times \frac{3.7 \times 10^{10}\ \text{d/sec}}{\text{Ci}} \times \frac{0.7\ \text{MeV}^*}{\text{d}} \times \frac{\text{ion pair}}{34 \times 10^{-6}\text{MeV}}$$

$$\times \frac{\text{esu}}{2.08 \times 10^9\ \text{ion pairs}} \times \frac{\text{m}^3}{10^6\ \text{cm}^3} \times \frac{97\ \text{ergs in tissue}}{\text{R-g}} \times \frac{1\text{R - cm}^3}{\text{esu}}$$

$$\times \frac{\text{rad-g}}{100\ \text{erg}} \times 0.5\ \text{(for the semispherical cloud)} = \frac{0.18\ \text{rad}}{\text{Ci-sec/m}^3}$$

*An average photon disintegration energy for fresh fission products of 0.7 MeV (ref.67,68) has been used. (ref.35,51).

It is emphasized that the conversion factor that has been used in the ARL-LV model, 0.18 rad per Ci-sec/m^3, is appropriate only for predicting ground-level gamma doses from a fission-product cloud for which the average gamma photon energy is 0.7 MeV. It is not possible to use this factor to estimate actual gamma exposures from measured air concentrations. Several factors contribute to the difficulty in relating measured air concentrations to measured gamma exposures. A significant part of the gamma exposure may be caused by shine from the cloud aloft and is therefore unrelated to ground-level air concentrations.[35,65] Clouds are generally non-homogeneous; concentration gradients are likely to exist within the cloud. Measurement of air concentrations of noble gases and short-lived gross fission products is difficult because air samplers that have been used in the NRDS surveillance program have not collected the noble gases and because many of the short-lived nuclides have decayed prior to the sample analysis (the NERC-LV aircraft program includes analysis of noble gases).

2. Other Approaches to External Gamma Exposure Predictions

Fultyn[33] developed a probabilistic model for estimating not only the mean external gamma dose as a function of distance but also the statistical deviation from the mean. Fultyn's model assumed that the gamma dose at a given distance was a lognormally distributed statistical variable. Fultyn described atmospheric diffusion with an empirical curve of normalized concentrations versus distance by normalizing ^{133}I air concentrations observed during ten reactor runs (1964-1966). A lognormal distribution was fit to the data for each distance and a curve relating concentration to distance was then fit to the means of these distributions.

Fultyn used a conversion factor (integrated gross beta air concentration to external gamma dose) of 2 rads per Ci-sec/m^3, roughly a factor of ten greater than the ARL conversion factor.[7,13] This empirical number related air concentrations to measured gamma exposures observed for the NRX-A4, NRX-A5, and Phoebus-1B reactor tests. Since the factor was based on measured air concentrations, the difference between it and the ARL factor may be explained in part by gamma exposure from shine and noble gases (not collected by air samplers) and by the non-homogeneous nature of the clouds. Although this model has been used in LASL reactor safety evaluation reports,[7,13] its use was discontinued in favor of adopting the ARL model for uniformity.

WANL has used a model similar to that of ARL-LV in its safety evaluation reports.[8]

Van Vleck proposed a gamma exposure conversion factor of 1.4 R per Ci-sec/m^3 for use with gross beta air sampling results.[32] This conversion factor requires the same qualifications as those discussed previously for the factor by Fultyn.

From the Fultyn and Van Vleck factors, it can be seen that a value greater than the theoretical value of 0.18 rad per Ci-sec/m^3 is necessary for conversion of actual measured air concentrations to gamma exposures. The NUS analysis of NRX-A4 data also bears this out.[69,p.20]

3. Evaluation

Stigall and Calley[40,p.21] noted in their analysis of effluent data for 1964-1966 that 84% of the gamma exposure estimates calculated from measured air concentrations were below the corresponding gamma predictions (using post-run source term and run-time meteorology). Wilson's analysis[39] and the Fultyn[7,13] and Van Vleck[32] conversion factors indicate that the discrepancy is caused not by any inherent conservatism of the model but

more by the difficulty of converting air concentrations to gamma exposures. Wilson[39] compared model predictions with measured gamma exposures and found a slight tendency to predict low (actually close to 50%-50%).

4. Thyroid Dose via Inhalation Pathway

The inhalation pathway consists of steps i, ii, iv, ix, and x of Figure 7. The following discussion outlines the calculation for these steps.(Ref.35,39,51,52).

i. The predicted source term for a specific nuclide is the product of reactor inventory[53], the release fraction (discussed in Section II) and exponential decay relations based on the radiological half-lives of the specific radionuclide and its precursors. Table 5 indicates the maximum activity of the various radioiodine isotopes per Mw-sec for a reactor operating time of 1800 seconds. The maximum for several of the isotopes does not occur until several hours after shutdown because they build up as their precursors decay. Table 5 also indicates the approximate time of occurrence for each maximum. The ARL model has assumed that this maximum activity is present at all times prior to its occurrence. Thus, it also assumes that the radioiodine isotopes and their precursors behave similarly during transport and biological uptake.*

The inventory of radioiodine produced for a given run (plus the remainder from previous tests) has been estimated from Kochendorfer.[53] Decay during transport may be accounted for by use of Reference 58 or appropriate radioactive decay relationships.

*The treatment of ^{132}Te-I has been an exception. Although the half-life of ^{132}Te was used during transport, the implications of inhaling it were not considered by the ARL model.

TABLE 5. PARAMETERS FOR RADIOIODINE(53)

Iodine Isotope	Ci/Mw-sec[a]	Time When Max. Occurs H + seconds[b]	Radiological Decay Half-Life
131	0.0200	63,000	8.05 days
132	0.115	0	3.24 days[c]
133	0.448	10,000	20.3 hours
134	6.05	1,600	52 minutes
135	1.29	160	6.68 hours

[a] Based on an operating time of 1800 seconds.(53)

[b] H is the time of the end of reactor run.

[c] Assuming ^{132}Te is also released, the rate at which the quantity of ^{132}I present is reduced is dependent on the ^{132}Te half-life. The ^{132}I half-life is 2.26 hours.

ii. The atmospheric diffusion factor (X/Q) has been calculated from one of the variations of Sutton's equation given in Section II.

iv. The breathing rate recommended for the International Commission on Radiological Protection(ICRP) for standard man[59] has been used-- $2.32 \times 10^{-4} m^3/sec$. (Ref.35,39,51,70).

The intake (for each isotope) equals

$$Ci = X(Ci\text{-}sec/m^3) \times 2.32 \times 10^{-4}\ m^3/sec$$

ix. The interaction in man may be estimated by the following assumptions and considerations:

a. 75% of inhaled radioiodine is retained in the body and goes to the blood stream[59], and

b. 30% of the radioiodine in the blood stream is transported to the thyroid.[59]

Thus, 0.75 x 0.30 = 0.23 of the inhaled radioiodine is assumed to be deposited in the thyroid.

x. The following indicates the dose to man based on a given intake, assuming:

a. Radioiodine is uniformly dispersed in the thyroid.[71]*

b. The energy absorbed in a unit volume of the thyroid is equal to the energy emitted by the quantity of radionuclide in the unit volume.[71]

c. The biological effective half-life and effective decay energies (H_E) from ICRP 2 are given in Table 6.[59]

---

*Hine and Brownell(71) indicate that iodine is not immediately taken up into the thyroid, as is assumed by the model that has been used. An uptake half-time of 5 hours is indicated. The ARL model is conservative by up to a factor of two for the shorter half-life radioiodine isotopes such as ^{135}I(Ref.71,p.837).

TABLE 6. BIOLOGICAL PARAMETERS FOR RADIOIODINE ISOTOPES

Iodine Isotope	Biological Effective Half-Life (59) Days	(Seconds)	Effective Energy (20-g Thyroid) (59) (MeV)	Rad/Ci-sec/m^3 (20-g Thyroid)[a]
131	7.6	6.6×10^5	0.23	3.4×10^2
132	0.097	8.4×10^3	0.65	1.2×10^1[b]
133	0.87	7.5×10^4	0.54	9.2×10^1
134	0.036	3.1×10^3	0.82	5.8
135	0.28	2.4×10^4	0.52	2.9×10^1

[a] The inhalation dose for an infant with a two-gram thyroid has been assumed to be 2.5 times that of a standard man.

[b] This dose conversion constant is based on the biological half-life of ^{132}I versus the chain controlling half-life of ^{132}Te. Assuming ^{132}Te is inhaled and deposited in the body according to the ICRP 2 assumptions (59), the dose from inhaled ^{132}I and ^{132}I produced from decay of ^{132}Te in the body indicates a dose factor of 51 rad/Ci-sec/m^3.

d. The thyroid weight (m) for standard man is 20 grams.

The following expression gives the dose rate to the thyroid from a thyroid burden:

$$\frac{Ci}{m(g)} \times 3.7 \times 10^{10} \frac{d}{Ci\text{-}sec} \times E_E \frac{(MeV)}{(d)} \times 1.6 \times 10^{-6} \frac{(ergs)}{(MeV)} \times \frac{rad\text{-}g}{100(ergs)} \quad (rads/sec)$$

To obtain the integral dose, the dose rate is integrated from the time of intake to infinity. Assuming the removal of iodine can be represented by a single exponential, indicative of a biological half-life, the removal of radioiodine can be represented by a biological effective half-life (T_{eff}) which is based on both the biological and radiological half-lives.

The approach to dose calculation parameters given in Table 6 has been to calculate the inhalation dose for an adult. Rather than actually using the parameters for an infant, it is then assumed that the infant's dose is 2.5 times that for an adult.

The calculation procedures used by the other organizations are similar to that indicated above. Stocum (58) evaluated the biological parameters and related them to statistical distributions. The analysis is largely related to the parameters associated with ingestion of radioiodine via the milk-food chain. In recent safety evaluation reports, LASL has applied the geometric standard deviation from this analysis to a mean based on ICRP(59) parameters. [3,13]

5. Thyroid Dose via Ingestion--Milk-Food Chain

Steps i, ii, v, vi, viii, ix and x of Figure 7 apply to the dose via ingestion. The calculations for steps i, ii, and x (transport and dose parameters) are the same as presented for the inhalation dose in the previous section although the only isotope that has been used in predictions for ingestion dose is ^{131}I. Iodine-131 accounts for the majority of the milk ingestion dose because of its longer radiological half-life (with respect to other referenced radioiodine isotopes). The NERC-LV considers the presence of the other radioiodine isotopes in sample analysis, and when estimating the possible dose from drinking milk.[46,47,50]

The following indicates the calculations for the steps pertinent to this dose pathway not covered in the previous section:

v, vi, and viii. When cows are on fresh forage susceptible to contamination by the effluent, the amount of radioiodine inhaled by the cow (vi) is insignificant. Thus, for practical purposes (vi) is considered to be included within (v). The conventional technique for determining cow forage contamination from passage of an effluent cloud is to use the product of the deposition velocity (m/sec) and the reciprocal of the mass of feed growing per unit area of the field (m^2/g), i.e., m/sec x m^2/g = m^3/g-sec). At the time the NRDS model was developed, insufficient data were available to evaluate each variable. Thus, a single parameter was used in the ARL model to relate the integrated airborne concentration of radioiodine to the resulting concentration in milk. The value now used in the model, 4×10^{-4} pCi/l per pCi-sec/m^3, was based on a literature survey. The value is only intended for ^{131}I concentrations because of the short half-lives of the other iodine radioisotopes.

Studies at NRTS[72,73] noted that about half of the variability in deposition velocity could be explained by the variation in the density of vegetation on the ground. In accordance with this, surveillance results from NRDS tests were fit to a log-normal distribution based on the ratio of radioiodine concentrations in milk and vegetation to integrated air concentrations.[59] This study indicated a geometric mean of about 4×10^{-4} pCi/l per

pCi-sec/m^3 and a geometric standard deviation of 2, which indicates the appropriateness of the original value used.

ix. The deposition of effluent from NRDS tests has been an acute or semi-instantaneous process. The concentration decrease subsequent to the peak for ^{131}I can be approximated by an exponential decay with an effective half-life in milk of five days (Ref.56, Report 5). The integral concentration subsequent to the peak has thus been estimated to be 7.2 times the peak; i.e., $\int_0^\infty (\exp - [\ln 2/5 \text{ days}]t)dt$. The Federal Radiation Council (FRC) Report 5[56] estimates that 20-25% of the total intake of ^{131}I via milk, subsequent to acute deposition, may be due to intake prior to the occurrence of the peak. Thus, the total intake has been assumed to be equal to about ten times the peak.

X. A convenient dose conversion parameter based on step ix (Ci intake/peak conc. in milk) and the previously mentioned dose conversion factors (rads/Ci intake) is 16 mrad thyroid dose as a result of a peak milk concentration of 100 pCi/l.[56] This is based on an infant with a 2-gram thyroid consuming one liter of milk per day.

The other organizations which have made effluent predictions have used similar techniques for estimating the ingestion dose. Stocum[58] analyzed the biological parameters associated with ingestion. Based on this analysis and a more recent evaluation,[74] he suggested a dose conversion factor of 12 mrad/100 pCi/l. Although this factor includes the dose contribution from consumption prior to the peak, it is identical to the FRC Report 5[56] value for the intake after the peak. The difference stems from an assumption of a lower value for the combination of milk intake and thyroid uptake parameters.[74]

The doses estimated by the WANL model[8] have been about 30-50% less than those of the ARL model because the WANL model has not considered the potential ^{131}I ingestion prior to the occurrence of the peak and used a 4.8 versus 5-day effective half-life for ^{131}I in milk.

B. Particle Dose Prediction Models

Models for prediction of biological hazards from particulate debris involve steps i, ii, iii, ix, and x of Figure 7. Methods for prediction of the

source term, step i, are discussed in Section II. For particle predictions, the source term may be expressed as a quantity of uranium, in grams, expected to be lost from the core. Steps ii and iii, discussed in Section II, yield predictions of expected ground concentrations in terms of particles per unit area (particles/m^2). Predictions at NRDS have generally used the Cluff-Palmer equation to scale ground concentrations of particles measured on previous tests to predict expected deposition from a future test, taking into account differences in source terms and meteorological parameters. Steps ix and x consist of evaluating various interactions of these particles with man and estimating doses and/or effects from these interactions. Step x for the particle model differs from that for the aerosol models in that there are no official radiation protection standards or guides for evaluating the implications of particle interactions; whereas, there are for the aerosol effluent.

Interaction of the particles with man is treated statistically by the model. Although there exists a possibility that a particle will fall at any downwind distance out to several tens of miles, the probability that a particle will fall at any particular location is small. The model assumes that this probability can be predicted from the Poisson distribution.

Modes of biological interaction of the particles with man that have been considered include localized skin doses, eye cataracts (from deposition of a particle in the eye), doses to the lung from inhalation of particles, and doses to the GI tract from ingested particles. These modes have been evaluated by several individuals and committees, including the AEC Division of Biology and Medicine, Space Nuclear Safety Committee, and it has been concluded that the localized skin dose has been the limiting or critical mode of interaction.[75,76,77]

The hazards of inhalation of particles have been discounted largely because there is evidence that nuclear rocket engine particles small enough to have a reasonable probability of being deposited in the deep pulmonary region of the lung have not contained sufficient activity to produce significant biological effects.[76,77,78]

Most of the information on biological effects produced by highly radioactive discrete particles in the lung is based on experiments with plutonium particles. The doses from these particles are much larger than doses which would result from inhalation of reactor particulate debris, and biological effects have been observed only at levels higher than expected from reactor debris. The two situations are not totally analogous; however, this analysis cannot be regarded as conclusive. Experiments with plutonium have emphasized the alpha dose, in which there is a sharp demarcation between tissue receiving a lethal dose and tissue receiving a sub-lethal but potentially carcinogenic dose. Beta and gamma emission from reactor debris produces a much more continuous depth dose distribution. Langham[79] noted that most investigations have given little attention to tissue outside the range of the alpha dose which may however receive a significant dose from x-rays. Biological effects in this tissue might be expected to be similar to effects in tissue surrounding particles containing fission products.

Another concept which deserves more investigation involves consideration of the number of cells at risk and the quantity of tissue that must be exposed to a sub-lethal but potentially carcinogenic dose to cause a cancer. Dean and Langham[79] in presenting a thought-provoking concept rather than a final model, suggested that this problem be approached by integrating the probability of cancer occurring for each exposed cell to determine the total probability of biological effects.

The proper understanding of the relationship between the mass of tissue exposed to a given dose (i.e., gram-rads) and the resulting biological effect is also relevant to analysis of skin effects. But there are differences between understanding the particle skin problem and understanding or evaluating the inhalation problem. First, micro-effects in the skin can be observed; whereas those in the lung are difficult to detect *in-vivo*. Past experience indicates that skin doses which do not produce ulcers will not produce skin cancer.[80] Second, skin

ulcers or an indication of their formation[80,81,82] can be detected soon after exposure (within about two weeks) and can therefore be related directly with the exposure, while the time involved in lung effects may be longer. Third, skin cancer is adaptable to successful therapeutic treatment, whereas lung cancer may not be.

As an example to illustrate the plausibility of the argument that inhalation hazards can be discounted, the activity in a particle of respirable size can be compared to the activity required in the same size particle to produce a dose of 750 rads at Krebs' depth.* Since this requires the assumption that the dose-effect relationships for the skin and the lung are similar, this exercise must be regarded as an example only and not as conclusive evidence.

Henderson[16] reported a value of 1.7×10^{18} fissions/gram of uranium for the Pewee I, EP-III, which is higher than that reported for other full-power runs. Data reported by the ICRP Committee II Task Group on Lung Dynamics[83] indicate that particles with aerodynamic diameters greater than 10 micrometers are not likely to be deposited in the deep pulmonary region of the lung. The NERC-LV reported an average particle density of 11 grams/cc from Phoebus 1B EP-IV[14], larger than average particle densities reported by PAA and the NERC-LV for other full-power runs.[15,17,84,85] Assuming a particle with an aerodynamic diameter of 10 micrometers, a density of 11 g/cc, and a specific activity of 1.7×10^{18} fissions/gram of uranium, there would be 3×10^{8} fissions per particle. The associated radioactivity is roughly two orders of magnitude less than that required to produce 750 rads at Krebs' depth for reasonable particle travel times.[16] This is based on a mean retention time of much greater than 10 hours.

---

*Krebs' Dose is the dose at the periphery of a circular field of 4 mm in radius at a depth of 100 μm below the surface of the skin.[80] This is discussed in Section V B.

As discussed below, the figure of 750 rads at Krebs' depth is a skin dose particle guide used at NRDS and does not necessarily apply to biological effects in the lung, especially since the geometry involved in particle doses to the lung is unknown. However, the example serves to illustrate the plausibility of conclusions by some workers that the skin dose is a more important mode of interaction than the lung dose.[75,76,78]

Sanders, et.al.,[86] summarized the implications of respiratory system irradiation by particles, in particular, UC_2 particles with a fission product inventory. They concluded that although nonuniform irradiation of the lung is more carcinogenic than uniform irradiation, there is no justification for inferring numbers of tumors incidence for doses less than 3000 rads, to the epithelium 100 μm from the particle. Doses of this magnitude are only related to particle sizes of about 10 μm or more (30 μm aerodynamic diameter) and travel times of less than one hour. But, Sanders, et.al., concluded that the data necessary for a comprehensive evaluation of inhalation probability and radiation effect are not available.

The remainder of this section will be devoted to the skin dose model. Discussion of models for the other modes of interaction (lung, eye, and GI tract) is presented in Appendix B.

1. Particle Skin Dose Model

For this model, steps i, ii, and iii of Figure 7 consist of predicting the source term in grams of uranium to be released from the core as particles and applying the Cluff-Palmer equation to predict ground deposition of particles in terms of particles/m^2 at points downwind, as discussed in Section II. Step ix concerns the interaction of particles with man. This interaction is evaluated by computing the probability that one or more particles will impact on an individual in the effluent trajectory and will produce a guideline skin dose. The NRDS

guideline dose is 750 rads at Krebs' depth,[80] as discussed in Section V.

The model assumes that the probability $P_n(n,\lambda)$ of a certain number of particles (n) impacting on an average individual and inflicting the guideline dose can be described by the Poisson distribution:

$$P_n(n,\lambda) = \frac{e^{-\lambda}\ \lambda^n}{n!} \qquad \text{IV-1}$$

where λ is the average number of radioactive particles per individual.[17] If n = 0, P_n is the probability that no particles will interact with the individual, Eq. IV-1 becomes

$$P_n(0,\lambda) = e^{-\lambda} \qquad \text{IV-2}$$

The probability P of at least one particle interacting with an individual to produce the guideline dose is

$$P = 1 - P_n(0,\lambda) = 1 - e^{-\lambda} \qquad \text{IV-3}$$

Here λ is defined as the average number of particles impacting on and retained by an individual with sufficient activity to produce the guideline dose. A useful approximation for small values of λ ($\lambda \leq 10^{-2}$) is

$$P \cong \lambda \qquad \text{IV-4}$$

Only a fraction of the particles will contain a sufficient inventory of fission products subsequent to a given transport time to produce the guideline dose, even if they impact on and are retained by the exposed skin of the individual. The inventory which a particle must contain to produce the guideline dose is a function of particle size and transport time; thus, both size and particle radioactivity inventory distributions must be considered in computing λ.

The NRDS model divides the size distribution into i classes and computes λ from Θ_i, the total number of particles in the ith size class which impact on and are retained by an individual, and σ_i, the fraction of the total number of particles in the ith size class with sufficient inventory to produce the guideline dose:

$$\lambda = \sum_i \Theta_i \sigma_i \qquad \text{IV-5}$$

In practice, Θ_i and σ_i are estimated empirically from size and radioactivity inventory distributions observed from past tests, appropriately extrapolated to the proposed test conditions.[16] For reasons of convenience and the accuracy of data, the size distribution is generally divided into three classes: less than 15 micrometers, 15 to 50 μm, with representative mean diameters for these classes of 10, 30, and 70 μm, respectively.

The average number of particles, Θ_i (x), which impact on and are retained by an individual at any downwind distance x is the product of the predicted ground concentration of particles in terms of particles/m^2 in the ith size class (developed in steps i, ii, and iii of Figure 7 and the exposed surface area of the individual in m^2. This assumes that the number of particles which impact on and are retained by the exposed skin of an individual is the same as the deposition on an equivalent horizontal surface area.[16] This is based on studies by Booz-Allen[87] which indicated that approximately the same amount of mass was deposited on the exposed surface area of a mannikin as was collected on an equivalent horizontal area. These results imply that the fraction of particles which impact but do not stick and the fraction which follows air streamlines around an object compensate for the differences between particle fluxes in the vertical and horizontal directions. This approach has the advantage of simplicity and bypasses more

elaborate theoretical approaches proposed by Kochendorfer and Ulberg[88], DeAgazio[89], Mikhail and Collins[76], and the Radiological Effects Working Group.[90]

The total exposed skin area is used rather than the cross-sectional area as suggested by Kochendorfer and Ulberg[88]. Henderson[91] assumed winter dress styles similar to Model A of Kochendorfer and Ulberg: long pants, long-sleeved shirt, and hat, with a corresponding exposed skin area of 0.0702 m^2 and summer dress styles similar to Model B of Kochendorfer and Ulberg: long pants, short-sleeved shirt, no hat, with a corresponding exposed skin area of 0.384 m^2.

The fraction of particles, $\sigma_i(x)$, at a given downwind distance, x, with sufficient inventory to produce a guideline dose depends on: (1) particle size distribution, (2) particle inventory distribution, (3) reactor run history, and (4) travel time from release of particles from the reactor to impaction on the individual. The travel time has been estimated by x/U, where U is the mean transport wind speed.[16] The number of fissions required in a particle to produce the guideline dose may be determined from the beta tissue dose model of Mikhail and Collins.[76] This model is based on the work of Ulberg and Kochendorfer.[92]

The dose/fission calculations have been based on the reactor power and run time profile and include self-absorption within the particle. It has been assumed that all particles are retained in the reactor until the end of the run.

The dose is obtained by integrating the dose-rate with time. This integral has been based on arrival time and a mean retention time. The mean retention time is estimated from an empirical equation fit to experimental data[76,90] which yields the probability of $P_r(t)$ of a particle being retained

a period of time t:

$$P_r(t) = e^{-t/\delta} \qquad \text{IV-6}$$

where t is in hours and δ is the mean retention time (hours) for a particle of given diameter on the skin. The value of δ for a given size class can be determined from references.[76,90] The particle activity distribution has been predicted by scaling a particle activity distribution observed on a previous test in accordance with the ratio of the relative radioactive inventories of the reactor cores for the two tests:

$$A' = A(F'/F) \qquad \text{IV-7}$$

where A is indicative of the radioactivity inventory in the particle, in terms of fissions per particle, F is the number of fissions/gram of uranium. The primed values are for the proposed test.[16]

Pre-run safety evaluations of reactor tests at NRDS have involved the use of Equations IV-3 and IV-6 to develop curves of the probability of an individual receiving 750 rads at Krebs' depth as a function of distance.

V. RADIATION PROTECTION GUIDES

This section is subdivided into guides and standards for total-body, inhalation, and ingestion doses and guides applicable to evaluating doses from discrete particles. Guides are recommendations of a committee, organization, or individual, whereas standards have the impact of law (i.e., the AEC regulations). Tests at NRDS have been conducted on a contractor basis with the AEC, and thus have been conducted under the standards of AEC Manual Chapter 0524 (MC 0524) versus Title 10, Code of Federal Regulations, Part 20 (10 CFR 20 is applicable to the licensee relationship).[57,93,94,95]

A. Guides for Total Body and Internal Organ Doses

1. Normal Operation

The standards for normal operations have been those of MC 0524,[57] which specifies standards for both occupationally exposed people and the general population. These standards generally follow the recommendations of the ICRP,[59] FRC,[56] and the National Council on Radiation Protection and Measurements (NCRP).[97,98] The standards are given both as organ doses and as concentration guides for air and water. Table 7 gives the occupational standards.[57]

TABLE 7. OCCUPATIONAL DOSE STANDARDS

Organ Exposed	Time Period	Dose (rem)
Whole body, head and trunk, active blood forming organs, gonads, or lens of eye	Accumulated	5(Age in yrs-18)
	Calendar Qtr.	3
Skin, thyroid, and bone	Annual	30
	Calendar Qtr.	10
Other organs	Annual	15
	Calendar Qtr.	5

The dose standards for the general population are generally one-tenth of the occupational standards.[56,59,96] For the thyroid, the FRC[56,Report 2] recommended that a value of one-twentieth the occupational standard be used. The AEC concurred with this recommendation.[57,93] To compensate for the variation of doses to individuals from the average of a suitable sample, the FRC recommended the guides for individuals be reduced by a factor of three when applied to the sample average.

A suitable sample of the population is defined as a sample of cohorts representing the critical receptor; i.e., the group of the population that receives the highest dose with respect to the standards or guides.

For example, a one-year-old infant with a two-gram thyroid is the critical receptor for ingestion of radioiodine in milk.

In January 1971 the NCRP issued an updating report, "Basic Radiation Protection Criteria," NCRP 39.[98] The NCRP recommended a basic dose guide of 0.5 rem per year for the total body and/or critical organs of individuals in the general population. The reduction of the critical organ guide, from 1.5 to 0.5 rem, was based on administrative simplification rather than biomedical need. The guide for an average of the population is 0.17 rem per year.

The Manager, SNSO[95], in 1967 stipulated the guides to be used in planning and approving the conduct of reactor tests at NRDS. The applicability of AEC MC 0524 and the FRC guides[56] was noted. The implication of the wording was that NRDS exposures would be considered separately from Plowshare exposures. This is similar to the implications of AEC MC 0524 which specifically excludes Plowshare activities, noting that guidance is "being developed." The FRC indicates that the guides of 0.5 rem/yr and 1.5 rem/yr for total body and thyroid doses, respectively, for individuals in the population are applicable for the summation of all normal doses from peaceful uses of nuclear energy.[56]

2. Accident Conditions

AEC MC 0524 does not stipulate appropriate standards for approving reactor tests based on hypothetical accident analysis. Although the AEC has issued standards for reactor siting in Title 10, Code of Federal Regulations, Part 100,[99] they have not been considered appropriate for evaluating the consequences of tests in the rocket engine program.[56,99]

In 1967 the Manager, SNSO,[95] recommended emergency guides to supplement the AEC standards.[57] It was stipulated that accident evaluation guides of 10 rem total body dose and 30 rem thyroid dose

for individuals in the off-site area would be used in approving the conduct of tests. Permission to conduct tests is also to be denied if the predicted on-site accident doses are above 12 rem and 36 rem to the total body and thyroid, respectively, of individuals. The dose guides for the general population are to be reduced by a factor of three where exposures cannot be adequately measured and evaluated on an individual basis.

The accident guides for the general population are based on the protective action guides (PAG) of FRC Reports 5 and 7.[56] The whole-body dose accident guide of 10 rem was evolved from the PAG for ^{137}Cs in FRC Report 7.[56] Although the dose from ^{137}Cs is a whole-body dose, the intake pathway is the food chain for FRC Report 7 versus external gamma dose for the NRDS guide. Actions to prevent or control external gamma dose in a fallout situation are generally more traumatic than those related to the food chain, and this use of the PAG appears reasonable.

The accident guide for total-body exposure for on-site personnel was based on MC 0524.[93] MC 0524 stipulates a quarterly dose of 3 rem for the total body. A year's summation of this standard would be 12 rem--the proposed accident guide. A similar treatment for an accident thyroid guide would be 40 rem, whereas the proposed accident is 36 rem or three times the total body guide. The factor of three between the total body guide and the thyroid guide was based on the ratio of the respective FRC guides.[56]

B. Guides for Exposure to Discrete Particles

In 1967 there was increased concern about the biological effects from discrete particles of fuel matter released from the reactor. This concern related to the lack of applicable radiation protection standards or guides and the increasing quantity and specific activity of the particulate matter with the increase in reactor run time and power level. Some of the increases--quantity, specific activity, etc.--were actually occurring whereas

some were projected for the future. Thus, although specific guides were not available for the Phoebus-1B test in February 1967, the effluent trajectory was limited to minimize the possibility of effluent interaction with on-site and off-site population. The NRX-A6 EP-III test was conducted in accordance with preliminary guides which were later adopted.

In May 1968, the Manager, SNSO, stipulated a particle probability-interaction guide to be used for approval of future tests.[100] The guide was given in terms of the probability of particles interacting with an individual and producing a skin tumor or cataract. The guide stipulates that this probability should be less than one in ten-thousand per person. This probability is to be based on the product of the probabilities of (1) a particle interacting with a person and (2) the probability of a skin tumor or cataract being produced from this interaction.

The guide allows credit for the protection afforded by buildings and/or special clothing or equipment provided the actual use and implied protection can be demonstrated. The probability of interaction is computed from the model in Section IV. The probability of an effect from an interaction is based on the Krebs' depth concept and the distribution of particle sizes and specific activities capable of giving doses exceeding Krebs' criteria. Although the probability of an effect, given an interaction, is greater for a cataract than for a skin tumor, the probability of deposition of a particle on skin compared to that of deposition in the eye is such that the basic guide and thus reactor safety evaluations have been limited to consideration of skin tumor probabilities.[16]

Krebs[80] evaluated available information concerning biological response of mammalian skin to irradiation with small, high-specific activity particles. Krebs concluded that serious radiation-induced acute lesions are caused primarily by the destruction of the germinal layer cells of the epithelium (stratum germinativum) and that the viable germinal cells must be reduced to a survival level of less than one-thousandth over an area large enough that cell proliferation in the margin of the exposed field will not be able to replace the dead cells.

Based on considerations of the area of skin irradiated and the characteristics of skin from the standpoint of biological effects, Krebs[80] proposed what has become known as Krebs' Dose. This is the dose at the periphery of a circular field of 4 mm in radius at a depth of 100 μm below the surface of the skin. The center of the field is the point on the surface of the skin where the particle rests.

Krebs postulated that at Krebs' Doses below 1500 rads, development of a moist desquamation or ulcer type injury was improbable.* Thus, a Krebs' Dose of 1500 rads was originally used as the criteria of producing an "effect" in the aforementioned guide. This was based on the hypothesis that "From a general medical viewpoint, the production of erythema or dry desquamation is probably inconsequential," whereas the development of an ulcer and/or cancer is serious. In rats and mice the development of skin cancer from radiation has consistently been associated with the prior occurrence of acute lesions at the time of irradiation.[80]

Experiments by Forbes[82] and the biomedical research group of LASL[81] in 1968 and subsequent work by Forbes[101] indicated that doses of less than 1500 rads (Krebs' criteria) could produce a moist desquamation or ulcer type lesion.** The experiments were comprised of implacing irradiated UC_2 particles on monkey, pig, and human skin. Experimental dosages ranged from 1300 to 7,400,000 rads for the point basal layer dose (i.e., dose at 100 μm below the particle skin interface) and roughly 3 to 35,000 rads Krebs' Dose.[102]

Preliminary results from these experiments indicated that moist desquamation and/or ulcer type lesions could be produced at doses below 1500 rads Krebs' Dose. Thus, based on the preliminary results, the dose guide was reduced from 1500 rads to 750 rads Krebs' Dose.[103, 104]

---

*Krebs denoted four degrees of lesions; erythema, dry desquamation (peeling or flaking), moist desquamation (moist discharge), and ulceration (open weeping lesion, which is slow to heal). Recent work by Forbes(ref.82,101) and LASL(ref.81,102) indicates that moist desquamation and ulceration are probably not separate entities for the type of lesions produced in this case, but rather they merge together. Thus, they will be referred to as ulcers.

**Preliminary information from these experiments was presented at a meeting of the safety agencies in Las Vegas, Nevada, on November 8, 1968.

The following summarizes the final results from the studies of LASL[81,102] and Forbes and Mikhail[101] and the status of the particle dose guide:

1. The present guide is a Krebs' dose of 750 rads.[103,104] Based on the original philosophy used by Krebs' (i.e., prevent moist desquamation or ulcers)[77], the work by Forbes and Mikhail[101] indicates the guide should be reduced.

2. The work reported by Forbes and Mikhail[101] using pigs indicated that the lowest doses used, 400 and 440 rads Krebs' Dose, produced ulcerous lesions; whereas the LASL studies using monkeys did not indicate the formation of ulcers at doses of 470, 500, or 770 rads Krebs' Dose.[81,102]

3. Additional studies are needed to determine the significance of the difference between the LASL and Forbes' results. The differences may be due to the different animal species, the measurement of the biological effect, etc. The highest human doses have been roughly 130 rads Krebs' Dose.

4. Forbes and Mikhail postulated that ulcer size might be a meaningful biological effects criterion. They noted that ulcers of 0.5 mm in diameter (400 rad dose) were probably of much less concern than those of 1 to 2 mm produced by doses of roughly 750 rads Krebs' Dose.

5. Krebs notes that the germinal cell layer surrounds the hair follicle. That is, the layer of germinal cells extends down to the depth of the hair follicle--roughly a millimeter. Krebs indicates that this provides a reservoir of germinal cells that are relatively protected against superficial injury. These cells would receive a much lower dose than the cells in the main basal layer. Thus, other things being equal, it is postulated that the dose effect relationship might vary between hairless and hairy skin. This may partially explain why the dose required to produce an "ulcer" on the sparsely

haired pigs is less than that for the monkeys used by LASL. This should also be considered in applying the results to man.

Appendix B includes a more complete review of the work by Krebs, Forbes and Mikhail, and LASL.

VI. ENVIRONMENTAL LEVELS AND DOSES

Since the beginning of reactor testing at NRDS in 1959, the effluent documentation program has included the efforts of a number of organizations. These have included:

1. EG&G - Long range aerial tracking--not discussed in this report.

2. NOAA/ARL - Documentation of meteorology and effluent predictions.

3. LASL - On-site surveillance including air sampling, external radiation monitoring, collection of discrete particles in fallout collecting mechanisms and fallout trays. Prior to 1966 most of the on-site sampling and monitoring was performed by LASL.

4. PAA - Primarily on-site surveillance with limited off-site sampling to obtain information for effluent transport modeling purposes. The program has included air sampling, gamma exposure measurements, and ground surveys for discrete particulate matter.

5. NERC-LV - Off-site surveillance program with limited on-site sampling for inter-program cross-checks and to obtain near-in samples to estimate potential implications in off-site populated areas. The program has included ground level surveillance for external exposure results (mobile monitoring personnel with survey instruments, fixed instrument stations, and thermoluminescent dosimeters); air sampling; sampling of milk, water and vegetation; and ground surveys for discrete particulate matter.

The aerial program has included sampling using equipment for analysis of particulate, halogen, and gaseous constituents of the effluent and monitoring equipment to measure gamma exposure rates and to track the effluent.

6. Reynolds Electrical and Engineering Company - sampling and monitoring on the Nevada Test Site--not discussed in this report.

A. Aerosol Effluent

The fission products in the effluent are fractionated because of the different migration constants in the fuel for the various radionuclides. The radioiodine isotopes have been of primary importance with regard to potential health implications because of their associated fission product yields and chain rates of migration, environmental transport, and biological parameters. Of the iodine isotopes, ^{131}I has been the most important because of its fission product yield, half-life, and potential transport to man through the forage-cow-milk-food chain.[3,61]

The chemical states of the various elements composing the effluent have not been fully documented. Several unsuccessful attempts have been made by NERC-LV to determine the chemical forms of the radioiodine effluent. At present, since methane is assumed to be present in the effluent (reaction of graphite and hydrogen), it is postulated that iodine is present in the effluent in numerous chemical forms.

1. Off-Site

Grossman[50] summarized exposure history for the off-site areas for the period 1959-1969, and the following discussion is taken largely from his summary.

At the time of the first Kiwi reactor in 1959, NERC-LV operated a network of 12 air sampling stations and a network of 28 film badge stations in the immediate off-site area. Mobile monitoring personnel

were used to supplement information from the networks. Prior to each test, these monitors were positioned at populated locations and on existing highways in the predicted effluent trajectory to measure radiation levels and to collect environmental samples (milk, water, cow feed, air) should airborne radioactivity be released. The monitors were also in two-way contact with a control center which followed reactor test operations and meteorological conditions, and could be repositioned, as required.

In subsequent years several changes in monitoring techniques and expansions in NERC-LV routine monitoring networks were made. Beginning in 1961, self-powered air samplers were included with the monitor's equipment, making the air sampling coverage for tests more adaptable. In the same year, the monitoring of NRDS test effluents by aircraft was begun, aiding in the locating of effluent trajectories and in the positioning of ground monitors.

In 1963 gamma-rate recorders were placed at 16 of the air sampling locations and in 1965, Model TL-12 thermoluminescent dosimeters by EG&G, Inc., were included in the film badge network and used off site by mobile monitors.

The film badge and air sampling networks were expanded after the latter part of 1961, due to the resumption of nuclear weapons testing.[50] These off-site networks were gradually expanded through the years so that they now number about 100 air sampling stations in Nevada and the Western United States, and include 30 gamma-rate recorders, 100 fixed TLD stations, and selected off-site volunteers who wear dosimeters. Use of film badges in the off-site dosimetry program was discontinued in 1970 because of the greater reliability and sensitivity of TLD's. The precise number of the various sampling stations varies with time.

Grossman[50] estimated whole-body gamma exposures (cloud passage plus infinite deposition exposure) from reactor effluent and calculated

hypothetical infant thyroid doses from inhalation of airborne radioactivity and from the assumed ingestion of milk contaminated with radioiodine from reactor effluent. Grossman's exposures and infant thyroid doses were hypothetical in almost all cases, since air samples were often taken at unpopulated locations and infants were seldom present at the locations where air and/or milk samples were collected.[50] Whole-body gamma exposures were integrated from G-M survey instrument data because no measurable exposure was ever detected with TLD's or film badges.[50]

Figure 8 taken from Grossman,[50] indicates the totals for exposures and hypothetical doses for reactor/engine tests for the period 1959 through 1969 for various sectors of the off-site area. Figures in Appendix D indicate hypothetical exposures and doses for shorter periods within the 10-year NRDS testing history. These figures were compiled by summing the maxima for each test occurring within each year and within a given sector and entering this value in that sector. Blank sectors indicate that no radioactivity was detected or that the hypothetical infant thyroid dose was less than 1 mrad. The reactor engine tests which released effluent which was detected off site are listed in Appendix D.

Table 8 [from Grossman[50]] compares the Radiation Protection Standards of AEC Manual Chapter 0524 and the FRC guides with the maximum hypothetical whole-body gamma exposures and the maximum hypothetical infant thyroid doses received by postulated receptors during the history of NRDS reactor testing. Within any given year the postulated whole-body gamma exposures were below 12% and 14% of the whole-body and thyroid dose standards respectively, for a sample of the population.

Table 9 presents some of the highest environmental concentrations observed during past reactor tests and the potential hypothetical doses from these concentrations. Higher values for the air concentrations were observed at close-in locations in some instances.

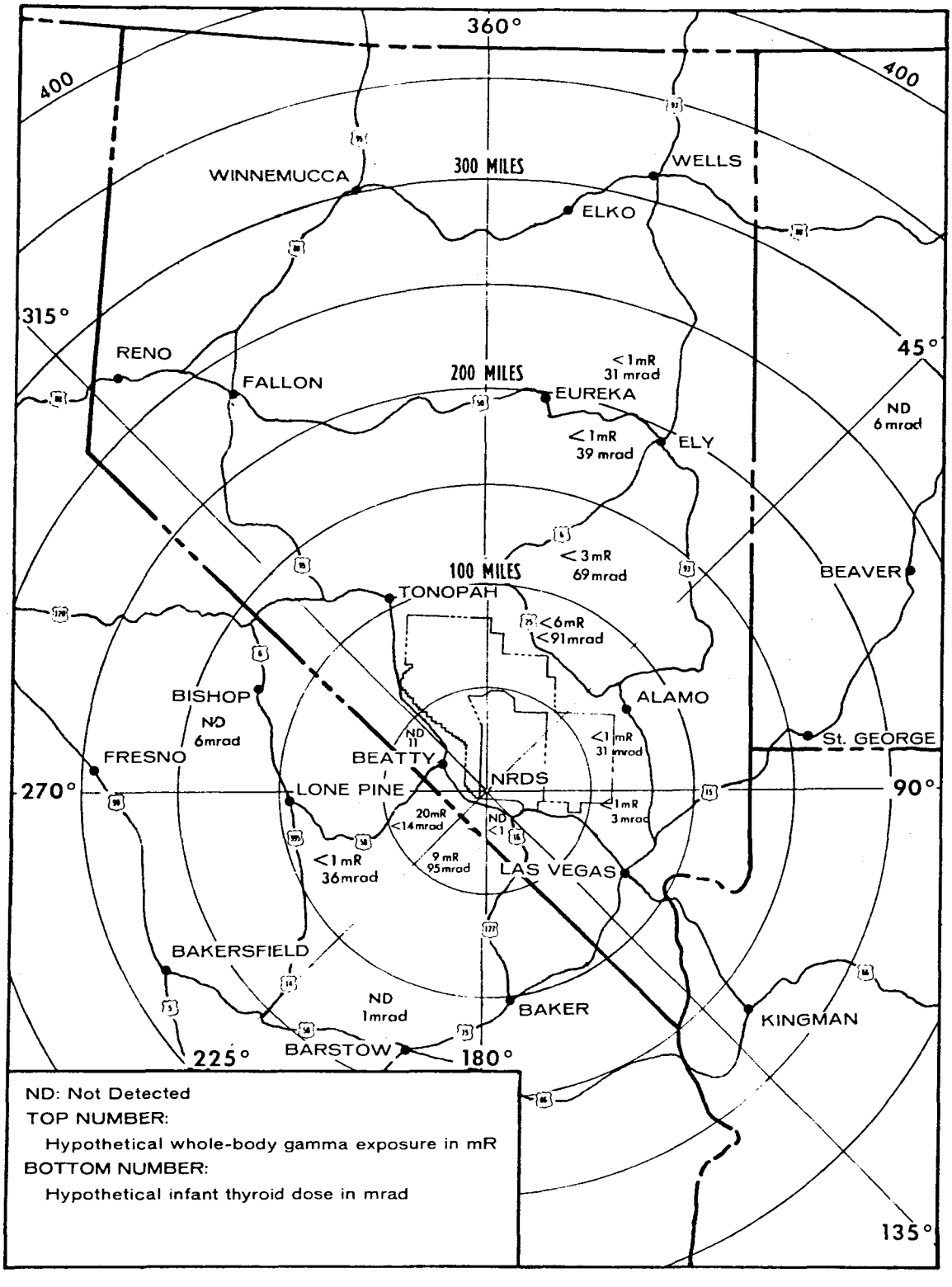

Figure 8 Off-Site Whole-Body Gamma Exposures and Infant Thyroid Doses Resulting from Reactor Engine Tests from CY 1959 to 1969

TABLE 8. COMPARISON OF MAXIMUM HYPOTHETICAL WHOLE-BODY GAMMA EXPOSURES AND INFANT THYROID DOSES WITH RADIATION PROTECTION STANDARDS.(50)

Type of Exposure/Dose	Radiation Protection Standard*	Maximum Whole-Body Gamma Exposure (mR) and Infant Thyroid Doses (mrad)**						
		'59-'63	'64	'65	'66	'67	'68	'69
Whole-body gamma exposure	170 mrem/yr	ND	<1	6	20	2	<1	<1
Thyroid dose	500 mrem/yr	<3	24	72	36	18	13	2

* Standards are for sample of population, AEC Manual Chapter 0524.(57)

**Units in mR and mrad are equivalent to mrem for this comparison.

TABLE 9. SUMMARY OF NRDS NUCLEAR ROCKET TESTING RESULTS

Event	Milk Results, ^{131}I - Infant			Air Concentrations - Adults		
	Distance from Test Cell (mi.)	Peak Milk Concentration (pCi/l)	Potential[a] Dose (mrem)	Distance from Test Cell (mi.)	^{131}I (μCi-sec/m^3)	Potential[b] Dose (mrem)
NRX/EST-A4, EP-IVA 3/25/66 (46)	95[c]	140	16	95[c]	7.4	4
NRX-A5, EP-IV 6/23/66 (47)	180	240	17[d]	60	9.7	7
Phoebus-1A, EP-IV 6/25/65 (105)	120	180	20	65	1.7	0.1
Phoebus-1B, EP-IV 2/23/67 (45,48)	193	100[e]	15[e]	78	2.8	6

[a] Potential thyroid dose for an infant drinking 1-liter of milk per day assuming a 2-gram thyroid.

[b] Potential thyroid dose for standard man; based on iodine-131, 132, 133, and 135.

[c] The meteorological conditions appeared to produce a subsidence and possibly rainout or washout at this distance, resulting in higher concentrations than would have been suspected from those near-in. The cows were receiving only about 1/10 of their feed from fresh forage.

[d] FRC 5 type assumptions (5-day effective half-life in milk) would indicate a dose of 48 mrem; but the observed half-life was shorter than 5 days.

[e] There were not complete daily results. The peak concentration is based on extrapolating values prior to the peak. The highest measured result was 60 pCi/l. Based on FRC Report 5 assumptions.

It is apparent from a comparison of Tables 8 and 9 that most of the totals for annual exposure and hypothetical thyroid dose given in Table 8 results from one or two tests for the indicated time period.

Figure 9[48,105] compares estimated hypothetical doses with pre-run dose predictions for Phoebus-1B EP-IV. The estimated doses were calculated from environmental surveillance data and are about an order of magnitude below the pre-event predictions. Estimated hypothetical external gamma exposures are not indicated on the graph. The off-site gamma exposure-rate was near the limit of detectability, with the highest measured exposure being less than 0.1 mR. Thus, all of the gamma exposures fall off the scale of the graph. The predicted external gamma exposure was based only on cloud passage (i.e., did not include exposure from deposited activity).

The difference between the pre-event predictions and the post-event estimates was in large part due to differences between pre-event estimates of parameters and what actually occurred. Table 10 compares some of these parameters and shows the effect of various assumptions on predicted doses.[48]

Figure 9 indicates that pre-event predictions were roughly an order of magnitude above the hypothetical dose estimates based on surveillance results. Table 10 indicates that the difference between pre-event predictions of parameters and post-event estimates of these parameters accounted for roughly a factor of 7 of the order of magnitude difference.[48]

Figure 10 shows the crosswind distribution of the effluent and indicates the relative quantity of ^{131}I on natural desert vegetation (relative pCi per unit wet weight of vegetation).

2. <u>On-Site</u>

This section is concerned with exposures produced by reactor test effluent and does not consider occupational exposures to personnel

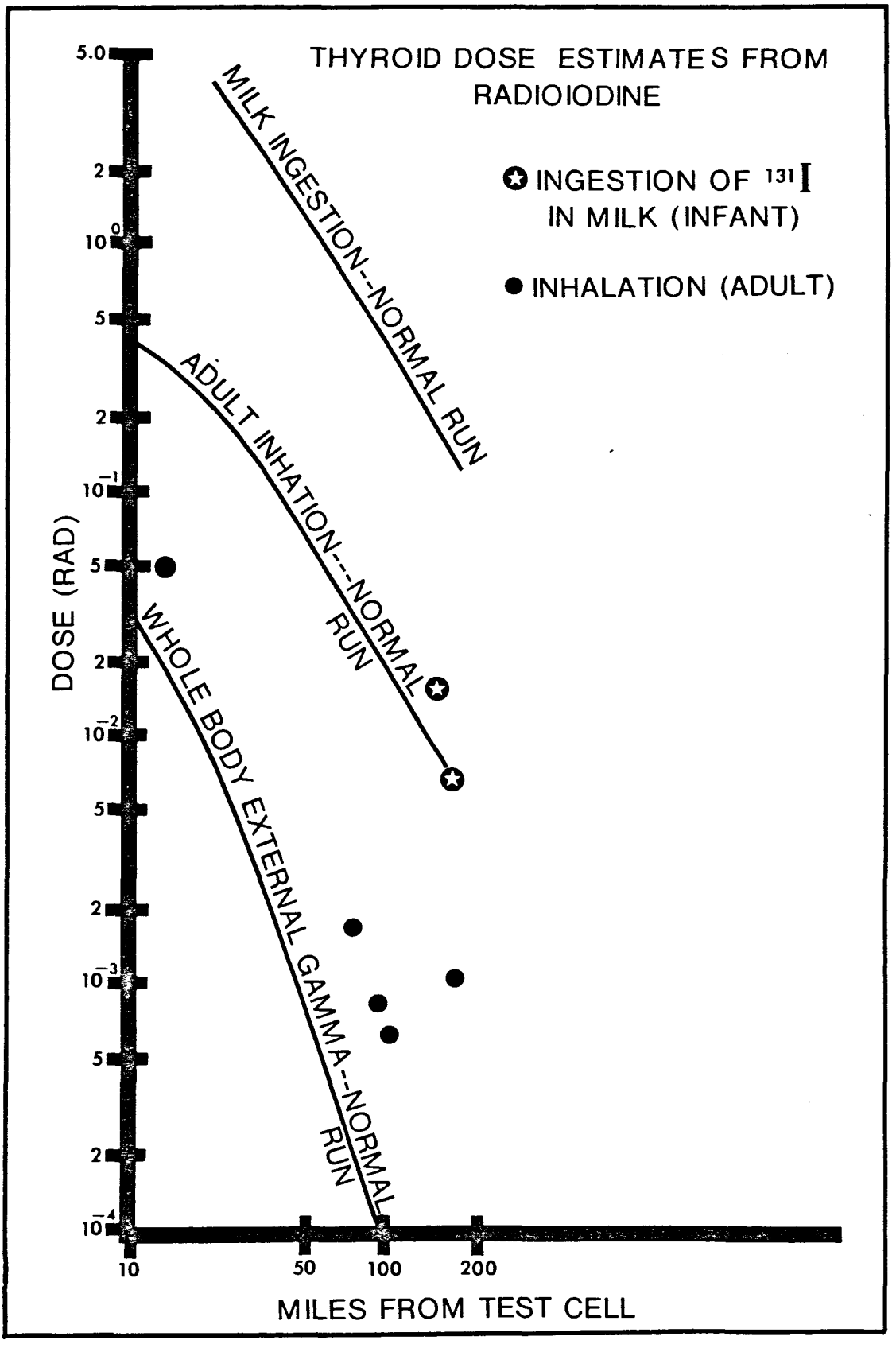

Figure 9 Pre-Event Dose Predictions and Dose Estimates from Surveillance Results[48]

TABLE 10. TYPICAL EFFLUENT PREDICTION PARAMETERS(48)

Parameter	Pre-Event Predictions Accident	Pre-Event Predictions Normal Run	Post-Event Normal Run	Factor Change In Prediction (+ increase; - decrease)*
Power Integral (Mw-sec)	2.7×10^6	2.7×10^6	3×10^6	+0.1
Fission Product Release Fraction for ^{131}I (percent)	50%	5%	1%	-5
Wind Speed (mph)	6	6	15	-2.5
Effective Stack Height (meters)	300	1,500	1,200	Minor for off-site area

*Summing this factor indicates that the pre-event prediction was roughly a factor of 7 above doses estimated by use of post-event parameters and the model.

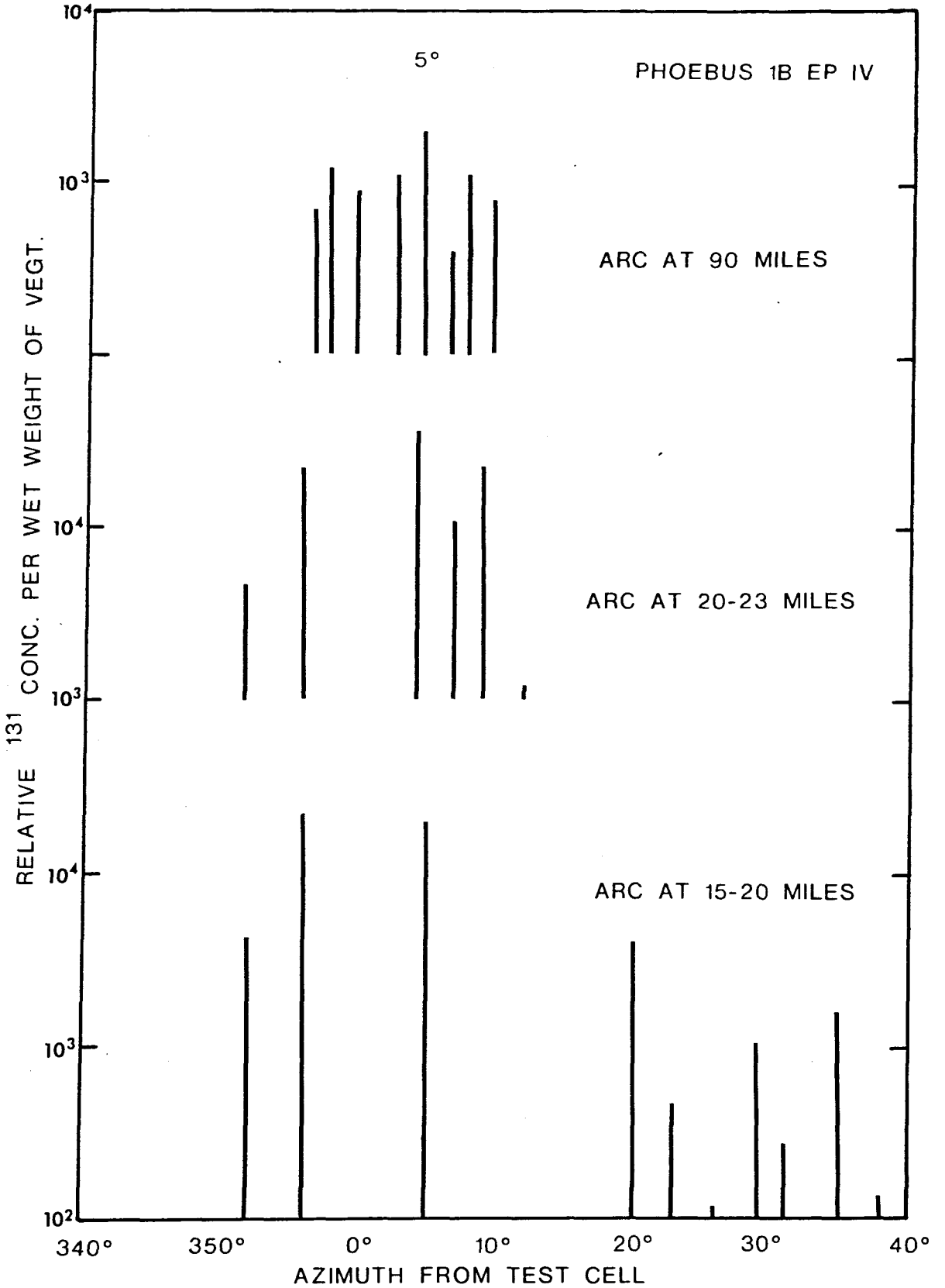

Figure 10 Relative Quantity of ^{131}I on Natural Vegetation (Sagebrush or Greasewood Phoebus 1B, EPIV)

involved in reactor disassembly or test operations. No comprehensive summary of surveillance data or actual absorbed doses in the on-site area is available, and information presented here is limited to hypothetical whole-body gamma exposures estimated from exposure-rate data compiled by Van Vleck[106] for several reactor tests. The on-site program has been conducted by LASL and PAA.

Figure 11 indicates the cloud centerlines for the following tests: NRX-A3, EP-V; NRX/EST-A4, EP-IV; NRX/EST-A4, EP-IVa; NRX-A5, EP-V; Phoebus-1B, EP-IV; NRX-A6, EP-IIIa; Phoebus-2A, EP-IV; Phoebus-2A, EP-V; and Pewee-I, EP-III.

Figure 12 presents estimated hypothetical whole-body external gamma exposures (infinite exposures integrated from time of completion of cloud passage) resulting from activity deposited by the tests whose cloud centerlines are indicated on Figure 11. Figure 12 excludes external exposure received during cloud passage. Past experience at NTS indicates that exposure during cloud passage may be about half of the infinite exposure from deposited activity. The integrated exposures are based on the assumption that the deposited activity decayed with time according to $t^{-1.2}$.

B. Deposition of Particulate Effluent

Simens[29] summarized the early history of environmental surveillance efforts related to particulate effluent. Ground deposition of particulate matter out to several miles from the test stand was noted commencing with the first NERVA test (NRX-A2, 1964). Prior to the NRX-A5, EP-IV test in June 1966, the particulate effluent was considered to be related to the immediate environment within several miles of the test point. Subsequent to the NRX-A5 test, particles were found on site 30 miles downwind of the test stand[14,107]. This initiated the concern for particles as a potential off-site safety problem.

Beginning with Phoebus-1B, EP-IV, LASL, PAA and NERC-LV mounted extensive field efforts to measure the extent of particulate contamination and to

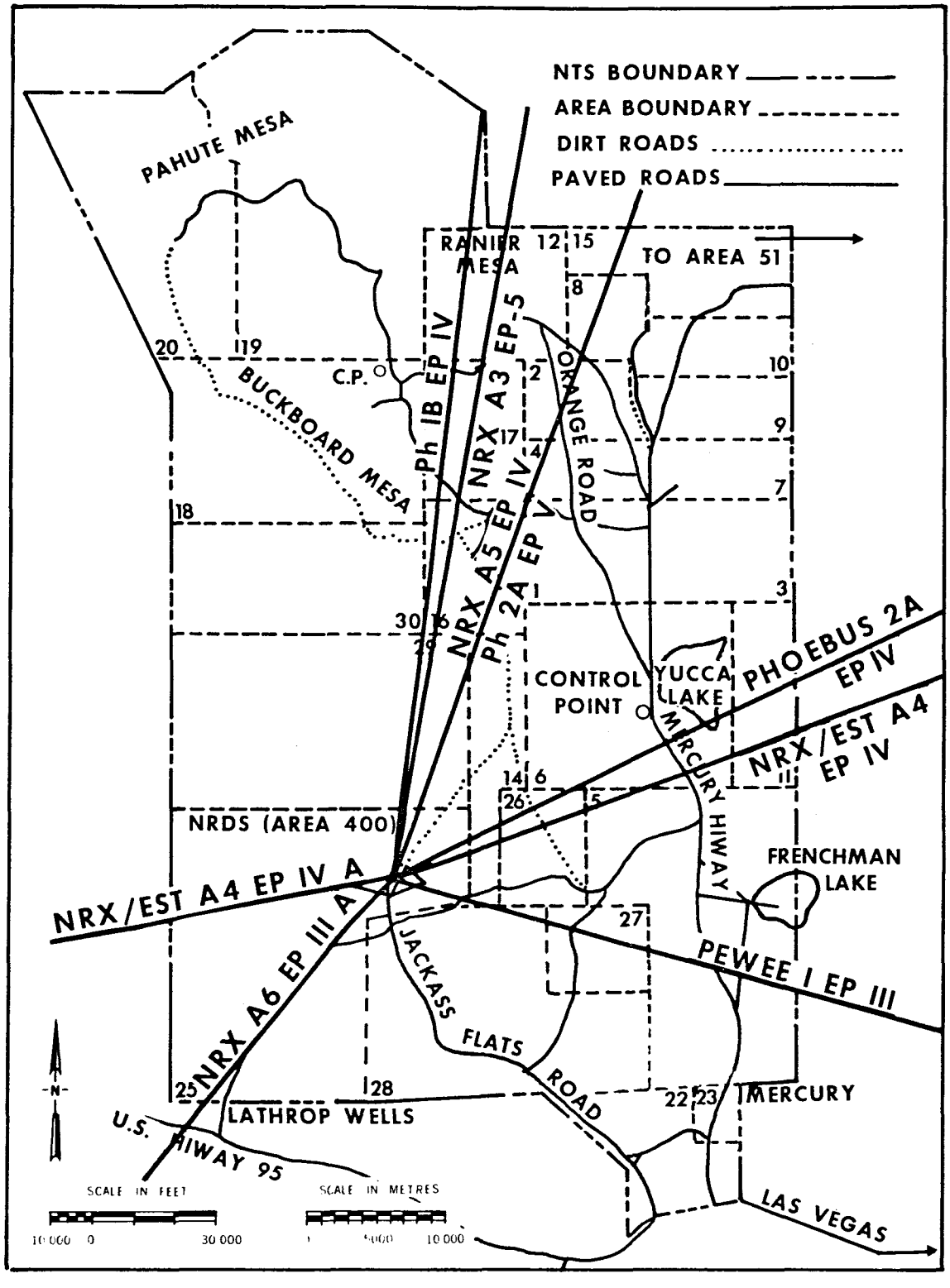

Figure 11 Cloud Centerlines for Selected Reactor Tests

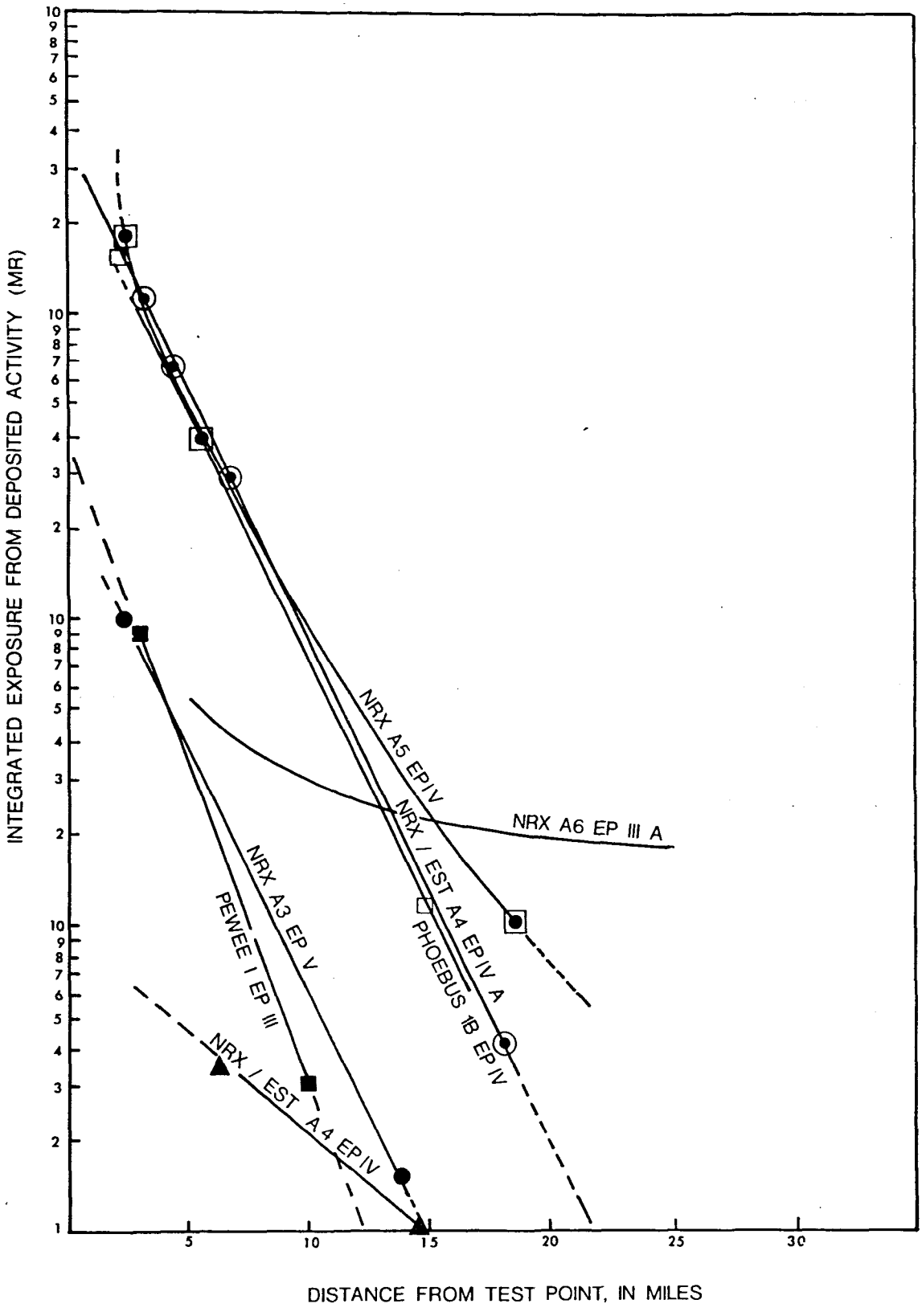

Figure 12 Estimated Hypothetical Whole-Body External Gamma Exposures from Activity Deposited by Selected Tests Indicated on Figure 11

estimate particle size and activity distributions. The findings of the organizations are described in their respective reports of surveillance operations for the Phoebus-1B, EP-IV; NRX-A6, EP-IIIa; Phoebus-2A, EP-IV and EP-V; and Pewee-I, EP-III reactor tests.[14,15,17,43,84,85,108,109,110,111]

Altomare and Coleman[43] compared the preliminary particle data obtained for effluent from Phoebus-1B, EP-IV, by PAA, LASL, and NERC-LV and found the data to be inconsistent. For this test, PAA and LASL data indicated a log-normal size distribution of particulates with a count median diameter of about 67 micrometers and a geometric standard deviation of 2.0. NERC-LV particulate data indicated a log-normal size distribution with a count median diameter of 11.5 micrometers and a geometric standard deviation of 2.9. PAA reported an average particle density of 6 gm/cc while NERC-LV reported an average particle density of 11 gm/cc. Altomare and Coleman indicate that the PAA data showed a decrease in particle size with distance and a correlation between particle size and activity.

Mikhail and Collins[76] also evaluated the Phoebus-1B, EP-IV, particle data. They divided the particles into size groups, greater than and less than 12 μm, and evaluated the associated inhalation, ingestion, and skin exposure implications of human interaction. They concluded skin exposure was the limiting mode of exposure.

The final NERC-LV report for the Phoebus-1B particle studies indicates an overall count median diameter of 12 μm.[14] The count median diameter for the particles over 10 μm in diameter and within 10 miles of the test cell was 35 μm. This latter number is somewhat analogous to the data of PAA and LASL, which only collected particles greater than 10 to 15 μm in diameter, the majority of which were within 10 to 15 miles of the test cell. It was also noted that the particle size generally decreased with distance although the correlation coefficient was not significantly different from zero at the 95% confidence level.

The "hot-lines" for the five reactor engine tests for which particulate data were collected in the off-site area are indicated on Figure 13,

Figure 13

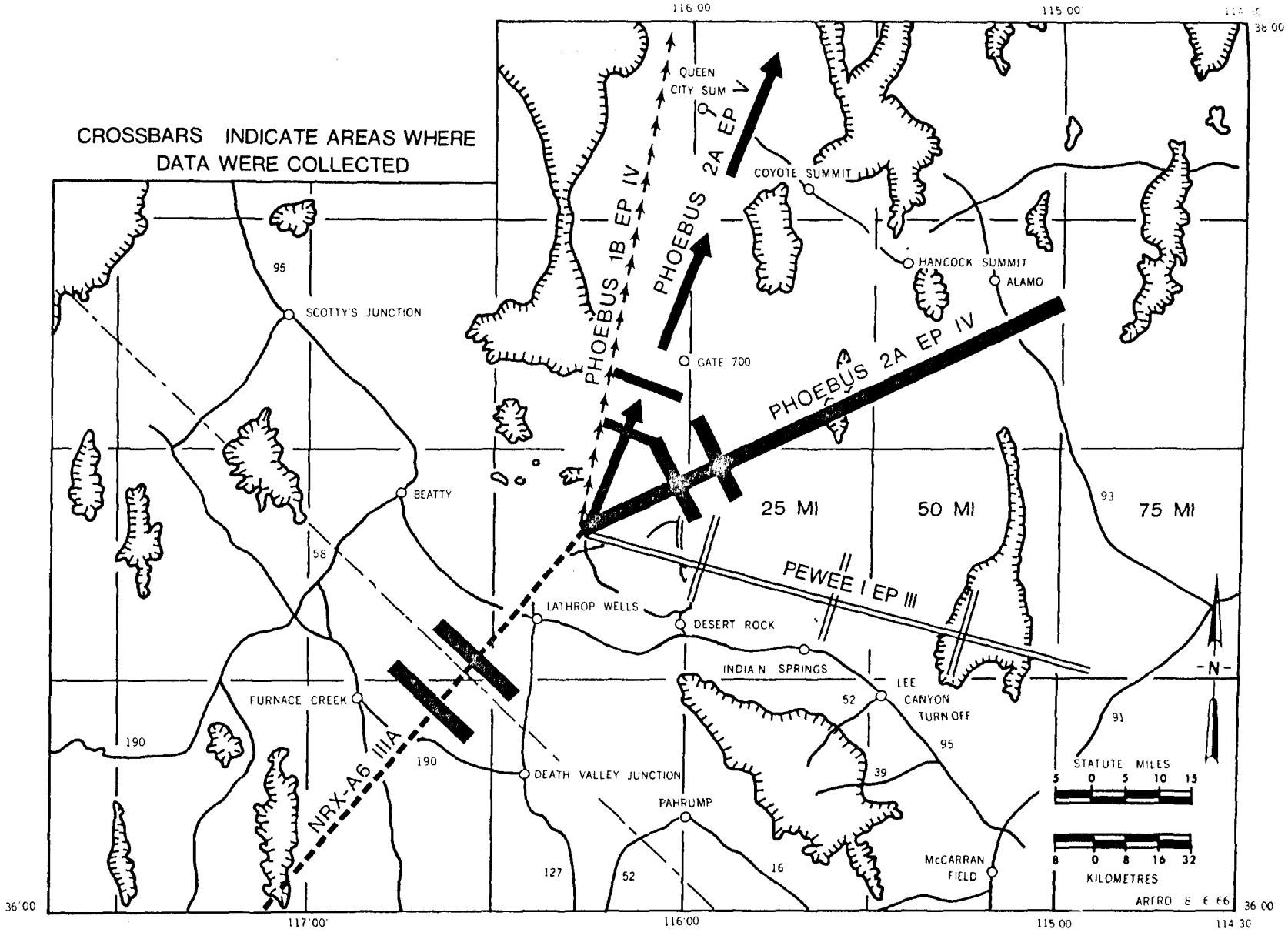

Cloud Centerlines for Reactor Engine Tests for Which Particle Deposition was Documented in Detail

together with the arcs on which particle data were collected. Particle sampling efforts for Phoebus-1B, EP-IV, were primarily devoted to locating the "hot-line" and determining concentrations along the centerline, rather than establishing lateral distribution about the centerline. Figure 14 indicates the particle concentrations observed by NERC-LV for the Pewee-I, EP-III test. Data for the other tests indicated in Figure 13 are in Appendix E.

NERC-LV data indicate particle concentrations for Pewee-I, EP-III, as high as 0.4 particles/m^2 at a distance of 38 miles,[110] somewhat higher values than NERC-LV reported for other tests at this distance. However, particle concentrations in themselves are not sufficient to appraise the hazards from particles. As outlined in Section IV, particle hazards have been evaluated in terms of the probability of receiving a specified skin dose at Krebs' depth. Initially, for operational purposes at NRDS, probabilities greater than one in ten thousand of receiving 1,500 rads at Krebs' depth were considered unacceptable in the off-site area. This dose value was later reduced to 750 rads.[16]* Figure 15 shows the potential probability of receiving the specified doses at Krebs' depth as a function of distance for NRX-A6, EP-IIIa; Phoebus-2A, EP-IV; Phoebus-2A, EP-V; and Pewee-I, EP-III; as estimated from particle data collected after the tests. The curve for Phoebus-2A, EP-IV, is the probability of receiving 1500 rads at Krebs' depth; the other three curves are calculated for a critical dose of 750 rads at Krebs' depth.

These probabilities were estimated using the ARL model and methods.[16] Kennedy and Henderson performed the calculations for Phoebus-2A, EP-IV, and Pewee-1, EP-III.[112] The curves for Phoebus-2A, EP-V and NRX-A6, EP-IIIa, were estimated from data reported by PAA[17,85] using the ARL model and values for the particle activity required to produce 750 rads at Krebs' depth calculated by Mikhail for XE Prime.[16] Comparison of curves of particle travel time versus particle activity required to produce

---

*See Section V on guides.

Figure 14

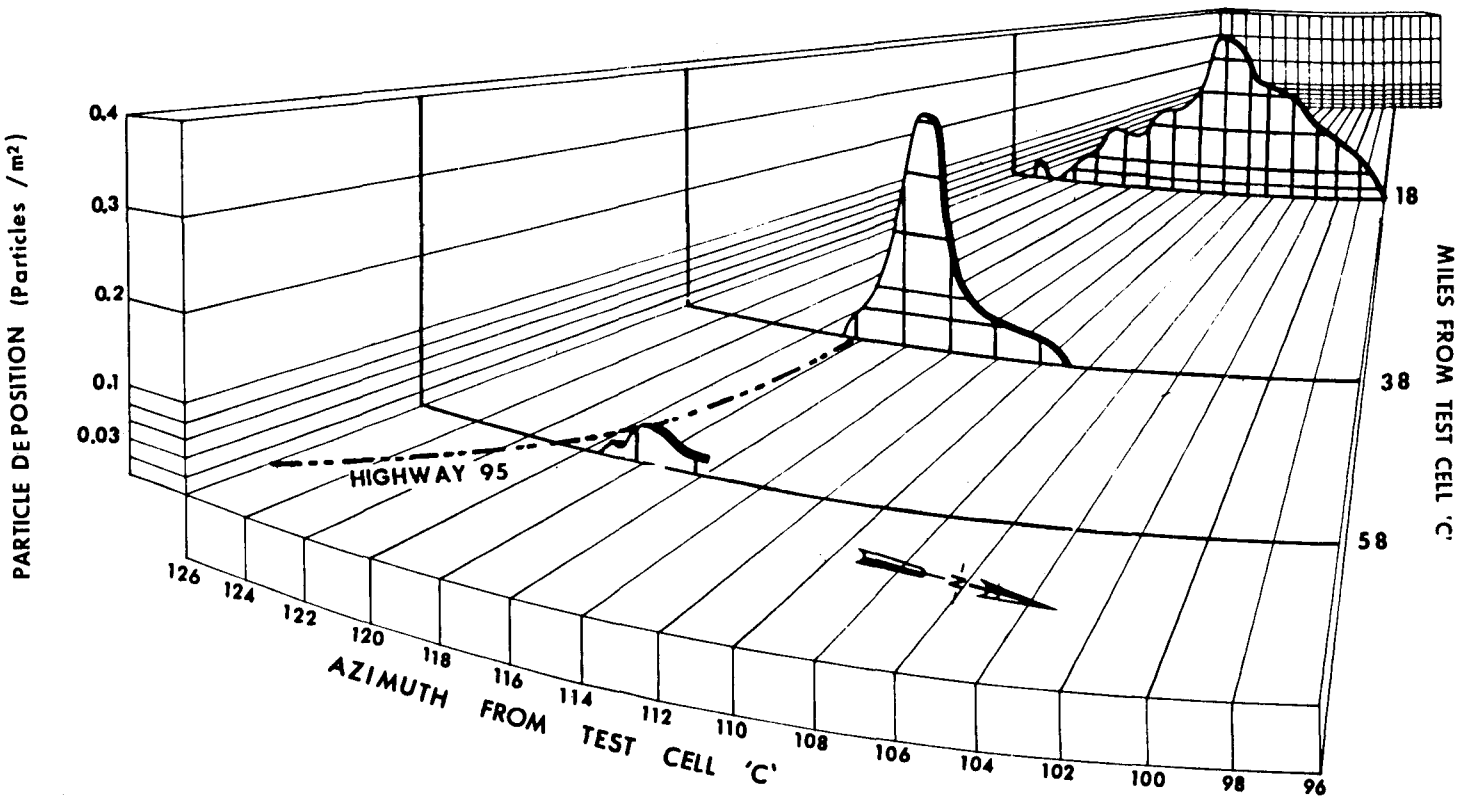

Three Dimensional Representation of
Particle Deposition for Pewee I, EP-III[110]

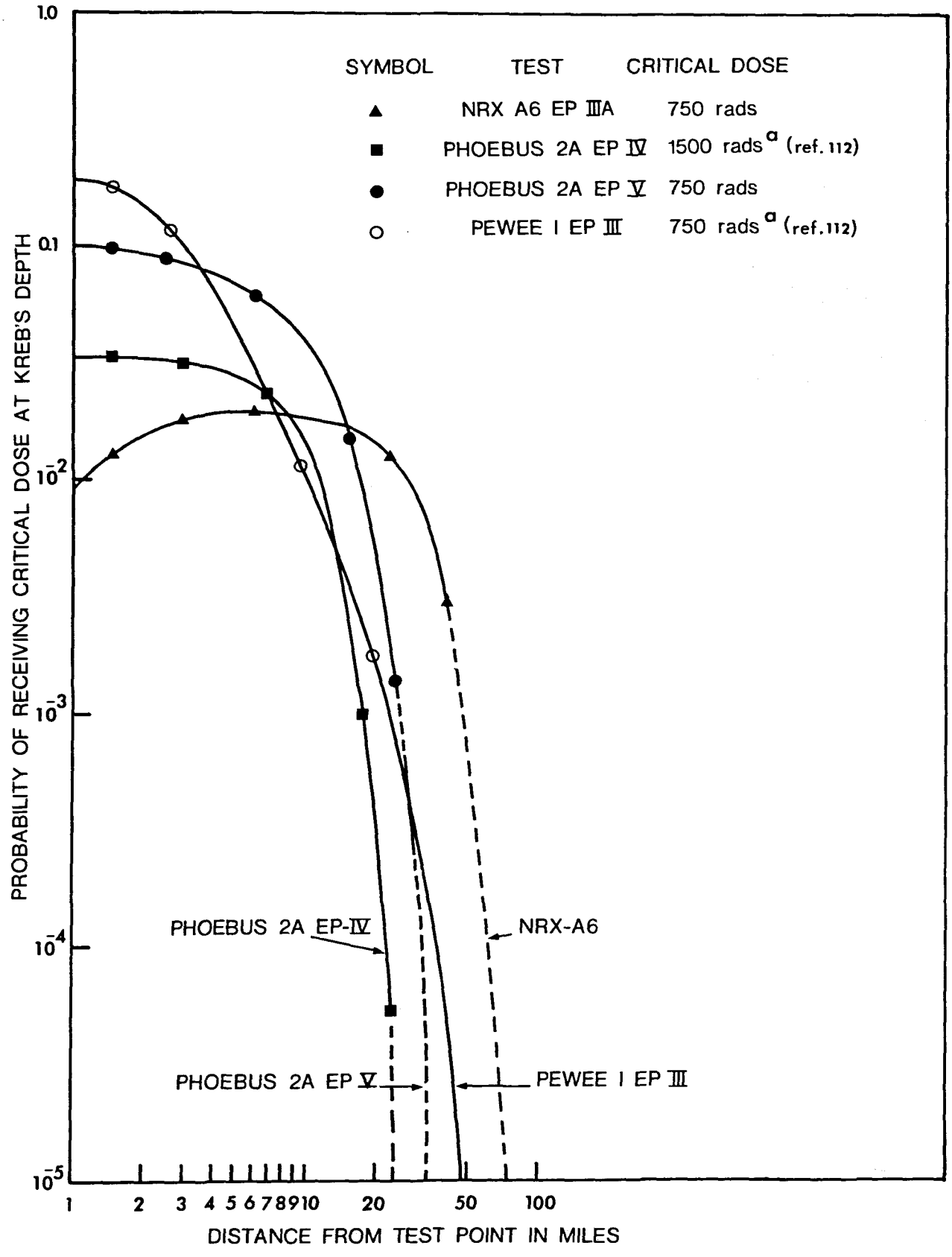

Figure 15 Probability of Receiving Critical Dose at Krebs Depth for Four Tests

750 rads at Krebs' depth for Pewee-I, EP-III,[91] (activity production time about one hour) with the corresponding curves for XE Prime, EP-V,[16] (activity production time about 6 minutes) indicated that the errors introduced by using the XE Prime curves for NRX-A6, EP-IIIa, and Phoebus-2A, EP-V, were relatively small, probably less than a factor of two.

For NRX-A6 (December 15, 1967) and Pewee-I, EP-III (December 4,1968), the exposed area of an individual was assumed to be 7.0×10^{-2} m^2, which corresponds to a dress style similar to Model A of Kochendorfer and Ulberg.[88] For the two Phoebus-2A runs (June and July 1968), the exposed area of the individual was assumed to be 0.384 m^2, corresponding to Model B of Kochendorfer and Ulberg.[88]

The data in Figure 15 indicate that the probability of receiving the critical dose (either 750 or 1,500 rads) at Krebs' depth exceeded 0.0001 at some locations in the off-site area for NRX-A6, EP-IIIa, and Pewee-I, EP-III (see Figure 16). The 0.0001 probability points for Phoebus-2A, EP-IV and EP-V, occurred at about 20 and 30 miles, respectively, from the test point; Figure 13 shows these points to be within the NRDS-NTS complex. For NRX-A6, EP-IIIa, off-site residents in the effluent trajectory within 25 miles of the test point were advised to stay indoors for at least one hour after the end of the test.[113] There were no residents in the range between 25 miles and 60 miles (the 0.0001 probability point for 750 rads). The 0.0001 probability point for Pewee-I, EP-III, occurred at about 40 miles and the effluent did not pass over any populated areas prior to reaching this distance.

There are no known instances of interaction of particles with individuals in the off-site area; although there are several instances of interaction of particles with NRDS test related personnel. These include the exposure of the individuals related to the Phoebus-1B, EP-IV, test[111]. Measurable biological effects from these interactions including erythema were not observed.

Henderson[17] analyzed particle deposition data collected for the five reactor tests where there was significant documentation (Phoebus-1B, EP-IV;

NRX-A6, EP-III; Phoebus-2A, EP-IV and EP-V; and Pewee-I, EP-III) by PAA, LASL, and NERC-LV. Maximum particle concentrations for these tests at each arc distance are plotted in Figure 16. Particle concentrations shown in Figure 16 have been normalized to all parameters in the scaling equation: wind speed, shear angle, and source strength (grams of uranium).

The downwind distance was normalized to the height of rise of the plume, which is an attempt to normalize the peak concentration for all runs at a constant dimensionless distance x/h (distance divided by release height). However, after normalization, there remains variations in the data of approximately an order of magnitude. Henderson[16] has indicated that some or all of this variation might be explained by taking into account the effects of terrain and variations in particle sizes. The lines on Figure 16 are indicative of the range of expected results, based on past data.

Values for the variables used in the normalizations shown in Figure 16 are given in Appendix F. Figure 16 can be used to scale particle deposition by forecasting normalization parameters.

VII. SUMMARY, CONCLUSIONS

This paper has reviewed the history of nuclear rocket reactor engine tests at the Nuclear Rocket Development Station, which adjoins the Nevada Test Site. The nuclear rocket engines tested during the period covered by this report, have primarily been based on single-pass hydrogen-cooled reactors with fuel rods of UC_2 (highly enriched uranium) beads in graphite matrices. NbC and other materials have been used for coolant channel coating to both protect the fuel and reduce the diffusion of fission products into the effluent.

The subject tests included planned radioactive effluent releases. Many of the changes and improvements in reactor design have been primarily intended to maintain reactor integrity and improve the operational characteristics of the reactor-power level, run-time, etc. In addition, these changes were intended to and did reduce the radioactive effluent releases.

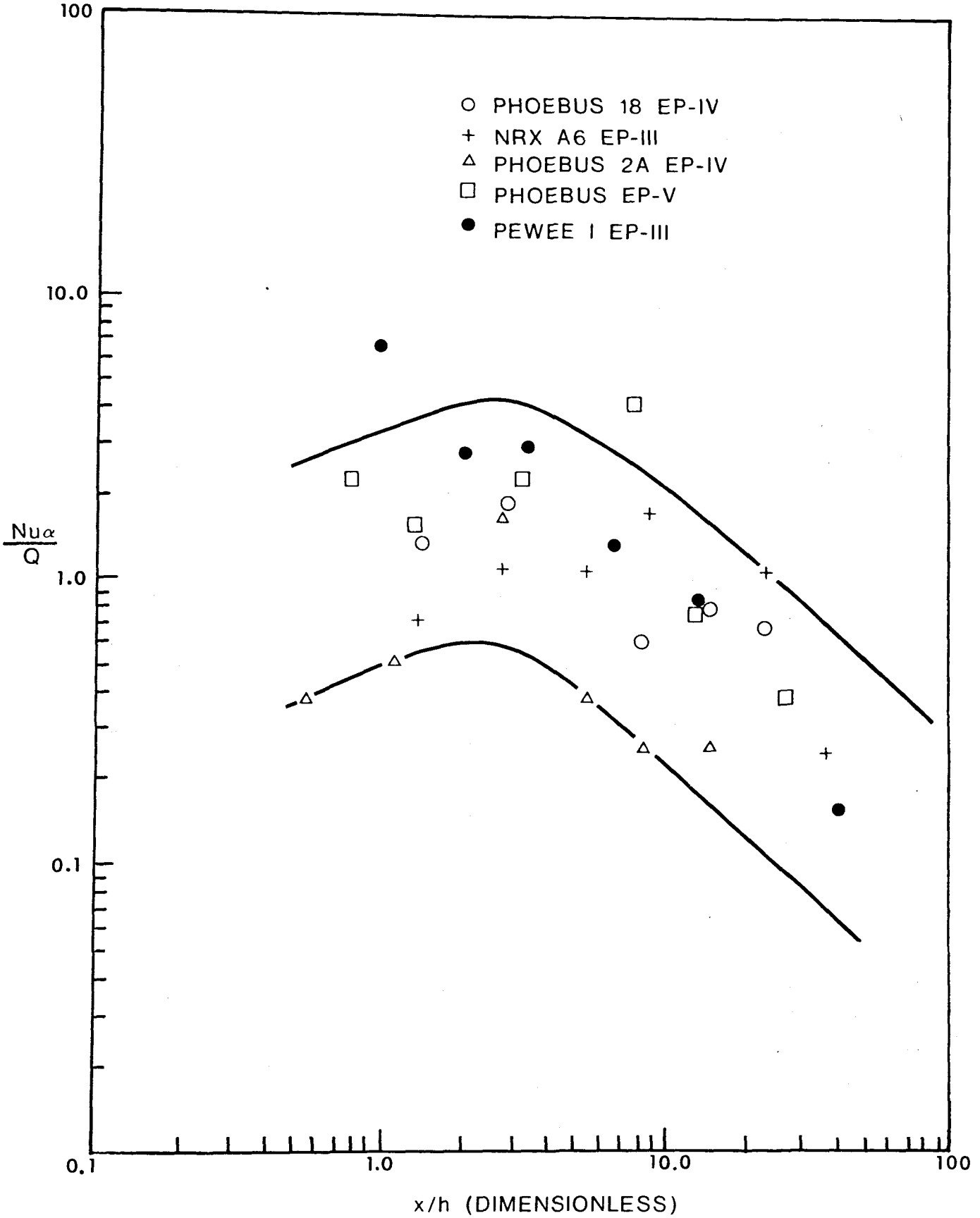

Figure 16 Normalized Maximum Particle Concentration[16]

The reactor effluent has been described under two categories: (1) fission products which migrated from the fuel into the coolant and were exhausted as gases and/or small particulate matter (micrometer size range)--denoted "aerosol effluent," and (2) discrete fuel fragments which were exhausted as a result of erosion, corrosion, and minor breakage of the fuel elements denoted as "particulate effluent." The potential effluent from reactivity insertion or loss of coolant accidents has also been considered. The accident effluent has been assumed to be characterized by the aerosol effluent, but has been postulated to be about an order of magnitude greater.

The biological or health implications of the effluent are evaluated by comparing effluent predictions and/or surveillance results to the appropriate radiation protection guides. Actual biological effects have not been observed at the low doses associated with the effluent from this program.

The surveillance results indicate that postulated hypothetical thyroid doses have been well below (roughly an order of magnitude) the FRC guides[56] and AEC standards[57,48,50,51,52]. The term postulated hypothetical doses refers to theoretical estimates which are based on environmental surveillance results (air, milk, etc.) which assume biological parameters for an infant---the critical receptor or person who might receive the highest potential dose.

Results from surveillance for discrete particles indicate that, although the administrative guide (less than a probability of 10^{-4} of a person receiving a Krebs' dose of 750 rads)[80,100,103,104] may have been exceeded in unpopulated areas, there have not been any reported interactions of particles with people in the off-site area. For the NRX-A6, EP-III test, the probability of 10^{-4} was exceeded in a populated area, but there was a specific operational field effort to request and insure that the off-site populace in the area of concern stayed indoors.[109] The guide[100,103,104] includes the latitude for use of appropriate countermeasures. It is concluded that off-site exposures or doses from nuclear

rocket engine tests at NRDS have been below the applicable guides. In general, it is felt that the program has been administered and conducted in a creditable manner and that the results reflect favorably on the management agencies. In reviewing the effluent program, several aspects were noted where possible improvements could be made. Potential areas for improvement include:

1. Consideration of the dose from ^{132}I resulting from the decay of ^{132}Te that is inhaled.
2. Additional investigation of techniques for estimating the external gamma dose from sky shine.
3. Resolve the remaining uncertainties related to the biological effects of human interaction with the particulate effluent. Proposed changes in fuel design, indicated in the preface, may cause these differences to be irrelevant to future nuclear rocket engine tests. The effluent from the nuclear furnace tests started in June 1972 was passed through a high-efficiency scrubber/filter system.

REFERENCES

1. Atomic Energy Commission and National Aeronautics and Space Administration. Environmental Statement, Reactor Testing, FY-1972. WASH-1508. (December 1971)

2. Atomic Energy Commission. Nuclear Propulsion for Space. Library of Congress 67-61704. Technical Information Center, P.O.Box 62, Oak Ridge, Tennessee. (February 1968)

3. Los Alamos Scientific Laboratory. Pewee I Effluent Effects Analysis. Memo P.V.Fultyn to H.T.Knight. (November 4, 1968)

4. Los Alamos Scientific Laboratory. Personal communication, E. A. Bryant and Luther Lyon. (May 1970)

5. Space Nuclear Systems Office. NRDS effluent data bank. Unpublished, undated manuscript received by the National Environmental Research Center, Las Vegas, June 1971.

6. Bryant, E.A., and A.E. Norris. Pewee 2 Fission Product Release Estimates. Los Alamos Scientific Laboratory, Los Alamos, New Mexico. (January 15, 1970)

7. Los Alamos Scientific Laboratory. Phoebus-2A Safety Analysis Report. JB-67-740, Sections 5.3 and 5.4. (July 1967)

8. Westinghouse Astronuclear Laboratories. NRX-A6 Safety Evaluation Report. WANL-TME-1633, Chapter 7. (October 1967)

9. Los Alamos Scientific Laboratory. Fission Product Release from a PH-2 Reactor. Memo E.A.Bryant to R.V.Fultyn. (August 8, 1967)

10. Westinghouse Astronuclear Laboratory. Source Term. Letter A. C. Sanderson to J. P. Jewett, Space Nuclear Systems Office. (October 28, 1969)

11. Southwestern Radiological Health Laboratory. Final Report of Aerial Surveillance for the NRX/EST, Experimental Plans IIB through IVA. Technical Information Center, P.O.Box 62, Oak Ridge, Tennessee. (May 1966)

12. Southwestern Radiological Health Laboratory. Final Report of Aerial Surveillance for the NRX-A5, EP-III and EP-IV. Technical Information Center, P.O.Box 62, Oak Ridge, Tennessee. (February 1967)

13. Fultyn, R.V. Effluent Effects Evaluation. Part of Pewee 2 Safety Analysis Report. Los Alamos Scientific Laboratory, Los Alamos, New Mexico. (Undated)

14. Southwestern Radiological Health Laboratory. Particulate Effluent Study Phoebus-1B, EP-IV. SWRHL-46r. Technical Information Center, P.O.Box 62, Oak Ridge, Tennessee. (April 1970)

15. Van Vleck, L. D. Summary of Results Effluent Monitoring Phoebus-1B, EP-IV. PAA-33-12. Pan American World Airways,Inc. (July 1967)

16. Henderson, Donald. Predicting Potential Skin Dose Effects Resulting from Particulates Released by Nuclear Rocket Engines. ARLV-351-6. Environmental Science Services Administration/Air Resources Laboratory, Las Vegas, Nevada. (September 1969)

17. Van Vleck, L. D. Summary of Results Effluent Monitoring Phoebus-2A, EP-IV and EP-V. PAA-33-31. Pan American World Airways, Inc. (December 1968)

18. Fultyn, R. V. Large Particles in the Phoebus-1B Effluent. LA-3799. Los Alamos Scientific Laboratory, Los Alamos, New Mexico. (June 1968)

19. Los Alamos Scientific Laboratory. Letter H.T.Knight to J.P.Jewett, Space Nuclear Systems Office. (October 10, 1968)

20. Strom, P. O., D. L. Love, A. H. Greendale, A. A. Delucchi, D. Sem, and N. E. Ballou. Nuclear Charge Distribution of Fission Product Chains of Mass Number 131-133. Phys. Rev. 144, 3, p. 984-993. (1966)

21. Katof, S. Fission Product Yields from Neutron-Induced Fission. Nucleonics 18:201. (1960)

22. Los Alamos Scientific Laboratory. Contribution to Pewee 2 Safety Analysis Report, transmitted L. L. Lyon to H. T. Knight. N-1-2537. (January 27, 1970)

23. Los Alamos Scientific Laboratory. Release of Fuel Beads from Phoebus-2A During EP-IV. Memorandum E. A. Bryant to distribution. (July 3, 1968)

24. Los Alamos Scientific Laboratory. Private communication, W. Stratton and R. V. Fultyn. (May 7, 1970)

25. Los Alamos Scientific Laboratory. Personal communication, W. Stratton. (May 11, 1970)

26. DiNunno, J. J., F. D. Anderson, R. E. Baker and R. L. Waterfield. Calculation of Distance Factors for Power and Test Reactor Sites. TID-14844. (March 1962)

27. Los Alamos Scientific Laboratory. Phoebus-2A Experimental Plan IV, Full Power Run. 64 J-17-393-68, pp 34. LASL, Mercury, Nevada. (June 26, 1968)

28. Coleman, R. D., and V. E. Andrews. Aerial Measurement of the Kiwi Transient Nuclear Test. Radiation Data and Reports 8:358-366. (July 1967)

29. Aerojet-General Corporation. Untitled, unpublished manuscript, Hugo Simens, Nuclear Rocket Development Station, Nevada. (1967)

30. Los Alamos Scientific Laboratory. The radioactive effluent from Pewee-I. A memorandum, E. A. Bryant. (December 27, 1968)

31. Quiring, R. F. Climatological Data, Nevada Test Site and Nuclear Rocket Development Station. ERLTM-ARL 7, UC-53, Meteorology. TID-4500. Environmental Science Services Administration. (August 1968)

32. Van Vleck, L. D. Meteorological Variables Applied to the Prediction of Dispersion from Nuclear Rocket Tests at the NRDS. PAA 33-25. Pan American World Airways, Inc. (June 1968)

33. Fultyn, R. V. A probabilistic scheme for predicting and evaluating hazards resulting from radioactive emissions to the atmosphere, and statistical nature of the radioactive effluent from ground tests of nuclear rocket engine prototypes. Proceedings of the Health Physics Society Symposium, Augusta, Georgia, January 1968. Environmental Surveillance in the Vicinity of Nuclear Facilities; edited by W. C. Reinig. Charles C. Thomas, Springfield, Illinois. (1970)

34. Briggs, G. A. Plume Rise, AEC Critical Review Series. Technical Information Center, P.O.Box 62, Oak Ridge, Tennessee. (1969)

35. Booth, H. G. The gas-cloud radiological dose prediction models used by ESSA in support of testing at the Nuclear Rocket Development Station. Environmental Science Services Administration/Air Resources Laboratory, Las Vegas, Nevada. Unpublished. (May 1968)

36. Air Resources Laboratory-Las Vegas, National Oceanic and Atmospheric Administration, Department of Commerce. Personal communication, Donald Henderson. (September 27, 1971)

37. Slade, D. H. (editor). Meteorology and Atomic Energy. Atomic Energy Commission. Technical Information Center, P.O.Box 62, Oak Ridge, Tennessee. (July 1968)

38. Wilson, D. A. Application of Diffusion Models to NRDS Effluent Released. A progress report. Environmental Science Services Administration/Air Resources Laboratory, Las Vegas, Nevada. (Unpublished May 1968)

39. Wilson, D. A. An Evaluation of Radiation Prediction Models Used by ARFRO at the NRDS. Environmental Science Services Administration/Air Resources Laboratory, Las Vegas, Nevada. (March 1967)

40. Stigall, G. E., and H. W. Calley. Summary and Analysis of Effluent Data from Nuclear Rocket Testing at the Nuclear Rocket Development Station. NUS-399, Vol. 1 and 2. NUS Corporation. (September 1967)

41. Environmental Science Services Administration/Air Resources Laboratory. A Fallout Scaling Model for the Prediction of Gross Gamma Dose Rates from Earth Cratering Detonations. An unpublished manuscript, F. D. Cluff and T. Palmer. ESSA/ARL, Las Vegas, Nev.(1964)

42. Hughes, D. C. Nuclear Construction Engineering Technology. NCG Technical Report No. 2. U. S. Army Nuclear Cratering Group, Livermore, California. (September 1968)

43. Altomare, P. N., and J. R. Coleman. Study of Particulate Effluent from Nuclear Rocket Engine Test. NUS Corporation. (September 1967)

44. Van der Hoven, I. A Diffusion Deposition Model for Particulate Effluents from Ground-Tested Nuclear Engines. Int., J. Air, Water Pollution 7:1023-32. Pergamon Press. (1963)

45. Southwestern Radiological Health Laboratory. Final Report of Off-Site Surveillance for the Phoebus-1B Reactor, EP-I, EP-II, EP-III, EP-IV Test Series. SWRHL-45r. Technical Information Center, P.O.Box 62, Oak Ridge, Tennessee. (July 1969)

46. Southwestern Radiological Health Laboratory. Final Report of Off-Site Surveillance for the NRX-A4/EST Test Series. SWRHL-30r. Technical Information Center, P.O.Box 62, Oak Ridge, Tennessee. (September 1966)

47. Southwestern Radiological Health Laboratory. Final Report of Off-Site Surveillance for the NRX-A5 Test Series. SWRHL-32r. (October 1968)

48. Bernhardt, D. E., and J. R. McBride. Normal Run and the Accident Case for a Nuclear Rocket Engine. Proceedings of the International Congress on the Diffusion of Fission Products, Saclay, France.(Nov.1969)

49. Southwestern Radiological Health Laboratory. Final Report of Off-Site Surveillance for the NRX-A2 Experiment. SWRHL-16r, p. 15. (Feb.3, 1965)

50. Grossman, R. F. Summary of Hypothetical Whole-Body Gamma Exposures and Infant Thyroid Dose Resulting Off-Site from Project Rover Nuclear Reactor Engine Tests at the Nuclear Rocket Development Station. SWRHL-92r. (August 1970)

51. Griffiths, P., and P. B. Erickson. Radiological Prediction and Monitoring of Tests at the Nuclear Rocket Development Symposium of the Institute of Electrical and Electronic Engineers, Space Nuclear Systems Office. (October 1969)

52. Goldman, M. I. Safety Aspects of Ground Testing for Large Nuclear Rockets. Nuclear Applications 2:94-98. (April 1966)

53. Kochendorfer, D. B. Calculated Activities of U-235 Fission Products for Very Short Nuclear Reactor Operation. USNRDL-TR-757, Vols. 1 and 2 (June 1964)

54. Westinghouse Astronuclear Laboratory. Rover Program Reactor Tests p. III-1, Performance Summary, NRX-A1 through NRX-A6. WANL-TME-1788. (July 1968)

55. Bernhardt, D. E. Milk-to-Air Ratios for Iodine-131 Concentrations (Project Rover). Proceedings of the Health Physics Society Symposium, Augusta, Georgia, 1968. Environmental Surveillance in the Vicinity of Nuclear Facilities; edited by W. C. Reinig. Charles C. Thomas, Springfield, Ill. (1970)

56. Federal Radiation Council. Background Material for the Development of Radiation Protection Standards, Report 1 (May 1960), Report 2 (September 1961), Report 5 (July 1964) and Report 7 (May 1965).

57. Atomic Energy Commission. Standards for Radiation Protection, USAEC Manual Chapter 0524. (November 8, 1968)

58. Stocum, W. E. Variability in the Parameters Used to Predict the Dose to the Thyroid from the Ingestion of Iodine-131 in Milk. Proceedings of the Health Physics Society Symposium, Augusta, Georgia, 1968. Environmental Surveillance in the Vicinity of Nuclear Facilities; edited by W. C. Reinig. Charles C. Thomas, Springfield, Ill. (1970)

59. International Commission on Radiological Protection. Report of Committee II on Permissible Dose for Internal Radiation. ICRP Publication 2. Pergamon Press. (1959)

60. Southwestern Radiological Health Laboratory. Ingestion of Iodine-131 from Food Products Other Than Milk. Memorandum to the Files, D. E. Bernhardt. (June 5, 1968)

61. Fultyn, R. V. Environmental Effects of the Kiwi-TNT Effluent: A Review and Evaluation. LA-3449. Los Alamos Scientific Laboratory. (April 1968)

62. Southwestern Radiological Health Laboratory. Kiwi-B Report, U. S. Public Health Service Off-Site Radiological Safety Organization. Distributed December 7, 1961.

63. Fitzsimmons, C. K., and W. H. Horn. Environmental Monitoring with Thermoluminescent Dosimeters. SWRHL-58r. Technical Information Center, P. O. Box 62, Oak Ridge, Tennessee. (1969)

64. Thompson, J. C. Comparison of Iodine-131 Intake from Milk and Foods. Health Phys. 14:483-489. (May 1968)

65. Imai, K., and T. Iijima. Assessment of Gamma Exposure Due to a Radioactive Cloud Released from a Point Source. Health Phys. 18:207-216. (March 1970)

66. Alonso, A. Generalization of Holland's Method to Assess Gamma Doses from Radioactive Clouds. Health Phys. 13:487-494. (May 1967)

67. Glasstone, S. Principles of Nuclear Reactor Engineering. D. Van Nostrand Co., Inc. (1958)

68. Glasstone, S., and A. Sesonski. Nuclear Reactor Engineering. D. Van Nostrand Co., Inc. (1963)

69. NUS Corporation, Environmental Safeguards Division. Effluent Report for the NRX/EST Test Series. NUS-311. (October 1966)

70. Space Nuclear Systems Office. Standard Effluent Concentration to Dose Conversion Factors for Rover Reactor Operations at NRDS. Letter R.S.Decker to B.P.Helgeson, April 1, 1966.

71. Hine, G. J., and G. L. Brownell. Radiation Dosimetry. Academic Press, Inc. (1956)

72. Bunch, D. F. (editor). Controlled Environmental Radioiodine Tests, Progress Report No. 2. IDO-12053, TID-4500. USAEC. (August 1966)

73. Hawley, C. A. (editor). Controlled Environmental Radioiodine Tests at the National Reactor Testing Station, 1965 Progress Report. IDO-12047. USAEC. (February 1966)

74. Stocum, W. E. Conversion Factors for the Child Thyroid Dose in the H-8 Prediction Model. LASL H-8 Division letter, H-8 M1045. Los Alamos Scientific Laboratory. (April 3, 1968)

75. Atomic Energy Commission. Conclusions of the Division of Biology and Medicine/Space Nuclear Safety Advisory Committee. Letter W. E. Lotz to D. S. Gabriel, June 6, 1968.

76. Mikhail, S. Z., and K. A. Collins. Analysis of the Particulate Effluent Data from Phoebus-1B, EP-IV Nuclear Reactor Test. USNRDL-TR-69-76. Naval Radiological Defense Laboratory. (July 15, 1969)

77. Sanders, C. L., R. C. Thompson and W. J. Bair. Carcinogenesis in the Lung from Inhalation of Radioactive Particles. NRDL-TRC-69-8. Battelle Memorial Institute, Pacific Northwest Laboratory (contract with the Naval Radiological Defense Laboratory. (March 18, 1969)

78. Mikhail, S. Z., and K. A. Collins. NRX-A6, EP-III Propulsion Reactor Test: Characteristics of Particulate Effluent and Comparison to Phoebus-1B, EP-IV. NRDL-TR-69-76. Naval Radiological Defense Laboratory. (July 15, 1969)

79. Dean, P. N., and W. H. Langham. Tumorigenicity of Small Highly Radioactive Particles. Health Phys. 16:79-84. (1969)

80. Krebs, J. S. The Response of Mammalian Skin to Irradiation with Particles of Reactor Debris. USNRDL-TR-67-118. Naval Radiological Defense Laboratory. (September 1967)

81. Dean, P. N., J. Langham and L. M. Holland. Skin Response to a Point Source of Fissioned Uranium-235 Carbide. Health Phys. 19:3-7. (July 1970)

82. Forbes, P. D. Acute Effects on Skin Produced by Radioactive Microspheres: A Progress Report. Undated, unpublished manuscript. The Skin Cancer Hospital, Temple University, Health Sciences Center, Philadelphia, PA. (USNRDL contract No. NOO-228 68C571).

83. Deposition and Retention Models for Internal Dosimetry of the Human Respiratory Tract. By the Task Group on Lung Dynamics for Committee - II of the International Commission on Radiological Protection. Health Phys. 12:173-207. (1966)

84. Southwestern Radiological Health Laboratory. Particulate Effluent Study - Phoebus 2A, EP-IV and EP-V. SWRHL-60r. (June 1969)

85. Pan American World Airways, Inc. Summary of Results Effluent Monitoring NRX-A6, EP-IIIa. PAA33-21. (April 15, 1968)

86. Sanders, C. L., R. C. Thompson and W. J. Bair. Lung Cancer: Dose Response Studies with Radionuclides. CONF-691001. AEC Symposium Series 18. Technical Information Center, P.O.Box 62, Oak Ridge, Tennessee. (April 1970)

87. Booz-Allen Applied Research, Inc. Empirical Relationships Between Deposition on Mannikins and Ground Contamination density from Particulate Clouds. Special memorandum No. 4 to Systems Analysis Division, Chemical Research and Development Laboratories, Edgewood Arsenal, MD. (1963)

88. Kochendorfer, D. B., and J. C. Ulberg. Human Exposure to Particulate Debris from Aerospace Nuclear Applications. USNRDL-TR-67-59. Naval Radiological Defense Laboratory. (June 8, 1967)

89. DeAgazio, A.W. Dose Calculation Models for Re-Entering Nuclear Rocket Debris. NUS-229. NUS Corporation. (May 1965)

90. Space Nuclear Systems Office, Naval Radiological Defense Laboratory. Rover Flight Safety Program Preliminary Review. IV. Safety Analysis Report: Radiological Considerations in Nuclear Flight Safety. USNRDL-TR-1010.(April 20, 1966)

91. Environmental Science Services Administration/Air Resources Lab. Post-Run Probability Calculation for Pewee I, EP-III. Memorandum D. Henderson to R. Nelson, Space Nuclear Systems Office. (Mar.26, 1969)

92. Ulberg, J. C., and D. B. Kochendorfer. Models for Estimating Beta Dose to Tissue from Particle Debris in Aerospace Nuclear Applications. USNRDL-TR-1107. Naval Radiological Defense Lab. (Dec. 12, 1966)

93. Federal Register. Standards for Radiation Protection, Title 10, Code of Federal Regulations, Part 20.

94. Atomic Energy Commission. Radiological Protection Criteria at the Nevada Test Site. Memorandum N. H. Woodruff, Director, AEC Division of Operational Safety, to J. E. Reeves, Manager, AEC Nevada Operations Office. (August 1, 1962)

95. Space Nuclear Systems Office. Radiation Dose Guides for Reactor Engine Test Approvals. Memorandum M. Klein, Manager, Space Nuclear Systems Office, to J. P. Jewett, Space Nuclear Systems Office-Nevada. (July 26, 1967)

96. Atomic Energy Commission. Off-NTS Radiological Safety Criteria for Reactor Runs at NRDS. Memorandum R. E. Miller, Manager, AEC Nevada Operations Office, to M. B. Biles, Director, AEC Division of Operational Safety. (June 26, 1969)

97. National Committee on Radiological Protection. Maximum Permissible Body Burdens and Maximum Permissible Concentrations of Radionuclides in Air and in Water for Occupational Exposure. National Bureau of Standards Handbook 69. (June 5, 1959)

98. National Council on Radiation Protection and Measurements. Basic Radiation Protection Criteria. NCRP Report No. 39. (Jan. 1971)

99. Federal Register. Reactor Site Criteria. Title 10, Code of Federal Regulations, Part 100. (April 5, 1966)

100. Space Nuclear Systems Office. Additional Radiation Criteria. Memorandum M. Klein, Manager, SNSO, to J. P. Jewett, SNSO-N, (May 20, 1968)

101. Forbes, P. D., and S. Z. Mikhail. Acute Lesions in Skin Produced by Radioactive Microspheres. Final Report, Contract SNSO-49. (April 1970)

102. Los Alamos Scientific Laboratory, Biological and Medical Research Group. Some Biological Aspects of Radioactive Microspheres. LA-3365-MS. (August 23, 1965)

103. Space Nuclear Systems Office-Nevada. Radiation Dose Guides. Memorandum J. P. Jewett to Milton Klein, Manager, SNSO. (January 1969)

104. Space Nuclear Systems Office. Particle Guides. Memorandum Milton Klein, Manager, SNSO, to J. P. Jewett, SNSO-N. (January 1969)

105. Southwestern Radiological Health Laboratory. Final Report of Off-Site Surveillance for the Phoebus-1A Experiment. SWRHL-19r. Technical Information Center, P.O.Box 62, Oak Ridge, Tennessee. (Jan. 1966)

106. Pan American World Airways, Inc. Personal communication, L. D. Van Vleck. (1970)

107. Southwestern Radiological Health Laboratory. Particulate materials. Memorandum D. N. McNelis to D. S. Barth. (Oct. 18, 1966)

108. Pan American World Airways, Inc. Summary of Results Effluent Monitoring Pewee I, EP-III. PAA 40-1. (March 24, 1969)

109. Southwestern Radiological Health Laboratory. Particulate Effluent Study of NRX-A6, EP-IIIA. SWRHL-57r. Technical Information Center, P.O.Box 62, Oak Ridge, Tennessee.

110. Southwestern Radiological Health Laboratory. Particulate Effluent Study, Pewee I, EP-III. SWRHL-66r. (in press)

111. Pan American World Airways, Inc. On-site Report for the Phoebus-1B Reactor Test Series. PAA 33-13. (August 18, 1967)

112. Kennedy, N. C., and D. Henderson. NRDS Radiation Prediction Model Evaluation. Environmental Science Services Administration/Air Resources Laboratory. Report No. ARLV-351-7. (June 1970)

113. Southwestern Radiological Health Laboratory. Final Report of Off-Site Surveillance for the NRX-A6 Test Series. SWRHL-78r. (August 1971)

114. Space Nuclear Systems Office. TWX concerning particle guides, J. P. Jewett, SNSO-N, to Milton Klein, Manager, SNSO. (Dec.2, 1968)

115. Spencer, L. V. National Bureau of Standards Monogr. 1. (1959)

116. Mikhail, S. Z. Tissue Beta Radiation Doses from Particulate Fission Product Sources: Comparison of Model Predictions with Experimental and Monte Carlo Values. ESA-TR-70-1. Environmental Science Associates. (May 1970)

117. Space Nuclear Systems Office. Particle Study. Letter S. Z. Mikhail, Naval Elect. Lab., to R. Nelson, SNSO-N. (Oct. 7, 1969)

118. Eve, I. S. A Review of the Physiology of the Gastrointestinal Tract in Relation to Radiation Doses from Radioactive Materials. Health Phys. 12:131-161. (February 1966)

119. Dolphin, G. W., and I. S. Eve. Dosimetry of the Gastrointestinal Tract. Health Phys. 12:163-172. (February 1966)

120. Coleman, J. R., and L. J. Perez. Consideration of Dose Models for the Eye and Lung from Nuclear Rocket Particulate Effluent. NUS-467. NUS Corporation. (May 15, 1968)

121. International Commission on Radiological Protection. Radiosensitivity and Spatial Distribution of Dose. Committee I. ICRP Publication 14. Pergamon Press. Glasgow. (1969)

122. Southwestern Radiological Health Laboratory. Personal communication, R. E. Stanley. (1970)

123. Los Alamos Scientific Laboratory. Personal communication, W. H. Langham. (May 1970)

124. Coleman, J. R., and L. J. Perez. Radiological Safety Studies of Space Nuclear Systems--Fourth Quarterly and Final Report. SC-CR-67-2729. Sandia Corporation. (October 1967)

125. Pestaner, J. F., D. A. Kubose and W. R. Balkwell. Beta Dose Rates from Neutron-Irradiated Uranium-235 Carbide Particles. USNRDL-TR-1082. Naval Radiological Defense Laboratory. (June 30, 1966)

126. Richmond, C. R., J. Langham and R. S. Stone. Biological Response to Small Highly Radioactive Sources. Health Phys. 18:401-408. Pergamon Press. (1970)

127. Altomare, P. M., L. J. Perez and J. R. Coleman. Method Applied for Calculation of Probability of Cataract and Probability of Exceeding Krebs' Depth Dose for Phoebus-2A, EP-IV. NUS Corporation. (June 20, 1968)

APPENDICES

Appendix	Title	Page
A.	Population and Milk Cow Distribution.	104
B.	Models and Information Related to Potential Biological Effects of Radioactive Particles.	105
B-1.	Acute Lesions in Skin Produced by Particulate Effluent.	106
	Dose Calculation Techniques.	106
	Results of Experiments.	108
	Summary of Particle Skin-Bioeffects Experiments.	110
	Summary.	113
B-2.	Potential Dose to the GI Tract from Particulate Material.	114
B-3.	Mathematical Models for Predicting Effects On the Lung From Inhalation and Deposition of Radioactive Particles.	117
	Introduction.	117
	Deposition of Particles in the Respiratory System.	118
	Estimation of Dose to the Lung from Deposited Material.	120
	Biological Effects of Doses to the Lung from Particulates.	121
B-4.	Model Used for Calculation of Probability of Cataract from Deposition of Particle in Eye.	122
	Schematic Drawings of the Model Eye.	123
	Anatomical Constants for Model Eye.	124
	Probability of Cataract Per Particle for Various Locations and Residence Times in the Eye as a Function of Total Particle Activity at Time of Deposition.	126
	Average Number of Particles Deposited in Eye Region Per Unit Air Concentration Versus Wind Speed.	129

Appendix	Title	Page
C.	Dosimetry and Air Surveillance Network Stations.	130
D.	Reactor Engine Tests at NRDS from Which Airborne Radioactivity was Detected Outside the Test Range Complex.	132
E.	Deposition Measurements and Survey Results.	140
F.	Particle Concentrations and Normalization Parameters.	145

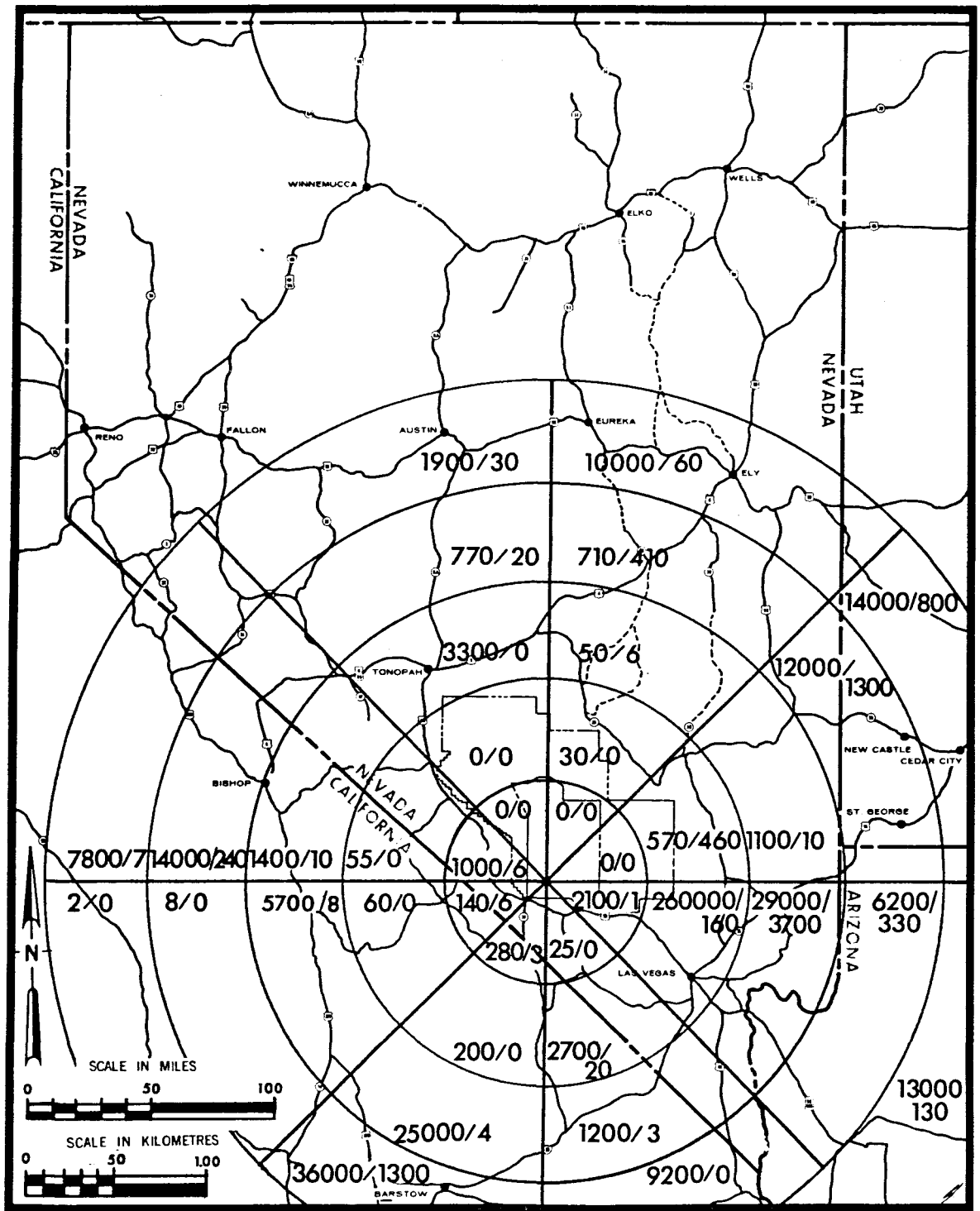

Figure A-1 Population and Milk Cow Distribution

APPENDIX B

MODELS AND INFORMATION RELATED TO POTENTIAL BIOLOGICAL EFFECTS OF RADIOACTIVE PARTICLES

1. Acute lesions in skin produced by particulate effluent.

2. Potential dose to the GI tract from particulate material.

3. Mathematical models for predicting effects on the lung from inhalation and deposition of radioactive particles.

4. Model used for calculation of probability of cataract from deposition of particle in eye.

APPENDIX B - 1. Acute Lesions in Skin Produced by Particulate Effluent.

This appendix includes information which supplements the information in Section V on guides for the particulate effluent.

Based on considerations of the area of skin irradiated and the characteristics of skin from the standpoint of biological effects, Krebs[80] proposed what has become known as Krebs' Dose. This is the dose at the periphery of a circular field of 4 mm in radius at a depth of 100 μm below the surface of the skin. The center of the field is the point on the surface of the skin where the particle rests. He postulated that Krebs' doses of less than 1500 rads would not produce serious skin lesions.

In 1968 preliminary results from experiments conducted by Forbes and Mikhail[82,101] and the Biomedical Research Group of LASL[81,102] indicated the need for reconsidering the dose guide for the skin. The experiments were based on implanting irradiated pyrolytic graphite-coated UC_2 beads on the shaved skin of monkeys and humans (LASL), and pigs (Forbes).

Based on the preliminary results of these experiments[81,82,101,102] the particle dose guide was reduced to 750 rads Krebs' dose.[103,104,114]

Dose Calculation Techniques

The following reviews briefly compares the dose calculation techniques used by the investigators.

Three types of dose calculations were made:

1. Beta dose at the surface of the particle.
2. Beta dose at the pstulated depth of the basal or germinal cell layer--100 μm.
3. The dose at the periphery of a 4 mm circular plane at a tissue depth 100 μm below the particle, Krebs' dose.

The Krebs' criterion has been used as a normalizing tool for presenting the results from particles of various sizes for the various studies referenced in this paper. The basal layer dose is also given. The surface dose has received limited use. Since the surface skin is composed of dead cells and the point dose gives no consideration to area distribution of the dose, it has limited biological meaning.

The LASL dose calculation technique is given in References 81 and 102. In summary the beta energy spectrum is measured using a plastic scintillator, the dose rate is then computed based on energy loss values for 100 keV intervals and integrated.[81,115] The dose at 100 μm is calculated based on exponential absorption.

The doses reported by Krebs and Mikhail are based on a determination of the number of fissions that have occurred in the particle using a specially calibrated high pressure ionization chamber and a combination of computer codes produced by the former Navy Radiological Defense Laboratory (NRDL) and known as the Transmission-Degradation-Dissipation (TDD) beta dose model. The first code estimates the build-up and decay of the fission products and a second code computes the beta energy spectrum for each beta emitting nuclide. A third code computes a composite spectrum weighted for the quantity of each nuclide present. A fourth code calculates the energy loss by self-absorption within the particle and a fifth code then gives the beta radiation emitted by the particle. A sixth code computes the beta depth-dose-rate in tissue and the integrated dose.[101]

Mikhail[116] has performed several evaluations of the NRDL model and compared it to the LASL model. In summary, there is good agreement between the LASL and NRDL models and between the NRDL model and empirical measurements. The following summarizes some of the conclusions:

1. A comparison of the NRDL and LASL techniques for calculating the basal layer dose (100 μm skin depth) for 11 particles indicated the maximum difference (difference/average) was 33 and the average difference was 27%. The NRDL dose estimate was always larger than the LASL estimate.[117]

2. An evaluation of the TDD NRDL program indicated that it gave invariably higher results than empirical experiments for shallow tissue depths (range of 100 μm).[116] The TDD doses ranged to roughly 50% higher than the measured doses (varied with particle size, radioactive decay, tissue depth, etc.). This gives reasonable confirmation for the LASL dose estimates.

The various dose models are in reasonable agreement. The apparent bias of the TDD model towards higher results is acceptable if it is used for both estimating the doses versus biological effects and the evaluations for hazards from reactor operations; as is presently done. Mikhail[116] discusses the possible biases in the model and these will not be discussed here.

The estimates for Krebs' doses for the LASL results were determined in several ways:

1. For the third experiment with monkeys, Dean, et al.,[81] the Krebs' dose was calculated by Mikhail using the TDD program.[117]
2. For the human experiments the Krebs' dose was estimated from a plot of particle size versus the ratio of the basal layer dose to the Krebs' dose (based on Mikhail's data in item one above).
3. For the first two experiments with monkeys, actual particle sizes were not reported.[102] The ratio of the LASL basal layer dose versus Krebs' dose for a 150 μm (a range of 140 to 160 μm was given) particle was used per the information in items 1 and 2 above. This ratio was 400.

Results of Experiments

The preliminary results of these studies indicated that the skin lesions did not fall into the four categories indicated by Krebs.[88] Rather, moist desquamation and ulceration did not appear to be separate entities, but merged together.[101] Thus, for simplicity the single term "ulceration" will be used.

The following sections summarize the results of the respective studies. Table B-1 indicates the particle size used, the resulting doses, and the lesion produced for all of the experiments. LASL, Experiments by Dean, et al.: [81,102]

1. The study utilized UC_2 beads of 100-200 μm in diameter which were placed on the skin of humans and monkeys. The resulting doses were calculated at a point 100 μm below the particle and at the skin surface. The LASL work is essentially composed of four experiments: two in 1965 on monkeys (basal skin layer dose ranged from 1,300 to 52,000 rads or 3 to 130 rads Krebs' dose); one on human skin in 1965 (basal skin layer dose ranged from 14,000 to 54,000 rads or 40 to 130 rads Krebs' dose); and a recent one on monkey skin with basal skin layer doses of 157,000 to 664,000 rads or 470 to 2,700 rads Krebs' dose.*
2. Ulceration, or moist desquamation, was observed at all sites with basal point doses of 261,000 rads or Krebs' dose of 850 rads or higher. The lesions remained open for approximately two days after exposure. Epithelization was complete by 71 days after exposure, the residual effect being a dimple.
3. Skin sites receiving less than a 261,000 rad basal layer dose showed only a dry desquamation over an area of 3-4 mm in diameter.
4. The LASL results bracketed the minimum dose which produced a moist desquamation and/or ulcer.

Forbes' and Mikhail's Experiments Using Pigs: [101]

1. Forbes' experiments dealt with implacement of 12 irradiated particles on pig skin. The particles ranged from 140-328 μm

*The LASL studies were not based on the concept of Krebs' dose. Estimates of Krebs' doses for the LASL studies are based on calculations, using LASL data, by Mikhail (Ref.117) or estimates by the authors of this paper using a plot of particle size versus the ratio of the basal layer dose to the Krebs' dose.

TABLE B-1. SUMMARY OF PARTICLE SKIN-BIOEFFECTS EXPERIMENTS.

Particle Size (μm)	Dose at Basal Layer (KRAD) NRDL	LASL	Calc by NRDL*	Krebs' Dose (RAD)	Ulcer Dia. (mm)	Type Lesion	Experimental Animal
Forbes & Mikhail[101]							
148	240			405	0.5	Ulcer-ation	Pig
140	286			444	0.5		
145	488			770	1		
153	514			771	2		
144	563			921	0.5		
148	569			944	0.5		
152	642			060	2		
154	717			210	2		
150	1370			310	3		
283	1230			400	4		
305	1530			320	5		
308	1510			490	5		
295	2350			10,980	5		
304	2320			11,100	5		
282	3550			15,100	6		
294	3800			17,300	6		
328	3850			19,800	7		
149	7400			35,200	8		
298	1700			28,900	4		
LASL--First Monkey Experiment(102)							
140-160		1.3	Not Calc.	3		Erythema	Monkey
		2.0		5			
		2.8		7			
		3.4		9			
		4.1		10			
		4.5		10			
		4.9		10			
		5.4		10			
		7.9		10			
		7.0		10			
		7.5		20			
		8.9		20			
		9.6		20			

TABLE B-1. Summary of Particle Skin-Bioeffects Experiments. (continued)

Particle Size (μm)	Dose at Basal Layer (KRAD) NRDL	LASL	Calc by NRDL*	Krebs' Dose (RAD)	Ulcer Dia. (mm)	Type Lesion	Experimental Animal
LASL--Second Monkey Experiment (102)							
140-160		15.8	Not Calc.	40		Erythemia	Monkey
		19.5		50			
		21.5		50			
		23.8		60			
		29.3		70		Possibly--Dry Desquam.	
		29.5		70			
		31.4		80			
		45.8		110			
		52.1		130			
LASL--Human Experiment (81)							
174		14.2	Not Calc.	43		Erythemia	Human
159		40.0		110		Erythemia	
140		54.0		130		Erythemia-Dry Desquam.	
LASL--Third Monkey Experiment (81)							
172		157	220	470		Dry Desquam.	Monkey
174		173	230	500			
186		242	320	770			
184		261	350	850		Ulceration	
186		270	360	890			
184		289	390	950			
191		313	420	1,100			
225		351	430	1,400			
204		472	600	1,800			
215		458	590	1,800			
213		664	870	2,700			

* Calculated from NRDL fission product beta dose calculation code.[116] The NRDL dose estimates for LASL experiments are presented to allow normalization of all of the data.

in diameter. Based on the Krebs' dose criteria, the doses ranged from 400 to 35,000 rads and the basal layer point doses from 240,000 to 7,400,000 rads.

2. The minimum dose used in the experiments, 400 rads (Krebs' dose), produced a small ulcer.
3. The authors suggested using ulcer size as a biological end-point versus ulceration, etc.
4. The various biological responses versus dose were evaluated. Straight line plots of lesion diameter versus the log of the dose resulted in correlation coefficients of 0.94 and 0.98, respectively, for dry desquamation and ulceration. Assuming a straight line extrapolation is applicable, the authors noted that the lines approached zero at 250 and 350 rads (Krebs' dose), respectively, for dry desquamation and ulceration.

The following items denote the uncertainties that occurred in attempting to correlate these experiments:

1. The doses were not uniformly distributed throughout the total dose interval.
2. The experiments were conducted on both pigs and monkeys, with limited experimental results on human skin. The range of experimental doses for each species was even more limited than for all of the experiments.
3. In addition to the uncertainties of the dose estimates, different dose calculation techniques were used by the different investigators. The uncertainties due to this were largely resolved by the dose calculation correlation efforts of Mikhail.[117]
4. The variation of the depth of the basal or germinal layer of cells on an individual animal can cause biological variability in addition to the biological variability between animals and across specie lines. There may be other sources of biological variability.

The AEC Division of Biology and Medicine, Space Nuclear Safety Advisory Committee met on February 15, 1968, to consider the hazards associated

with nuclear rocket ground tests--concerned primarily with particulate effluent. They were asked to consider only the implications of various modes of interaction of particulate material with humans--not the probability of the interaction. Based on their conclusions, and upon considering probabilities of interaction, the dose to the skin from particles residing on the skin was considered to be the limiting situation.

This committee did not have the benefit of the previously mentioned studies (Forbes and LASL final results) and thus their dose-effect relationships were not in full agreement with the aforementioned information. But, one of their recommendations is of special interest. The committee endorsed the concept of Dean that the skin tumor hazard could be estimated from an integration of the expected tumor yield for each exposed cell. The tumor yield per cell would be based on the dose yield per cell and published dose-tumor response data for rats.[79]

Summary

The present guide is a Krebs' dose of 750 rads.[103,104] This is based on minimizing the probability of ulceration occurring. Moist desquamation was not considered as a separate entity.

The work reported by Forbes and Mikhail[101] using pigs indicated that the lowest doses used, 400 and 440 rads Krebs' dose, produced ulcerous lesions; whereas the LASL studies using pigs did not note the formation of ulcers at doses of 470, 500, 770 rads Krebs' dose.[81,102]

Additional studies are needed to determine the significance of the difference between the LASL and Forbes results.

Forbes and Mikhail postulated that ulcer size might be a meaningful biological effects criterion. They noted that ulcers of 0.5 mm in diameter (400 rad dose) were probably of much less concern than those of 1 to 2 mm produced by doses of roughly 750 rads Krebs' dose.

Krebs[83] notes that the germinal cell layer surrounds the hair follicle. That is, the layer of germinal cells extends down to the depth of the hair

follicle--roughly a millimeter. Krebs indicates that this provides a reservoir of germinal cells that are relatively protected against superficial injury. These cells would receive a much lower dose than the cells in the main basal layer. Thus, other things being equal, the authors postulate that the dose effect relationship might vary between hairless and hairy skin. This may partially explain why the dose required to produce an ulcer on the sparsely haired pigs is less than that for the monkeys used by LASL.

APPENDIX B - 2. Potential Dose to the GI Tract from Particulate Material.

Several investigators have evaluated the implications of ingesting discrete radioactive particles either directly or through clearance from the respiratory system to the gastro-intestinal tract (GI). Several of these investigators and their general area of investigation are indicated below:

1. The LASL Bio-Medical group experimentally evaluated the solubility of coated and uncoated UC_2 particles in the gastric juices of monkeys. They also determined the clearance time for particles of various densities for the GI tract of man.[102]
2. Kochendorfer and Ulberg evaluated various modes of intake.[88] They noted that a mouth breather had a higher probability of exposure than a nose breather.
3. The Radiological Effects Working Group of SNSO developed a complete model from potential intake to dose to the GI tract.[90] The model considers both the average gamma dose to the GI tract and the beta dose at a depth of 300 μm from the gut wall. The depth of 300 μm is based on the depth of the dividing crypt cells. The model also considers transfer of radionuclides from the GI tract to the blood.
4. Mikhail and Collins[76] evaluated the effluent data from the Phoebus-1B reactor test. They used the intake model of item 2 above, and indicated intake probability and potential doses at a 300 μm tissue depth. They apparently calculated the integral dose from the passage of particles through the intestines versus the dose to discrete volumes of tissue. They concluded that the dose to the skin was more limiting than that to the GI tract.

5. Altomare and Coleman[43] evaluated the ground deposition and transport data from the Phoebus-1B reactor test and developed dose prediction models for human interaction, including the GI tract. Their dose calculation is based on the beta energy loss to the GI contents during transit. This is the basic model used by the ICRP[59] for GI tract dose calculations. The transit times suggested by Eve[118] were used.
6. At the request of SNSO, the AEC Division of Biology and Medicine Space Nuclear Safety Advisory Committee evaluated the various modes of potential particle interaction with humans.[75] They were requested not to consider the probability of interaction--only the implications of an interaction. They concluded that for the GI mode of interaction, "...the impact on a person's health would be roughly the same or less than the effects resulting from skin exposure." Mikhail and Collins,[76] indicated that the probability of a particle reaching the GI tract was at least two orders of magnitude less than that for interacting with the skin.

The above models have little in common other than that they indicate that the probability of interaction with, and irradiation of, the skin is more limiting than that for the GI tract. The following steps indicate a general approach for estimating the dose to the GI tract. As with the skin and lung, the basic uncertainty is the appropriate tissue, both depth from the surface of the GI lining and tissue mass and/or distance along the GI tract that should be used for the dose calculation.

1. The intake of particles can be based on evaluations in references 43, 76, 88 and 90. These references use similar approaches. It would appear that the particles cleared from the respiratory tract to the GI tract are of prime importance. The ICRP Task Group report on lung dynamics[83] is a good basic reference from which the transfer of material from the respiratory system to the GI tract can be calculated.
2. The transfer time through the various segments of the GI tract is important for all of the various dose calculation techniques.

There are several values given in the literature:

	Stomach	Small Intestine	Upper Large Intestine	Lower Large Intestine
a. The ICRP in Report 2, 1959 recommends(ref.59)	1 hr	4 hr	8 hr	18 hr
b. Kochendorfer and Ulberg (ref.88) indicate that Snyder of ORNL indicates that the ICRP will change the values to	1 hr	4 hr	13 hr	31 hr
c. Kochendorfer and Ulberg (ref.88) also refer to work at Argonne that indicates some retention for several days				
d. Eve (ref.118) recommended	1 hr	4 hr	13 hr	24 hr

3. Eve's[118] work concurs with the SNSO Radiological Effects Working Group[90] in that the mitosing cells are at some depth below the GI surface lining. Her literature review indicated that this depth varies from 140 μm for the small intestine (SI) to possibly 420 μm for the large intestine (LI). But, she also notes that it is not certain that some of the GI contents do not penetrate the wall to some extent.

In summary, it appears reasonable to select the large intestine (upper or lower--ULI or LLI) as the critical organ (due to the transit time) and calculate the dose at 300 μm. The dose can be calculated by the techniques indicated in references 102 and 116.

Dolphin and Eve[119] recommend changing from the ICRP 2[59] concept of calculating the dose at the entrance to a given section of the GI tract to calculating the average dose for the section. They note that this would be more consistent with dosimetry used for other body organs. Due to the relatively short half-life of the gross fission products in the particles (based on roughly 2 hours transport time prior to ingestion) the dose for the various sections will change by roughly a factor of two between the

beginning and end of a section. Considering the lack of information on the bio-effects to the GI tract from irradiating various masses of tissue, this factor of two is probably minor.

Due to the generally low solubility of the particles,[90,102] uptake of radionuclides from the particles to the bloodstream does not appear to merit further consideration.

APPENDIX B - 3. Mathematical Models for Predicting Effects On the Lung From Inhalation and Deposition of Radioactive Particles.

Introduction

Prediction of biological effects on the lung from inhalation of particulate debris from nuclear rocket engine tests is best visualized as a four step process: (1) prediction of debris transport; (2) prediction of inhalation and deposition of the particles in the lung; (3) estimation of the dose to the lung from deposited particles; and (4) prediction of biological effects resulting from the estimated doses. The techniques for carrying out each of these steps are not equally well defined; in particular biological effects on the lung from radiation are not well understood.

Particle air concentrations at points downwind can be estimated with one of the several available models. Examples include the ARL-LV model described by Henderson[16] and the Van der Hoven model adapted for computer usage reported by Stigall and Calley.[40]

Several methods have been proposed to accomplish the second step, prediction of inhalation and deposition of particles in the lung. Perez and Coleman[120] summarized and compared five deposition models contained in the literature. From a knowledge of particle characteristics such as activity and size distributions and the particle residence time, doses to the lung from deposited particles can be estimated (the third step).

The fourth step, prediction of biological effects on the lung from inhaled particles, is not well-defined. A question which is central to this problem is the relative tumor-producing effectiveness of a relatively small dose to a

large mass of tissue (kilograms) compared to a large dose to a small mass of tissue close to the particle (grams or fractions of a gram). The question is whether averaging the dose from the inhaled particle over the entire lung is more conservative from a health standpoint than computing the dose to the small mass of tissue which is actually exposed. The ICRP in Publication 14[121] notes that "the same radiation energy absorption might well be less effective when distributed as a series of 'hot spots' than when uniformly distributed." While there is uncertainty regarding biological effects from lung irradiation, it appears on the basis of present evidence that for the particular particle size and activity distributions expected from reactor engines, exposure to the skin is more limiting than exposure to the lung.[76,78]

Prediction techniques such as those of the eye model for predicting cataract probability have not been developed for the lung. Studies are in progress to better define dose-effect relationships for the lung. These studies include projects specifically dealing with reactor engine effluent such as that of Stanley at NERC-LV[122] where activated UC_2 particles are implanted in rat lungs. The studies of Langham[123] and Sanders, et al.,[77] are concerned with alpha and x-radiation from plutonium particles. Sanders, et al.,[86] summarized a number of lung radiological bio-effects studies and evaluated the hazard of particles from nuclear rocket engine tests.

Deposition of Particles in the Respiratory System.

Several models for prediction of particle deposition in the respiratory system have been proposed. The detailed description and comparison of these models is beyond the scope of this appendix. Perez and Coleman reviewed and compared five of these models, and further information can be obtained from their work and references 59, 83, 88, 90, 124.

Coleman and Perez[124] developed a mathematical representation of the most comprehensive deposition model, that of the Task Group on Lung Dynamics of Committee II of the International Commission for Radiological Protection.[83] This model is distinct from the ICRP 2[59] lung model.

On the basis of purely geometrical considerations, the respiratory system acts like a multicompartment selective sampler which filters out most of the larger particulate material in the upper respiratory tract. The mechanisms and efficiencies of dust or particle clearance differ considerably for various regions of the respiratory tract. Consequently the various models for particle deposition generally separate the respiratory system into three compartments for purposes of estimating particulate deposition and movement. Coleman and Perez's[124] adaptation of the ICRP Lung Dynamics Task Group model uses the following separation scheme: Compartment I includes the nasopharynx and oral pharynx to the larynx; Compartment II includes the oral pharynx starting at the larynx, trachea, bronchus, and connecting and terminal bronchiole; and Compartment III includes respiratory bronchiole, alveolar duct and alveolar sac.

The model[124] considers only the entrance of particles through the nose, ignoring mouth breathing. It assumes that all particles, regardless of size, have some probability of entering the system and that the size range available for entrance may be approximated from inertial properties of the particles.

One of the problems involved in evaluating biological hazards from inhaled particles is that even though the probability of inhalation of particles with aerodynamic diameters greater than approximately 10 μm may be very small, the consequences of deposition of particles this large and containing the associated quantities of radioactivity in the lung are so serious that even this small probability should not be neglected.

The raction of particles deposited in each of the various compartments is calculated from an empirical equation which Coleman and Perez fitted to deposition data reported by the ICRP Task Group on Lung Dynamics.[83] The model also attempts to incorporate data presented by the ICRP Task Group on clearance of dust and particles from the various respiratory compartments. Clearance actions by the blood, lymph system, and ciliary-mucus transport to the stomach are estimated by the model, based on the assumption that

material available for clearance is cleared according to first-order kinetics (the rate of clearance is assumed to be proportional to the amount of material present). The output of the deposition and clearance models is used to integrate the lung activity burden with respect to time, yielding a figure in curie-days or equivalent units.

Estimation of Dose to the Lung from Deposited Material

Doses to the lung from radioactive particles are usually computed using either of two approaches. One approach is to assume that the energy from particle radioactivity is deposited uniformly throughout the lung; this is referred to as the "smeared dose" concept. The other basic approach is to calculate the dose to the relatively small quantity of tissue near the particle. Some combination of these two approaches may also be used, analogous to the Krebs' depth dose concept used for the skin.

Coleman and Perez use the smeared dose concept. The estimated time-integrated organ activity burden is multiplied by a dose conversion factor; this factor depends on (1) radiation type and average energy; (2) physical properties of the particle material when activity is associated with a particle, since self-absorption must be considered; and (3) physical properties of the organ. This process yields what the authors describe as an average dose which is satisfactory if the number of particles per person is large. That is, if the number of particles inhaled is large, then the fraction of each size range deposited in each region of the lung can be estimated with satisfactory accuracy from the ICRP Task Group data. However, most cases encountered in estimating hazards from nuclear rocket effluent involve probable deposition of a very few particles or of only a fraction of a single particle per person. In such a case the NUS model gives an average dose for a number of individuals.[124] To overcome this shortcoming, the authors also developed a method of generating dose distribution, using the deterministic or average-dose model as a basis. Using this approach estimates can be made of the probability of an individual receiving a particular dose.

The model by Coleman and Perez[124] yields dose estimates in terms of the "Smeared dose" to the lung. Mikhail,[116] Mikhail and Collins,[76] Ulberg and Kochendorfer,[92] and Pestaner, et al.,[125] developed techniques for computation of point doses to tissue from deposited particles. Mikhail and Collins[76] calculated energy deposition in the lung by integrating the beta dose rate from each particle with respect to volume (equivalent to mass-integration, since they assumed a lung density of 1 gram/cc). The integration is performed by summing the dose rates absorbed in successive differential volume shells. Dividing this mass integrated dose rate (rad-g/sec) by the total mass of the lung and integrating over the particle lung residence time produces the smeared dose to the lung.

Biological Effects of Doses to the Lung from Particulates

Two primary points of contention remain concerning the lung models. First, which is appropriate, the smeared dose concept or the point dose concept? If the point dose concept is selected, then the tissue volume of interest must be defined. Sanders, Thompson, and Bair[77] indicate that most studies have used, as a standard, the dose at 100 μm from the particle. Second, the effect or biological endpoint must be defined (e.g., scar tissue or cancer). The dose-effect relationship then determines what volume of tissue must receive what dose to produce a given probability of incidence for this endpoint.

Sanders, et al.,[77,86] indicate that non-uniform irradiation of the lung from deposited particles is clearly more carcinogenic than uniform exposure to the entire lung. ICRP Publication 14[121] formally indicates that, based on general considerations and limited experimental data, localized "hot spot" doses are probably not as deleterious as average lung doses (based on gram-rad integral doses).

Sanders, et al.,[86] summarized most of the pertinent literature and developed a model for evaluation of pulmonary carcinogenesis from inhaled radioactive particulates. They also pointed out that the necessary data for precise evaluation of the hazards do not exist. They further state, however, that

the doses required for an observable tumor incidence are very high, on the order of several thousand rads if measured in tissue very close to the particle. There are no data to establish the low incidence end of a dose-effect curve and extrapolation of high-incidence data would be of questionable validity. While there is apparently no basis for postulating a threshold dose, the doses apparently required for observable tumor incidence (several thousand rads) could be delivered only by particles so large (aerodynamic diameter greater than 10 μm) that their probability of being respired would be extremely small.[77,86]

Several dose calculation approaches have been proposed, notably that of Dean and Langham,[79] which was based on the observation that tumor incidence exhibits a non-linear response with increasing dose, there being an optimum tumorigenic dose beyond which tumor incidence decreases because higher doses simply kill the cells, preventing cell mitosis and tumor formation. Another recent paper by Richmond, Langham, and Stone[126] reports the results of experiments which indicate that biological response to doses from highly radioactive particles is definitely influenced by the number of cells at risk.

APPENDIX B - 4. Model Used for Calculation of Probability of Cataract from Deposition of Particle in Eye.

Coleman and Perez[120] developed a mathematical model for computing the probability of cataract production by radioactive particles deposited in the eye. Use of the model was described by Altomare, et al.[127] Only the physical dimensions and the basic dose-response relationships will be described here.

Figure B-1, views a and b, are schematic representations of the eye assumed by the model. Coleman and Perez[120] selected the values for anatomical constants for the eye given in Table B-1 as composites of compromises from four medical references. In addition, they assumed that the eyelids could be described by ellipsoidal surfaces with a thickness of approximately 1 mm at the free margin when closed and that the conjunctiva fornix is completely symmetrical at a distance of approximately 8 mm from the corneal limbus.

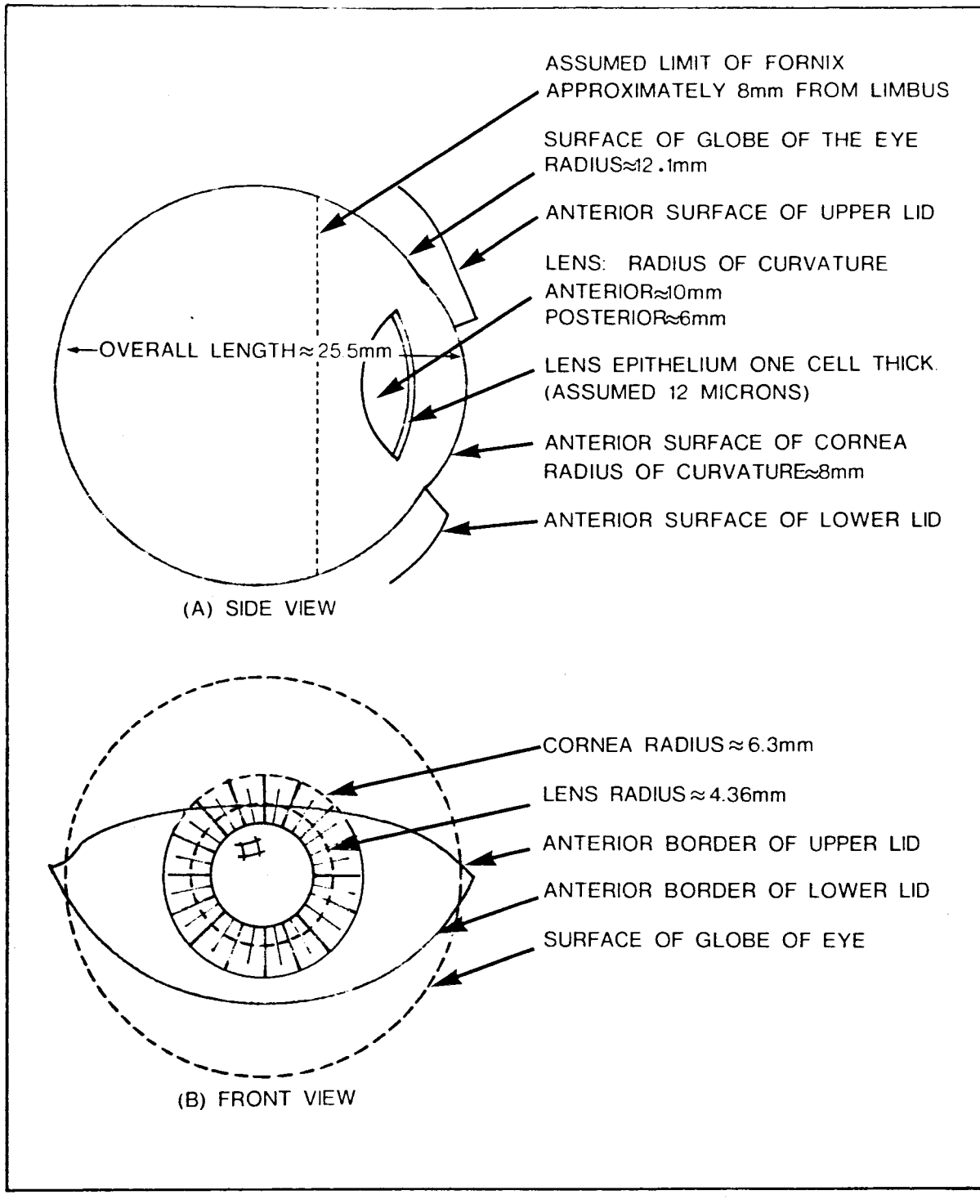

Figure B-1 Schematic Drawings of the Model Eye[120]

TABLE B-1. ANATOMICAL CONSTANTS FOR MODEL EYE(120)
(all dimensions are given in millimeters)

Eye Area	Measurement	
Eyeball	anterior-posterior length	25.5
	radius of curvature	12.1
Cornea	radius of curvature	8.0
	radius in vertical plane	6.3
Lens	radius of curvature anterior surface	10.0
	radius of curvature posterior surface	6.0
	radius in vertical plane	4.4
	distance anterior cornea to anterior lens	3.5
	epithelium thickness, single cell	0.012

Apparently the lens epithelium of the lens equator is the location of most cell mitosis within the lens and is consequently more radiosensitive than the rest of the lens.[120] Coleman and Perez accordingly incorporated a weighting function into the model such that the epithelium at the lens equator is considered to be 10 times more radiosensitive than epithelium at the lens center. The figure of 10 for the relative radiosensitivity was based on clinical observations.

A dose-response relationship was assumed such that the probability of cataract formation with 150 rads uniform dose to the lens is 0.01% (essentially zero) while 620 rads uniform dose to the lens produces a cataract formation probability of 99.99% (essentially unity). Coleman and Altomare then performed calculations assuming both normal and log-normal dose-response curves between these limits and concluded that the log-normal distribution more accurately represented reality.[120]

Residence time of particles in the eye is another variable of importance to the eye model. Opthalmologists consulted by Coleman and Perez recommended use of a residence time of 5 to 15 minutes.[120] The final form of the model assumed residence times of 4 hours and 24 hours for particles on the lid, 24 hours in the corner of the eye, and 5 minutes on the limbus.[127]

From the physical model of the eye represented by Figure B-1, views a and b, Table B-1, and the dose-response relationships outlined above, the probability of cataract production as a function of total particle activity at the time of deposition can be computed. Figures B-2 and B-3[120] show the computed probabilities for particles resulting from a 30-minute reactor run and transport times of 30 minutes and 2 hours.

For purposes of pre-run prediction, the ARL-LV scaling model described by Henderson[16] has been used with estimated particle fall velocities to predict air concentrations of particles as a function of distance downwind from the test point. Particle activity distributions are estimated for various distances downwind, and the activity distribution is broken into activity groups or ranges. For a representative activity within each group,

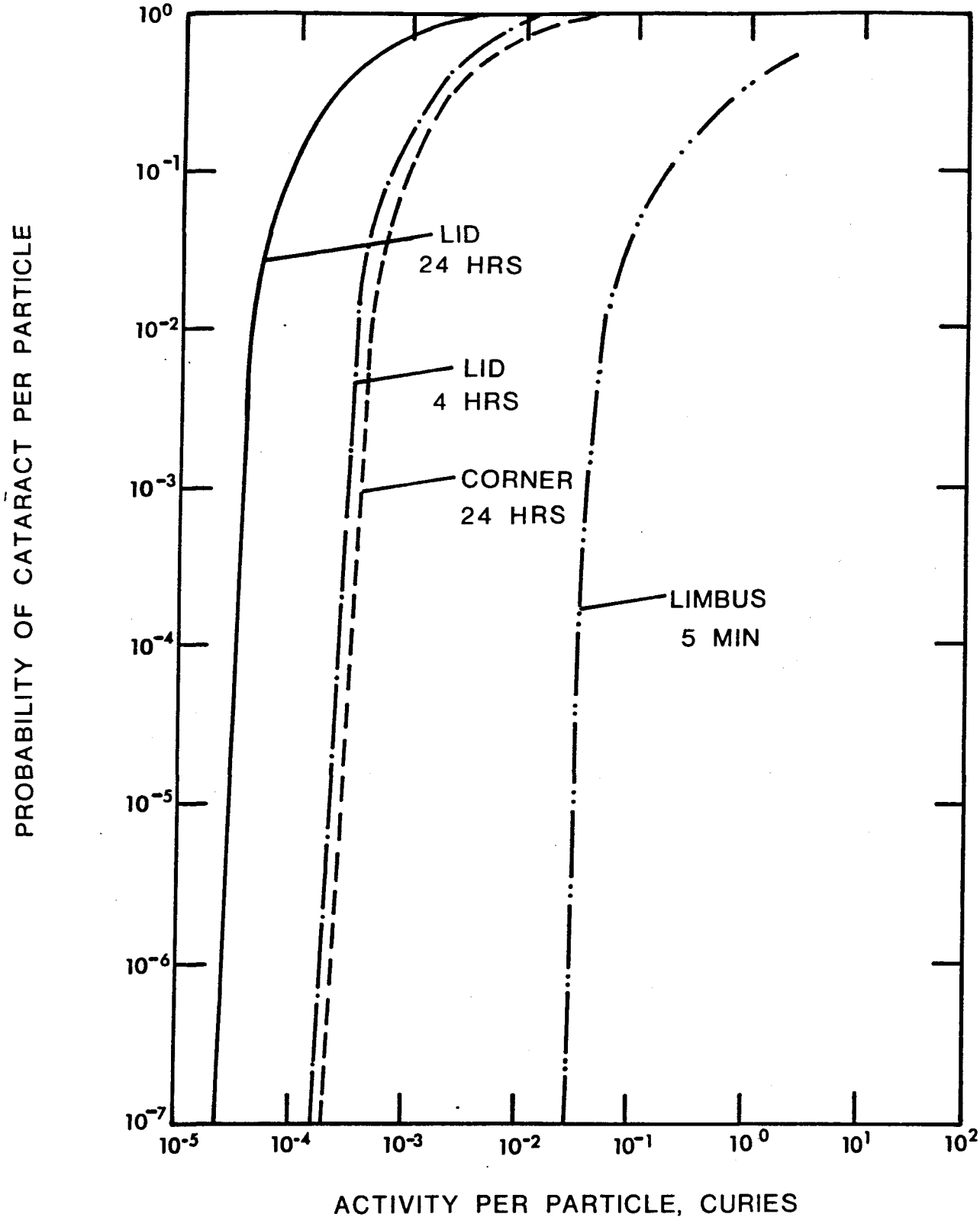

Figure B-2 Probability of Cataract Formation as a Function of Particle Activity (Based on 30-minute reactor run and 30-minute transport time)[120]

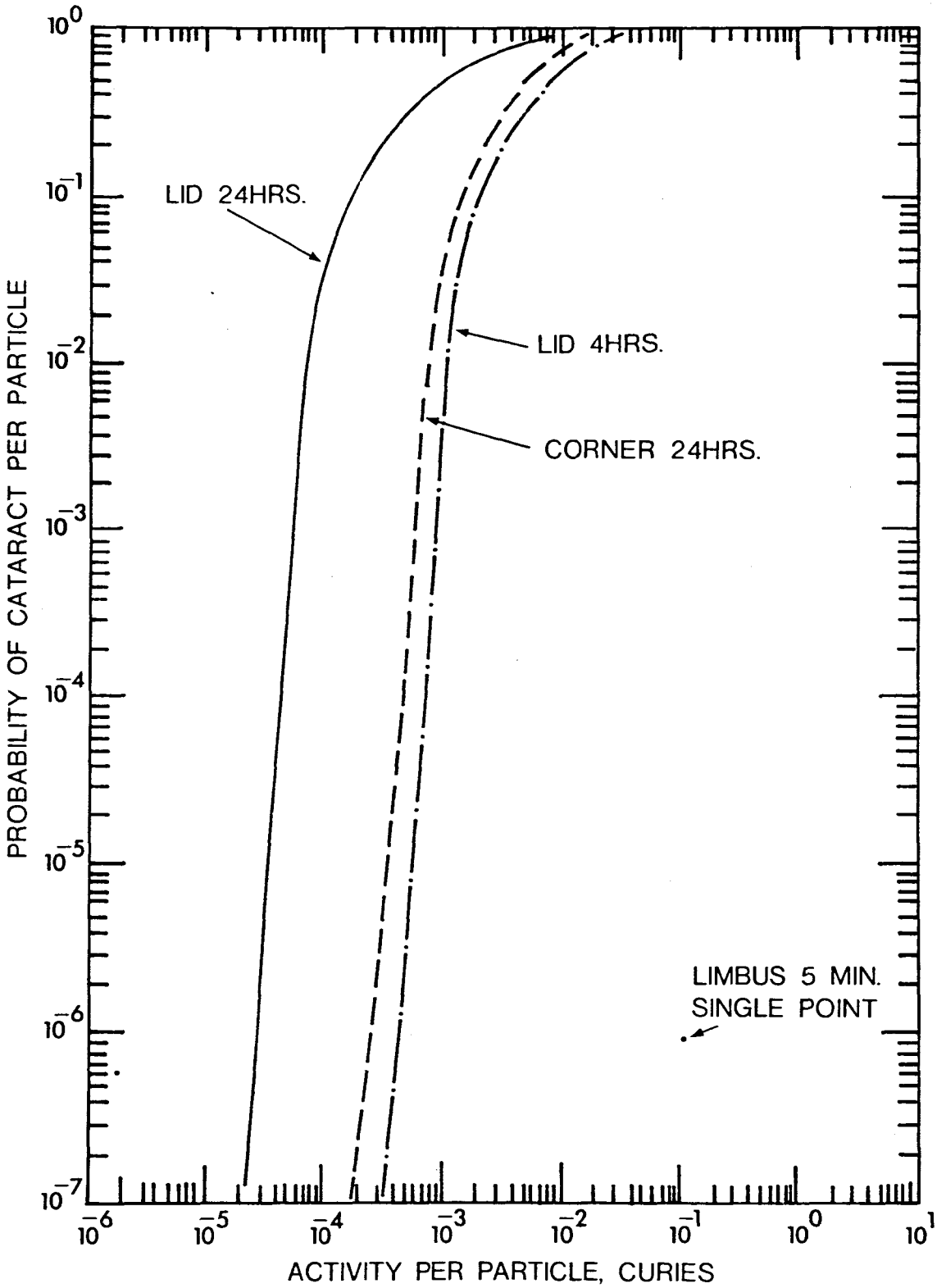

Figure B-3 Probability of Cataract Formation as a Function of Particle Activity (Based on 30-minute reactor run and 2-hours transport time)[120]

the probability of cataract formation, Pi, for a particle of that group deposited in the eye is determined from curves such as Figures B-2 and B-3. The total probability, P, of cataract formation for a particle at some location in the eye is then

$$P = \sum_i P_i N_i \qquad \text{Eq. B-1}$$

WHERE

N_i is the fraction of the particles in activity group i.

The NRDL deposition model for particle deposition,[88] assuming a 5 square cm area for the eye, is used to generate a curve such as Figure B-4, giving the average number of particles deposited in the eye region per unit integrated air concentration as a function of wind speed. These results are used to estimate the average number of particles in the eye region, λ_e, as a function of distance downwind. Assuming a Poisson distribution, the probability of one or more particles being deposited in the eye, K, is given by

$$K = 1 - e^{-\lambda e} \qquad \text{Eq. B-2}$$

The probability of cataract formation, P_c, is

$$P_c = (P)(K) \qquad \text{Eq. B-3}$$

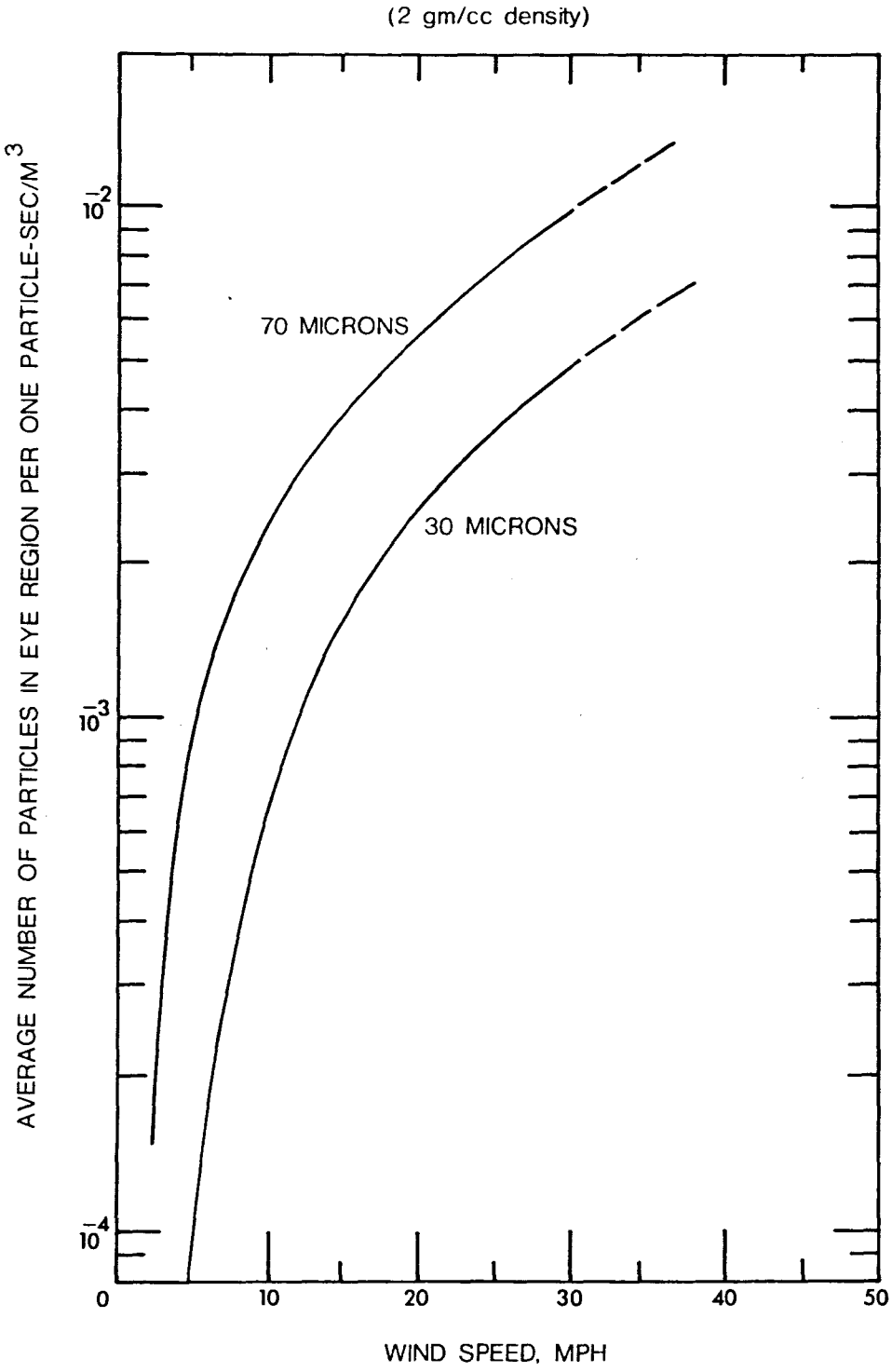

Figure B-4 Potential Number of Particles Deposited In Eye[120]

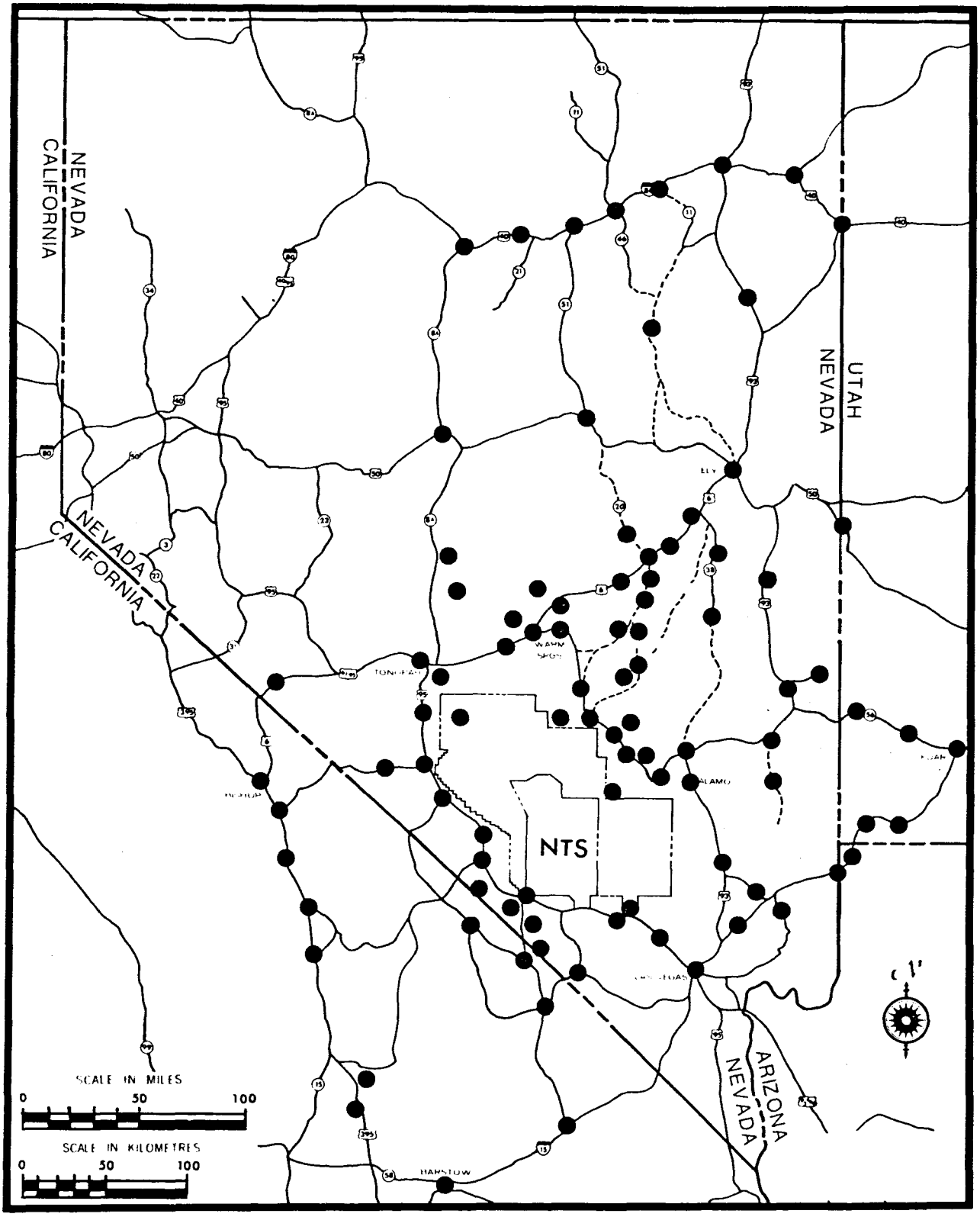

Figure C-1 Routine TLD Dosimetry Stations

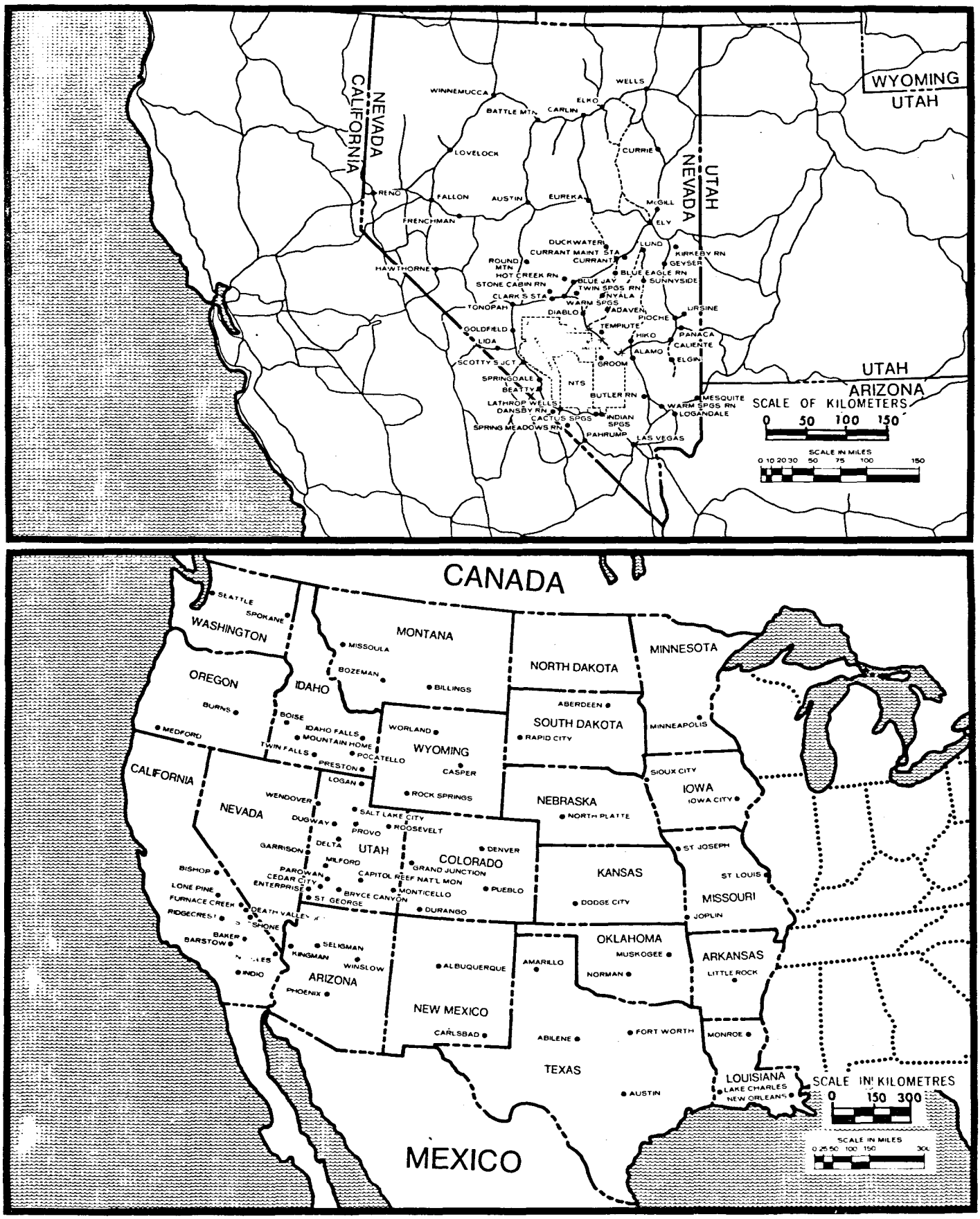

Figure C-2 Air Surveillance Network Stations

TABLE D-1. REACTOR ENGINE TESTS AT NRDS FROM WHICH AIRBORNE RADIOACTIVITY WAS DETECTED OUTSIDE THE TEST RANGE COMPLEX(5)*.

Reactor/ Engine	Experimental Plan	Date	Maximum Chamber Temperature (°R)	Nominal Power (Mw)	Integrated Power (10^6 Mw-sec)
Kiwi A	XVI	07/01/59	--	70	0.02
Kiwi A'	VII-116-B	07/08/60	--	85	0.06
Kiwi A3	VII-216-B	10/19/60	--	100	0.06
Kiwi B-1A	VI/A	12/07/61	--	300	0.03
Kiwi B-1B	IV	09/01/62	--	800	0.01
Kiwi B-4A	VI	11/30/62	--	500	0.04
Kiwi B-4D	IV	05/13/64	4280**	915	0.11
Kiwi B-4E	V	08/28/64	4240**	914	0.5
Kiwi B-4E	VI	09/10/64	4000**	882	0.18
NRX-A2	IV	09/24/64	3600	1100	0.3
NRX-A2	V***	10/15/64	--		~0.3
Kiwi	(TNT)	01/12/65	--	--	0.009
NRX-A3	IV	04/23/65	4900	1110	0.32
NRX-A3	V	05/20/65	3940	1080	0.84
NRX-A3	VI***	05/28/65			~0.5
Phoebus-1A	IV	06/25/65	4370**	1070	0.74
NRX-A4/EST	IIB***	02/03/66	2576	442	
NRX-A4/EST	III	03/03/66	4100	1140	0.88
NRX-A4/EST	IV	03/16/66	4000	1100	1.0
NRX-A4/EST	IVA	03/25/66	4150	1200	1.1
NRX-A5	III	06/08/66	4000	980	1.2
NRX-A5	IV	06/23/66	4100	1030	1.0
Phoebus-1B	III	02/10/67	2900**	588	0.14
Phoebus-1B	IV	02/23/67	4500**	1340	2.6
NRX-A6	IIIA	12/15/67	4150	1140	4.5
Phoebus-2A	III	06/08/68	2680**	1930	0.63
Phoebus-2A	IV	06/26/68	4060**	4010	4.5
Phoebus-2A	V/A&B	07/18/68	3900**	3430	2.5
Pewee-I	III	12/04/68	4600**	503	1.5
XE Prime	V/C	06/11/69	4200	1070	0.42
XE Prime	IXA	08/28/69	4200	680	0.34

* Data for experiments prior to 1964 are not included in Reference 5 and are thus unofficial estimates.

** Average maximum fuel temperatures.

*** Data not given in Reference 5.

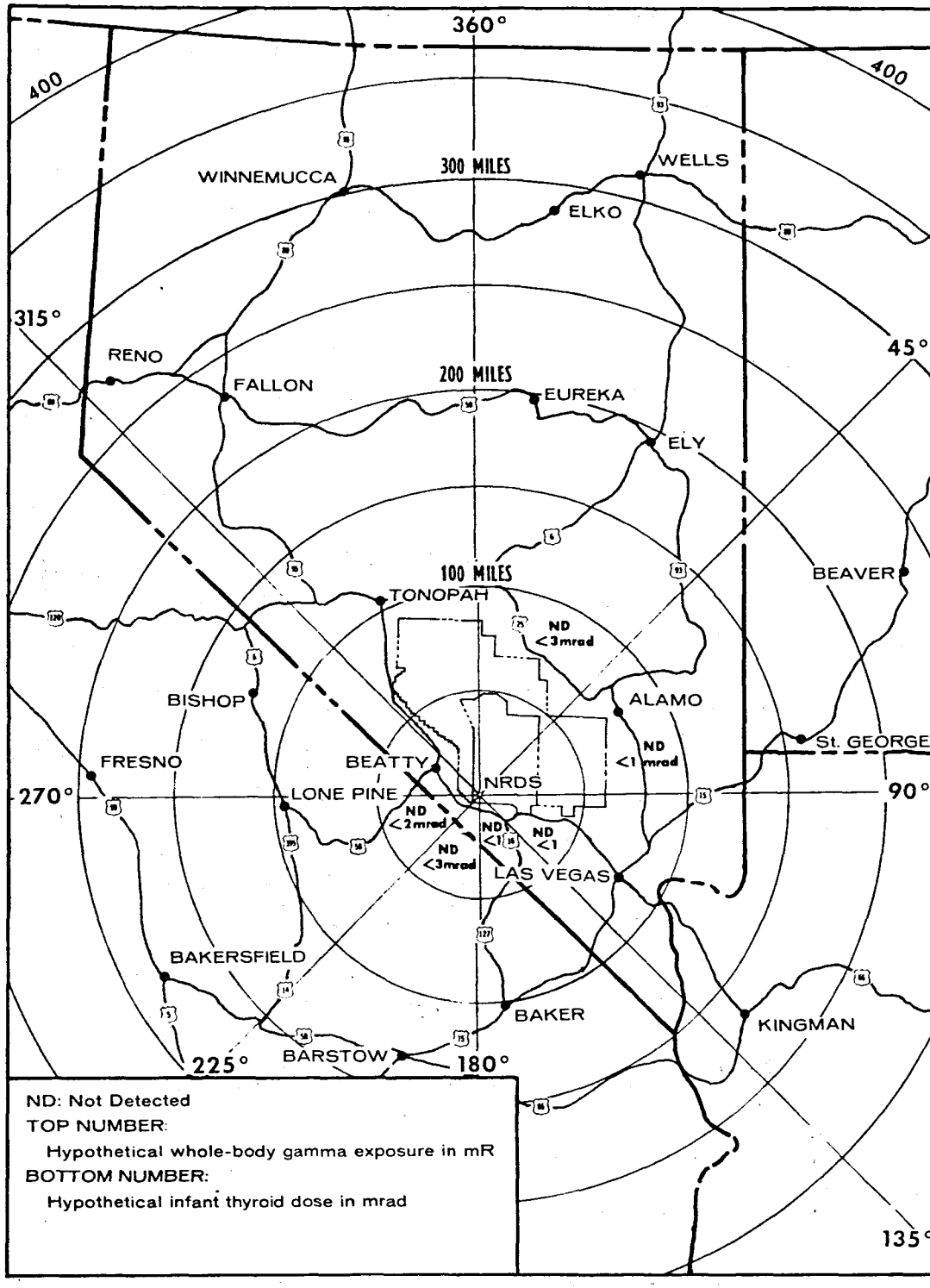

Figure D-1 Off-Site Whole-Body Gamma Exposures and Infant Thyroid Doses Resulting from Reactor/Engine Tests from CY 1959 to 1963 [50]

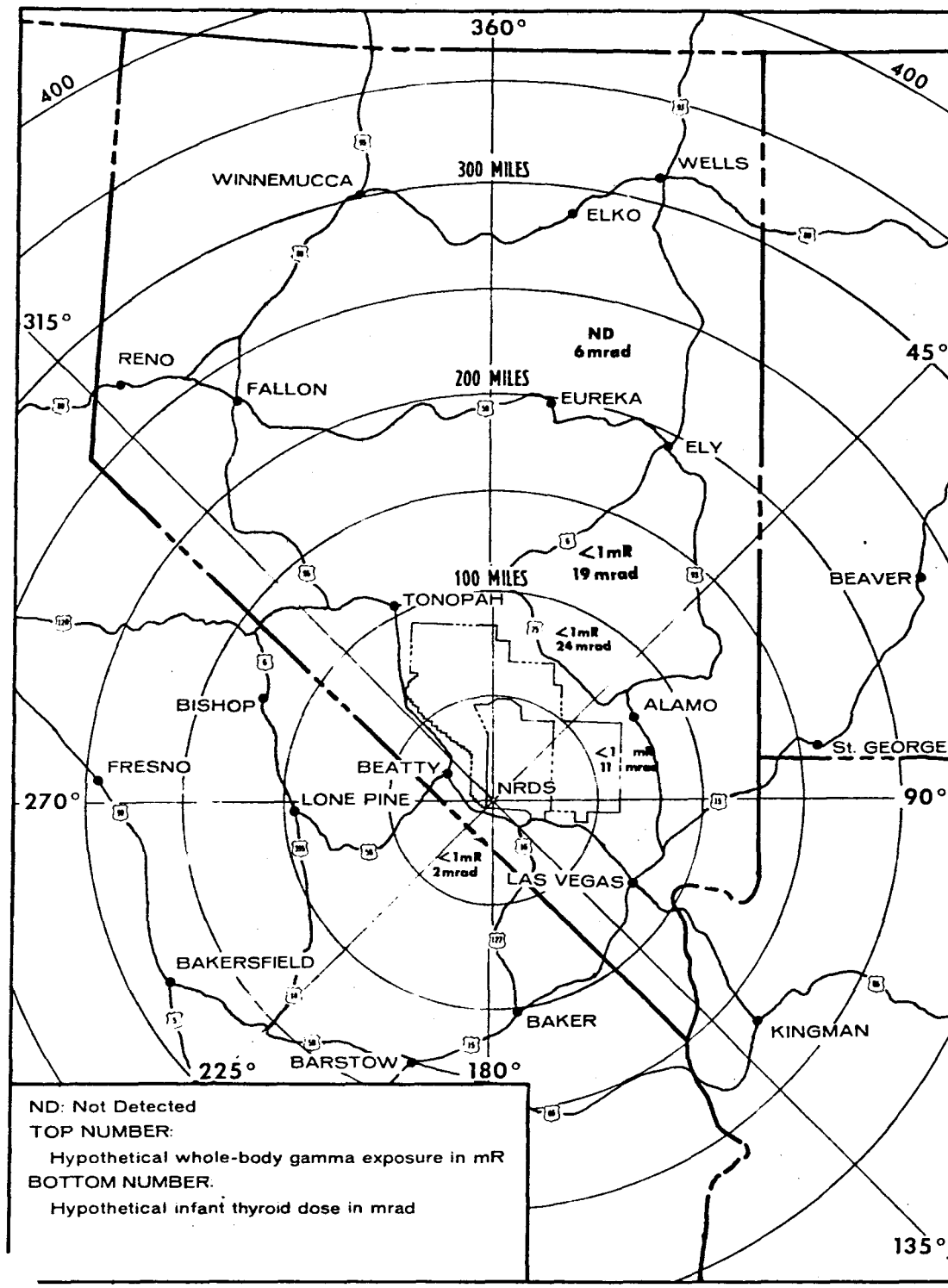

Figure D-2 Off-Site Whole-Body Gamma Exposures and Infant Thyroid Doses Resulting from Reactor/Engine Tests During CY 1964 [50]

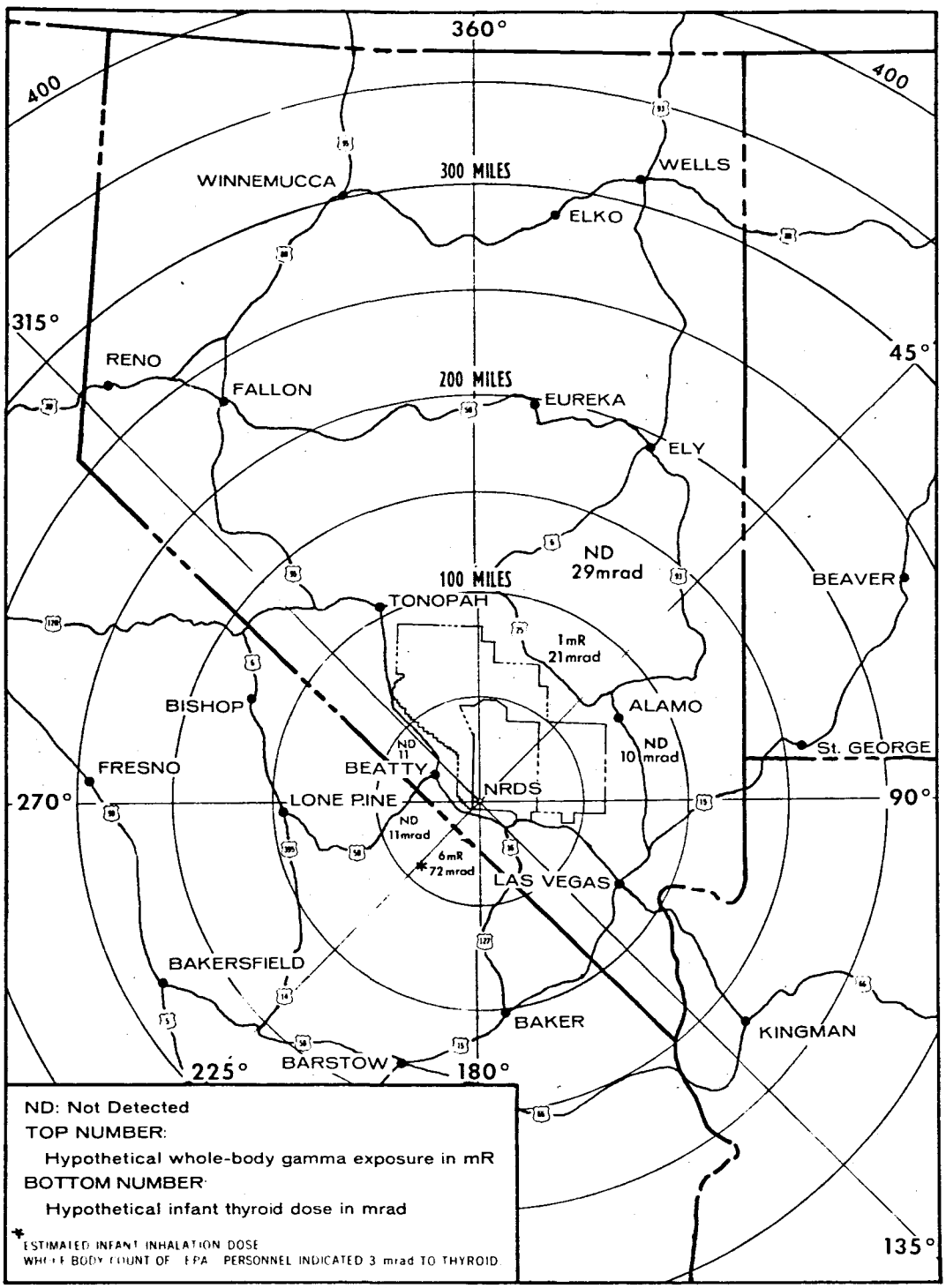

Figure D-3 Off-Site Whole-Body Gamma Exposures and Infant Thyroid Doses Resulting from Reactor/Engine Tests During CY 1965 [50]

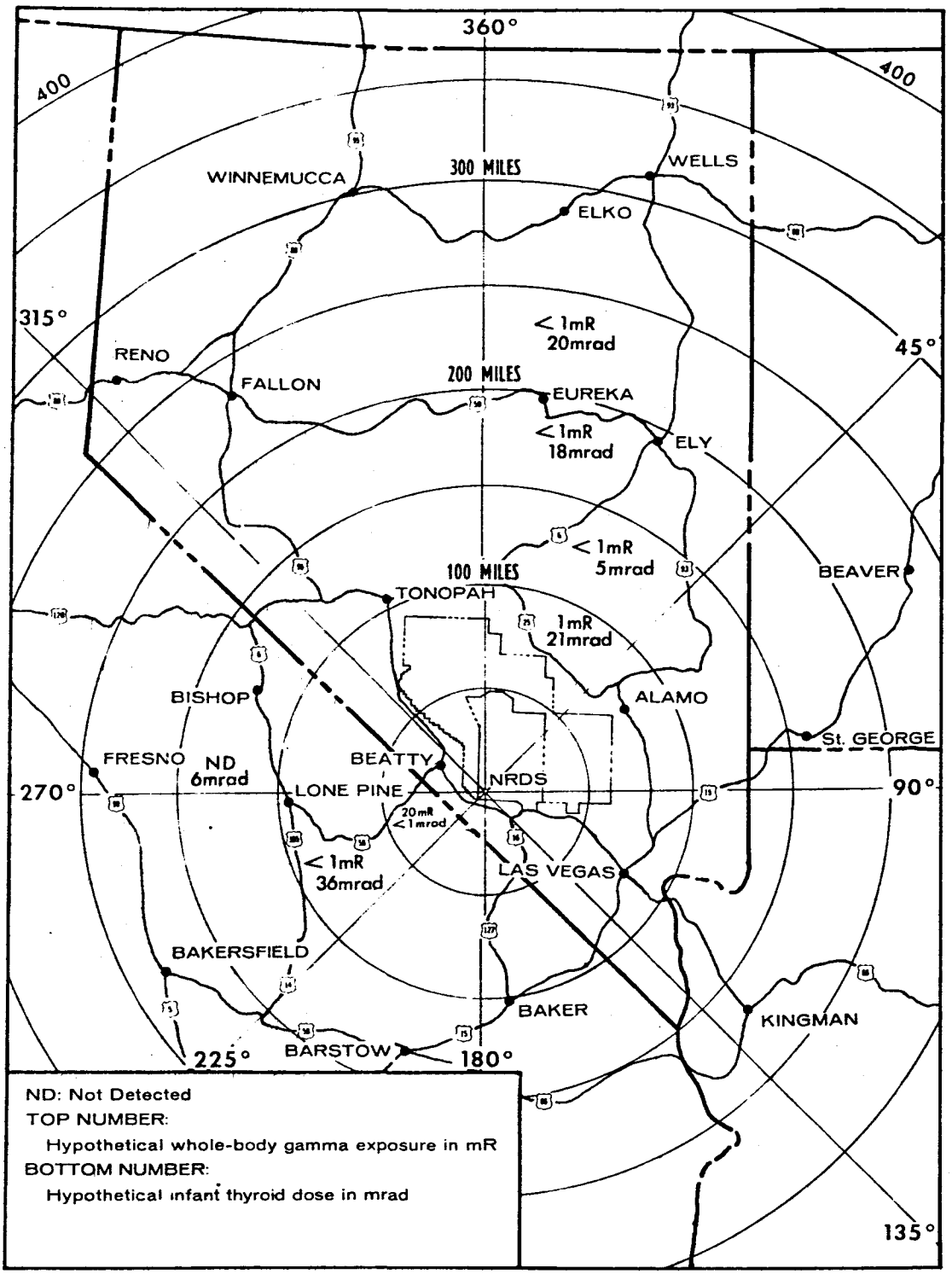

Figure D-4 Off-Site Whole-Body Gamma Exposures and Infant Thyroid Doses Resulting from Reactor/Engine Tests During CY 1966 [50]

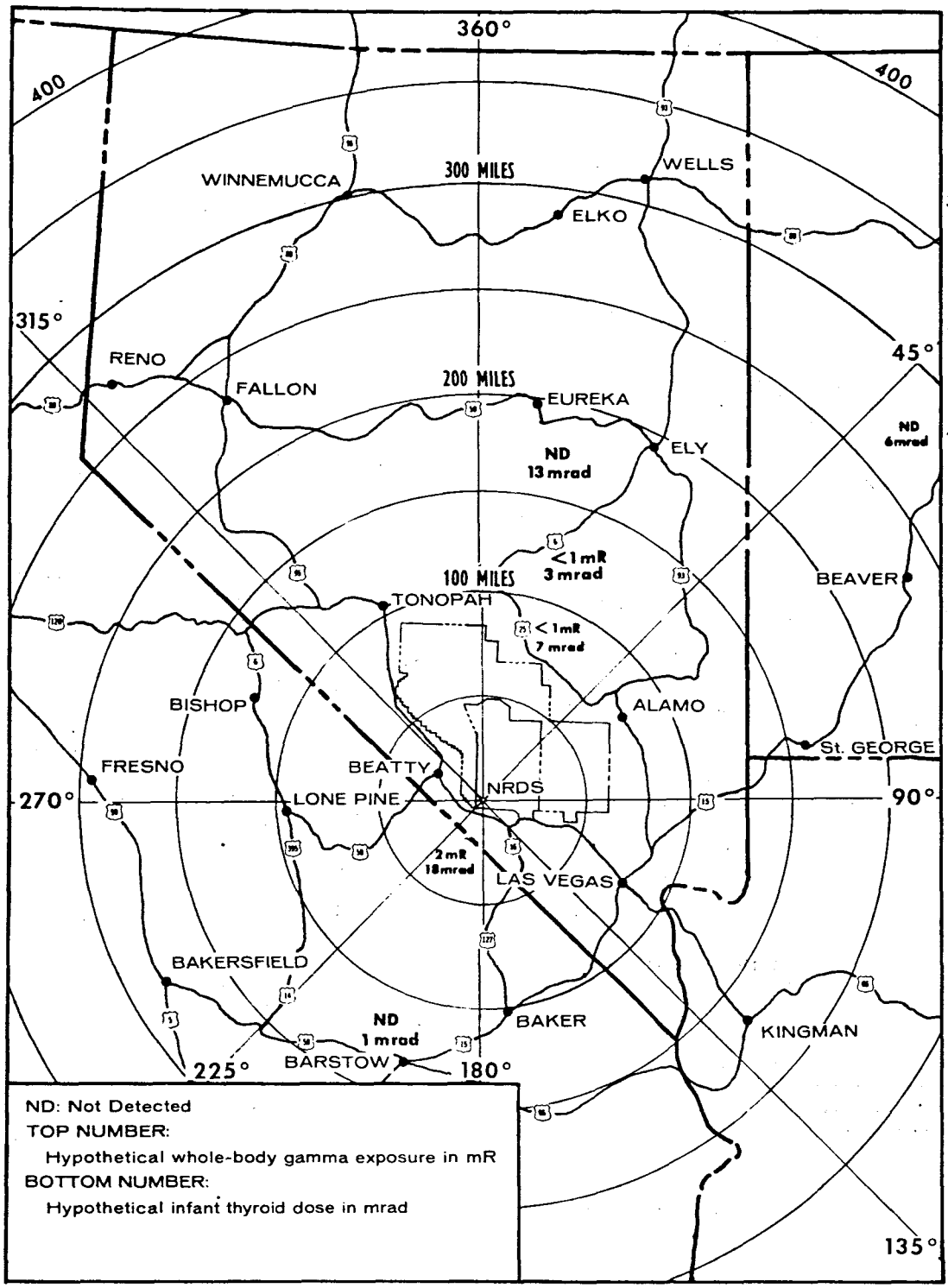

Figure D-5 Off-Site Whole-Body Gamma Exposures and Infant Thyroid Doses Resulting from Reactor/Engine Tests During CY 1967 [50]

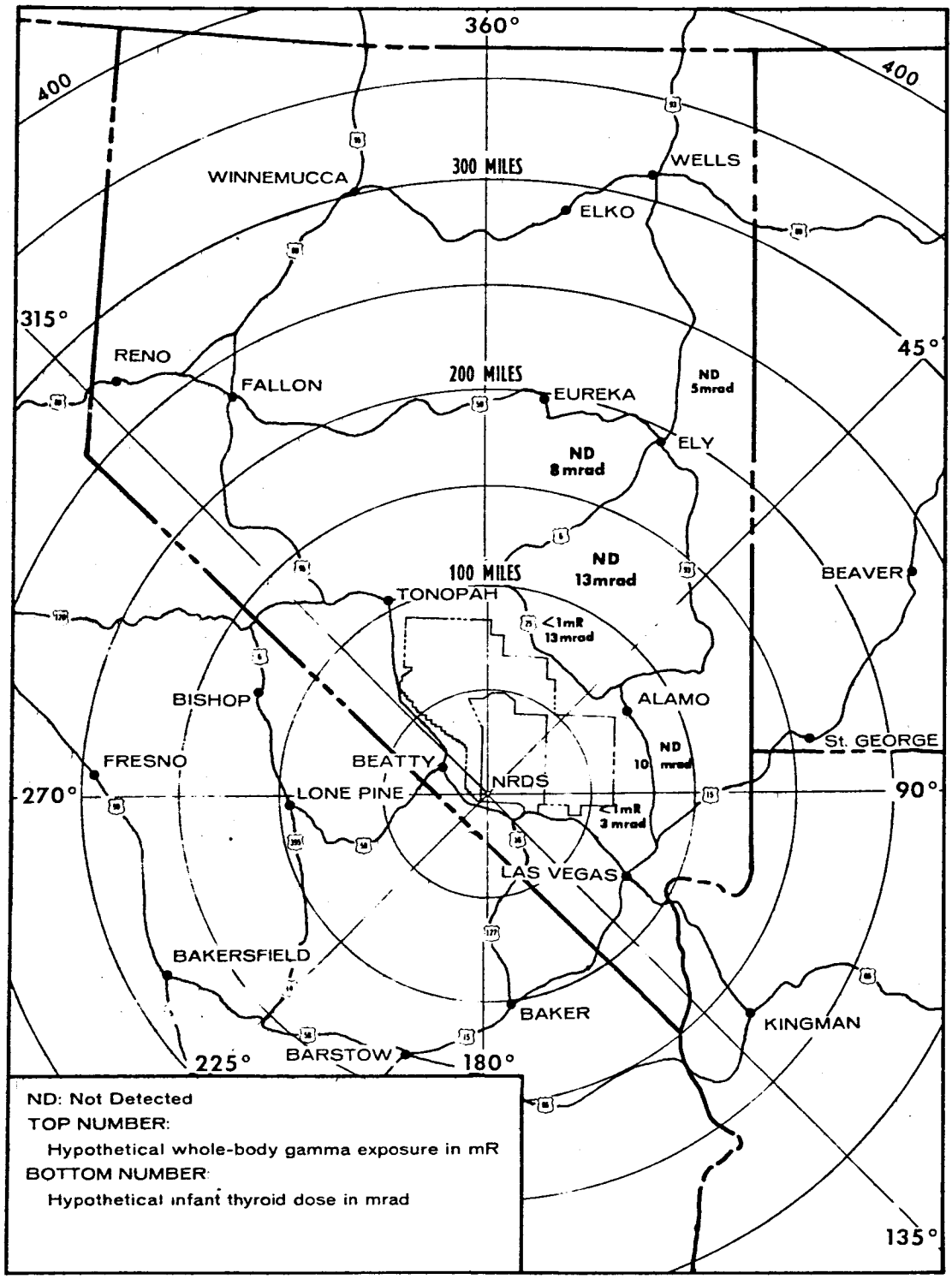

Figure D-6 Off-Site Whole-Body Gamma Exposures and Infant Thyroid Doses Resulting from Reactor/Engine Tests During CY 1968 [50]

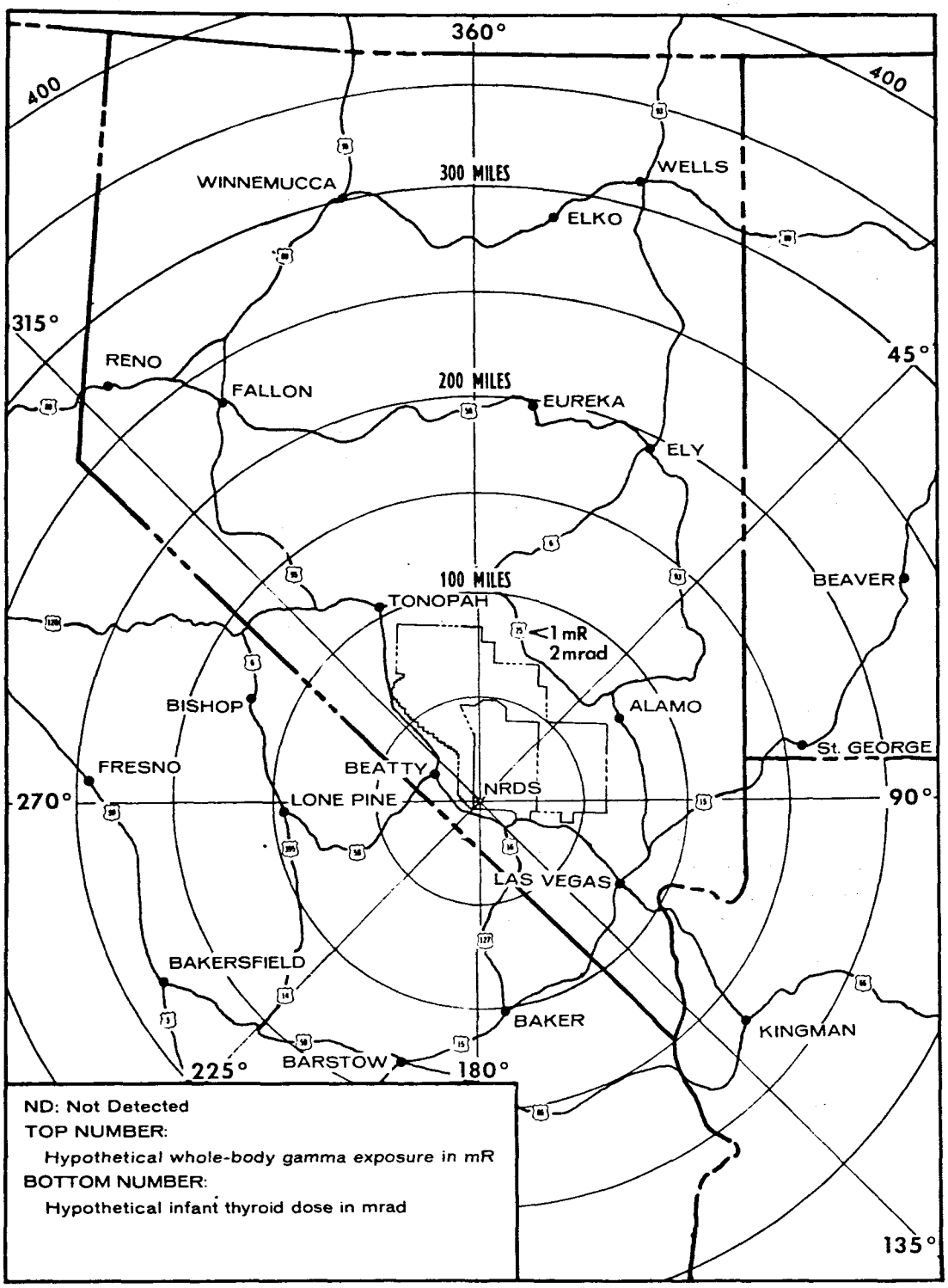

Figure D-7 Off-Site Whole-Body Gamma Exposures and Infant Thyroid Doses Resulting from Reactor/Engine Tests During CY 1969 [50]

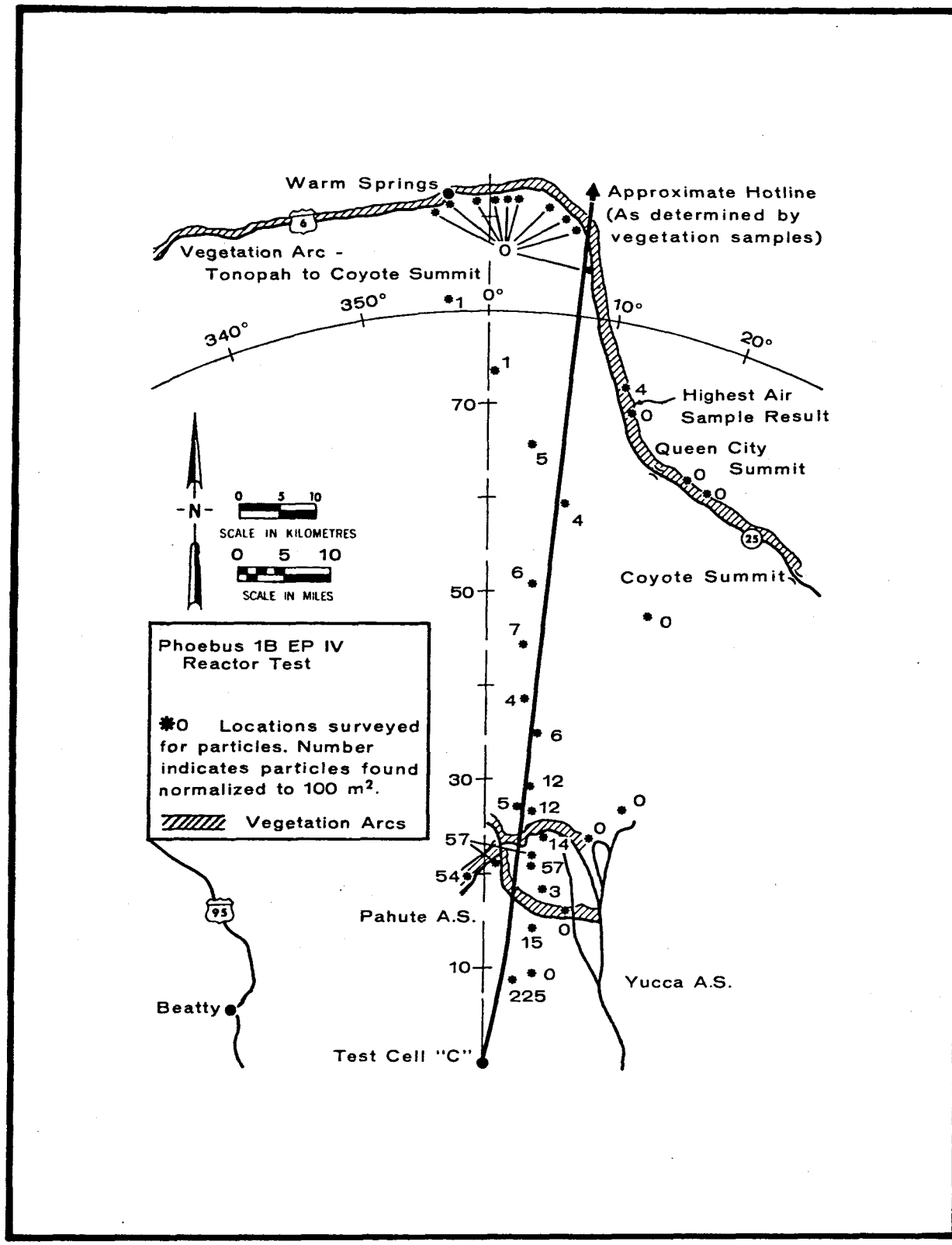

Figure E-1 Particle Deposition Measurements, Phoebus 1B-EPIV[14]

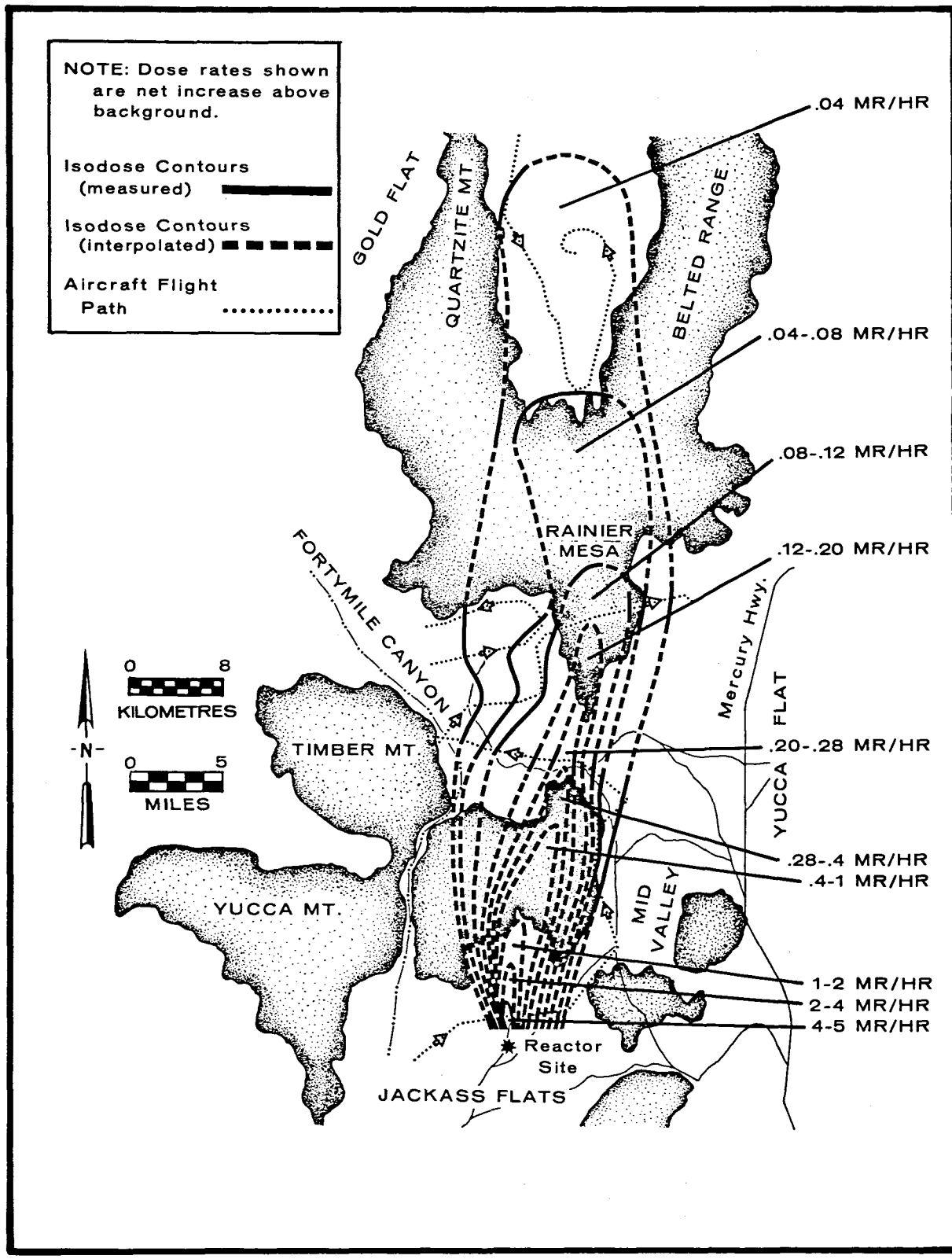

Figure E-2 Reactor Test Ground Depositon Pattern for Phoebus 1B, EPIV (Data used by permission from EG&G[14])

Figure E-3

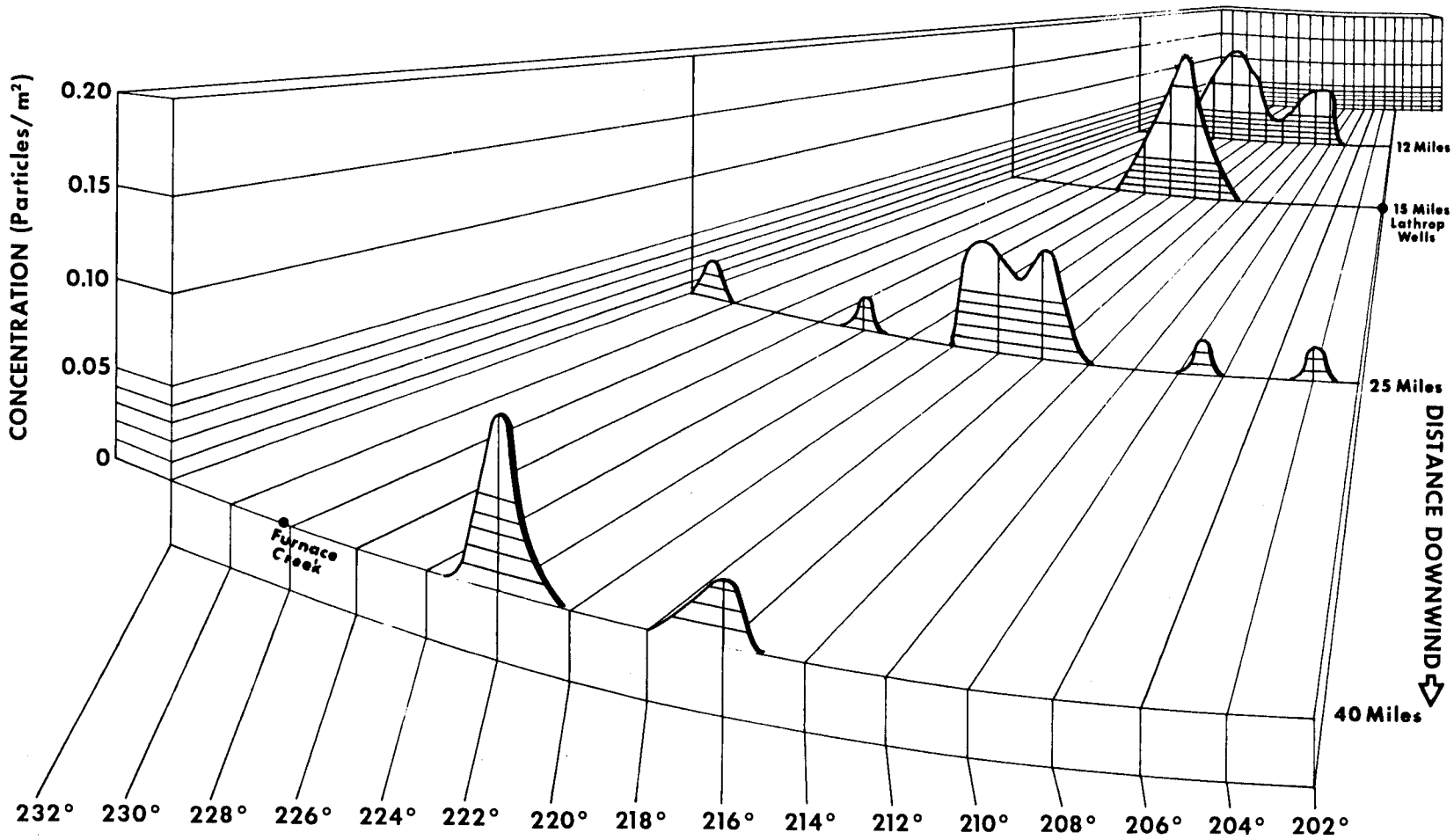

Three-Dimensional Representation of
Particle Survey Results for NRX-A6, EPIIIA[109]

Figure E-4

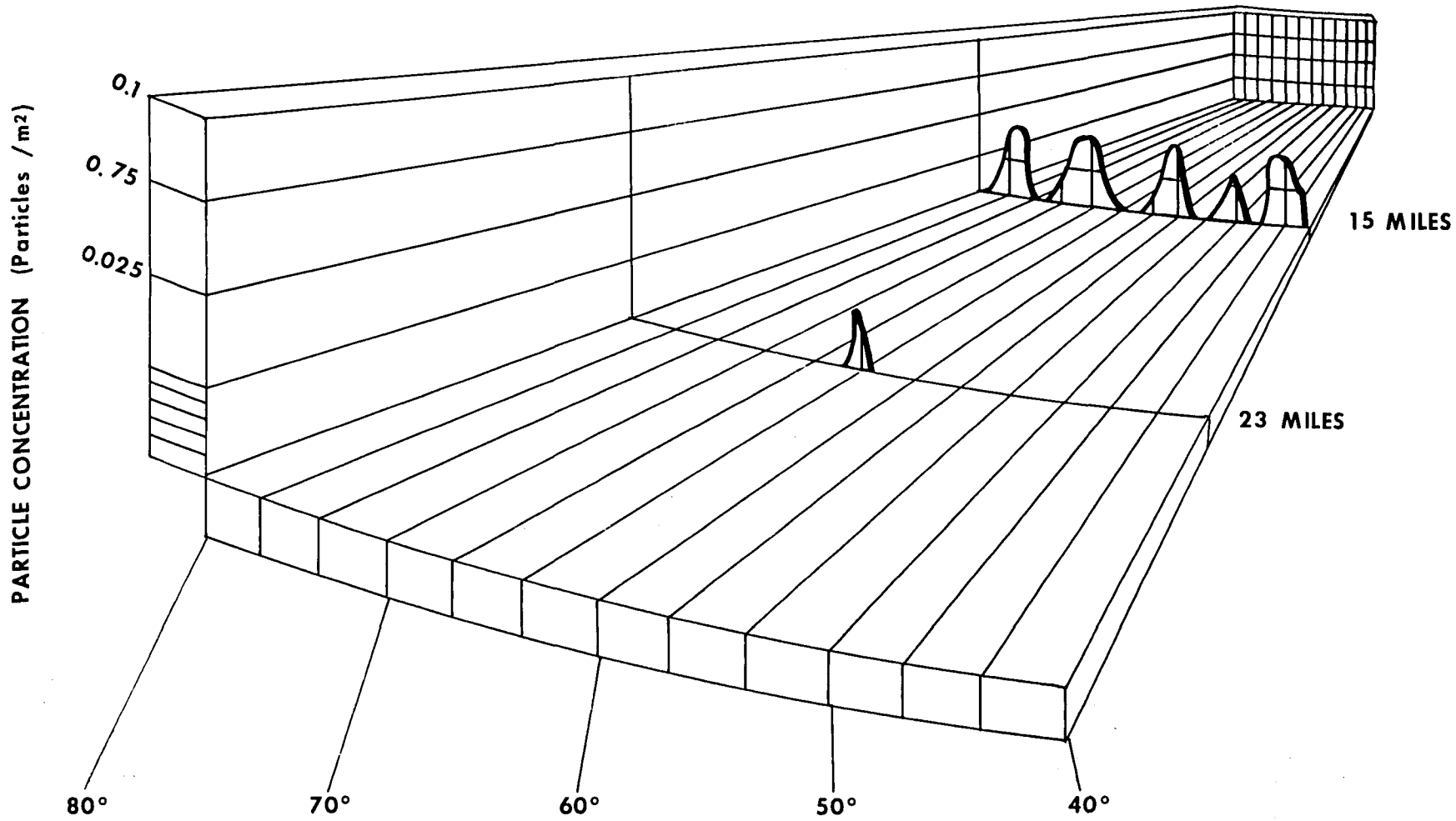

Three-Dimensional Representation of Particle Survey Results for Phoebus 2A, EPIV[84]

Figure E-5

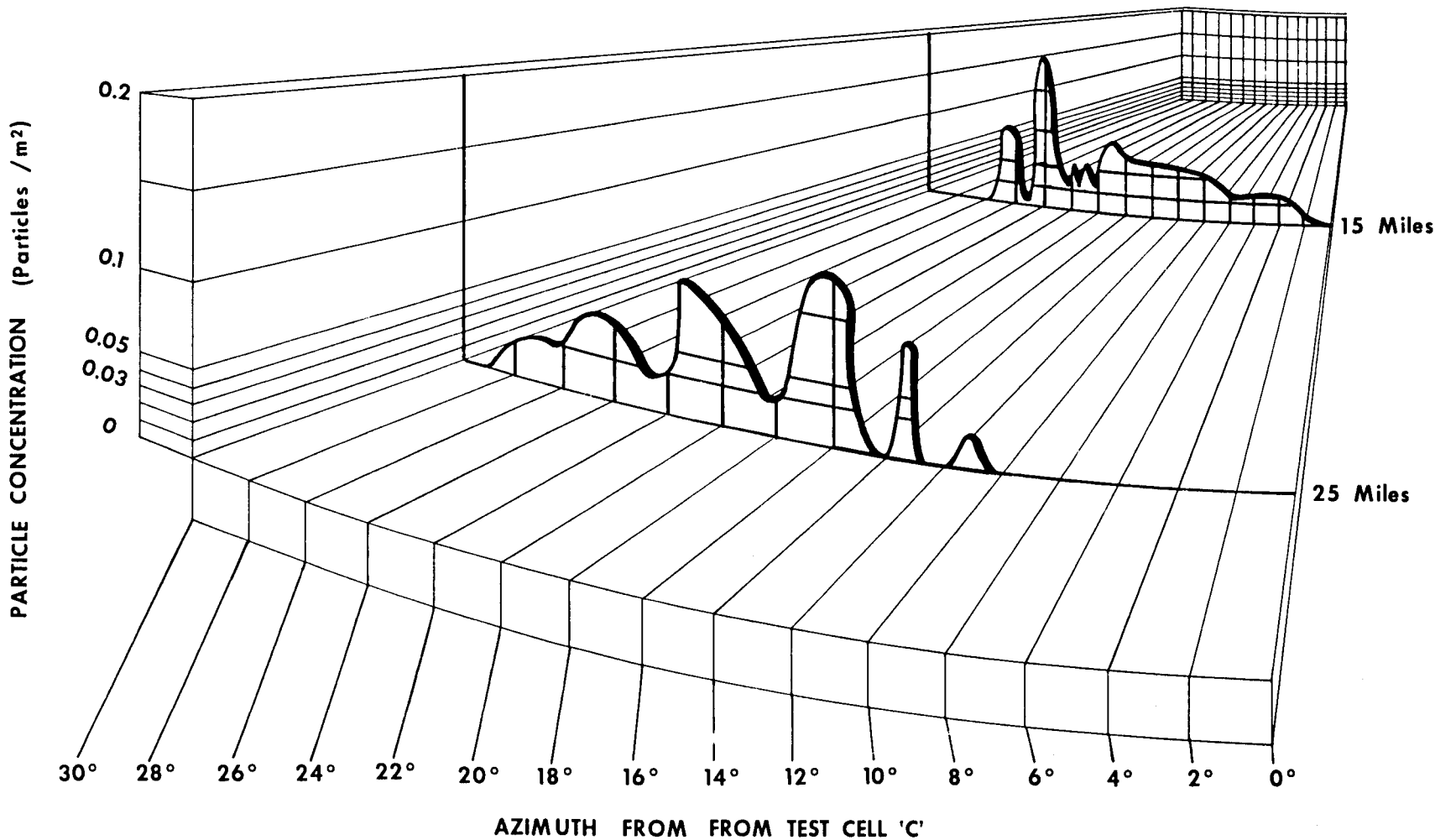

Three-Dimensional Representation of
Particle Survey Results for
Phoebus 2A, EPV[84]

APPENDIX-F

TABLE F-1. MAXIMUM PARTICLE CONCENTRATIONS AT INDICATED DISTANCES

Reactor Run	Arc Distance (miles)/Particles/m^2					
Phoebus-1B, EP-IV		2.5/2.4	5.0/3.3	15.0/1.1	25.0/1.4	40.0/1.2
NRX-A6, EP-III	1.5/0.6	3.0/0.9	6.0/0.9	10.0/1.4	25.0/0.9	40.0/0.2
Phoebus-2A, EP-IV	1.5/0.3	3.0/0.4	7.5/1.3	15.0/0.3	23.0/0.2	40.0/0.2
Phoebus-2A, EP-V	1.5/0.6	2.5/0.4	6.0/0.6	15.0/1.1	25.0/0.2	50.0/0.1
Pewee-I, EP-III	1.5/8.5	3.0/3.6	5.0/3.8	10.0/1.7	20.0/1.1	60.0/0.2

TABLE F-2. NORMALIZATION PARAMETERS

Reactor Test	Source Q (grams)	Cloud height h (feet MSL)	Mean Layer Wind $\bar{u}$ (knots)	Hodograph Shear α (degrees)
Phoebus-1B, EP-IV	450	13,000	10	25
NRX-A6, EP-III	210	9,500	25	10
Phoebus-2A, EP-IV	70	18,000	5	20
Phoebus-2A, EP-V	55	13,500	8	25
Pewee-I, EP-III	103	11,500	8	10

DISTRIBUTION

1 - 15 National Environmental Research Center, Las Vegas, NV
16 Mahlon E. Gates, Manager, AEC/NV, Las Vegas, NV
17 Robert H. Thalgott, AEC/NV, Las Vegas, NV
18 David G. Jackson, AEC/NV, Las Vegas, NV
19 Arthur J. Whitman, AEC/NV, Las Vegas, NV
20 Robert R. Loux, AEC/NV, Las Vegas, NV
21 Mail & Records, AEC/NV, Las Vegas, NV
22 Technical Library, AEC/NV, Las Vegas, NV
23 Chief, NOB/DNA, AEC/NV, Las Vegas, NV
24 P. J. Mudra, AEC/NV, Las Vegas, NV
25 B. W. Church, AEC/NV, Las Vegas, NV
26 Harold F. Mueller, ARL/NOAA, AEC/NV, Las Vegas, NV
27 Howard G. Booth, ARL/NOAA, AEC/NV, Las Vegas, NV
28 D. T. Schueler, AEC/NV, Las Vegas, NV
29 C. P. Bromley, AEC/NV, Las Vegas, NV
30 K. M. Oswald, LLL, Mercury, NV
31 James E. Carothers, LLL, Livermore, CA
32 Ernest A. Bryant, LASL, Los Alamos, NM
33 Harry S. Jordan, LASL, Los Alamos, NM
34 Charles I. Browne, LASL, Los Alamos, NM
35 Jerome E. Dummer, LASL, Los Alamos, NM
36 Eastern Environmental Radiation Facility, EPA, Montgomery, AL
37 Donald R. Martin, AEC/NV, Las Vegas, NV
38 Martin B. Biles, DOS, USAEC, Washington, DC
39 F. K. Pittman, WMT, AEC, Washington, DC
40 J. Doyle, EG&G, Las Vegas, NV
41 Richard S. Davidson, Battelle Memorial Institute, Columbus, OH
42 Carter D. Broyles, Sandia Laboratories, Albuquerque, NM

43 Maj. Gen. Ernest Graves, AGMMA, USAEC, Washington, DC

44 Albert C. Trakowski, Act. Ass't Administrator for Research & Development, EPA, Washington, DC

45 William D. Rowe, Deputy Assistant Administrator for Radiation Programs, EPA, Washington, DC

46 Ernest D. Harward, Act. Dir. of Technology Assessment, Office of Radiation Programs, EPA, Washington, DC

47 - 48 Charles L. Weaver, Dir., Field Operations Div., Office of Radiation Programs, EPA, Washington, DC

49 Gordon Everett, Dir., Office of Technical Analysis, EPA, Washington, DC

50 Library, EPA, Washington, DC

51 Kurt L. Feldmann, Managing Editor, Radiation Data & Reports, Office of Radiation Programs, EPA, Washington, DC

52 Regional Radiation Representative, EPA, Region IX, San Francisco, CA

53 Arden E. Bicker, REECo, Mercury, NV

54 John M. Ward, President, Desert Research Institute, University of Nevada, Reno

55 - 56 Technical Information Center, USAEC, Oak Ridge, TN (for public availability)